

LABORATORY MEASUREMENTS OF WAVE FORCING AND REACTIONS ON A
MODEL SUBMERGED MESH BREAKWATER

A Thesis

by

ALEX BAXTER KNOLL

Submitted to the Office of Graduate and Professional Studies of
Texas A&M University
in partial fulfillment of the requirements for the degree of

MASTER OF SCIENCE

Chair of Committee,	Robert Randall
Committee Members,	Hamn-Ching Chen
	Gerald Morrison
Head of Department,	Robin Autenrieth

August 2014

Major Subject: Ocean Engineering

Copyright 2014 Alex Knoll

ABSTRACT

The purpose of this thesis is to design the test setup, perform the model tests, and process the data to find the wave forces on a submerged breakwater. Breakwaters are coastal protection structures used to help prevent the erosion of the shoreline. Submerged breakwaters are a more recently developed type of offshore detached breakwater that does not interfere with the ocean view and still helps prevent the longshore transport of sediment. For submerged breakwaters that are made of a single structure and placed on the seafloor, the forces must be estimated to ensure proper anchoring.

The prototype submerged breakwater that was examined was a 40 ft long 14 ft diameter half cylinder. The model tested in the laboratory was a 4:1 scale, with a model diameter of 3.4 ft and a length of 10 ft. The estimated forcing on the structure came from measurements during model testing in the Haynes Coastal Engineering Laboratory wave tank. Both regular sinusoidal waves and irregular waves were generated. The significant wave heights ranged from 0.75 ft to 1.0 ft and wave periods varied from 2.0 sec to 3.0 sec using a JONSWAP wave spectrum with a peak enhancement factor of 3.3. Theoretical calculations were completed to help size the instrumentation needed to conduct the experiments. Theoretical calculations were based on the drag law to obtain the force, and Airy as well as Stokes 2nd Order wave theory to obtain the orbital velocities.

It was found that the maximum expected load for all cases at the anchor without any factor of safety (FOS) is 38 lb in shear and 9.9 lb of uplift force. This equates to prototype forces of 2,433 lb of shear and 633 lb of uplift force. Using a FOS of 2.0 the prototype horizontal reaction force required is 4,866 lb and the prototype uplift reaction is 1,266 lb. A total prototype reaction force of 5,028 lbs per anchor is needed. These anchors could be gravity anchors, driven piles or screw anchors.

ACKNOWLEDGMENTS

I would like to thank my committee chair, Dr. Robert Randall, and my committee members, Dr. Hamn-Ching Chen, and Dr. Gerald Morrison, for their guidance and support throughout the course of this research.

Thanks also go to my friends and colleagues and the department faculty and staff for making my time at Texas A&M University a great experience. Thanks go to John Reed for helping set up and run the experiments. Thanks also go to the other graduate students, Joseph Girani and Yuanzhe “George” Zhi, at the Haynes Coastal Engineering Laboratory for helping with running the experiments and processing the data. I wish to thank the undergraduate student workers, Sara Clark, Shelby Clark, David Patterson, Billy Schoelman, Keaton Savoie, Cory Taylor, Jacob Triska, and Colton Wylie for assisting me in the construction of the test setup, placing instrumentation, and helping with general activities around the laboratory.

I also want to extend my gratitude to the Texas Land Grant Office for providing the project and allowing me to use the data for my thesis. I would also like to thank the Western Dredging Association (WEDA) for the scholarships provided to me for my entire length of my master’s studies.

Finally, thanks to my mother and father for their encouragement and support throughout my graduate and undergraduate career at Texas A&M University and for helping me grow as an engineer over the years.

NOMENCLATURE

2D	Two-Dimension
3D	Three-Dimension
A	Wave Amplitude
A	Projected Area
ADV	Acoustic Doppler Velocimeter
CAD	Computer Aided Design
Cd	Drag Coefficient
cal	Calibration
CFD	Computational Fluid Dynamics
cm	Centimeter
DAQ	Data Acquisition System
deg	Degrees
f	Frequency
FOS	Factor of Safety
Fr	Froude Number
FSO	Full Scale Operating
ft	Foot
g	Acceleration Due to Gravity
H	Wave Height

h	Water Depth
H _s	Significant Wave Height
H _{1/3}	Significant Wave Height
Hz	Hertz
in	Inch
JONSWAP	Joint North Sea Wave Project
k	Wave Number
kN	Kilo Newton
L	Wave Length
lb	pound Force
m	Meter
mm	Millimeter
N	Newton
psi	Pounds per Square Inch
RMS	Root Mean Square
sec	Seconds
SPM	Shore Protection Manual
T	Wave Period
t	Time
T _p	Peak Wave Period
TGLO	Texas General Land Office

u	Horizontal Velocity
USACE	U.S. Army Corps of Engineers
v	Vertical velocity
WG	Wave Gauge
z	Depth Below Water Line (negative value)
α	Alpha
σ	Wave Radial Frequency
ρ	Fluid Density
γ	Gamma – Peak Enhancement Factor

TABLE OF CONTENTS

	Page
ABSTRACT	ii
ACKNOWLEDGMENTS.....	iv
NOMENCLATURE.....	v
TABLE OF CONTENTS	viii
LIST OF FIGURES.....	x
LIST OF TABLES	xiv
INTRODUCTION.....	1
OBJECTIVES	2
LITERATURE REVIEW.....	3
TEST CASES FOR EXPERIMENT.....	8
EXPERIMENT SET UP	11
Test Facility.....	11
Breakwater Model.....	12
Design of Model Support Structure for Force Measurements on 10 ft Breakwater	16
Wave Absorber.....	18
Instrumentation and Data Acquisition.....	19
Capacitance Wave Gauge Data and Calibration	20
Load Cells.....	22
Acoustic Doppler Velocimeters	23
Data Acquisition System.....	24
Location of Instrumentation	26
PROCEDURES AND THEORY	28
Experimentation Procedures	28
DATA PROCESSING PROCEDURES	30
Force Data	30

	Page
Wave Transmission and Reflection.....	31
Position of Wave Gauges	31
Wave Transmission and Reflection.....	32
THEORETICAL WAVE FORCING.....	34
MODEL TEST RESULTS.....	41
Horizontal and Vertical Force Measurements.....	41
Horizontal Irregular Wave Force Measurements	43
Vertical Irregular Wave Force Measurements	46
Horizontal Regular Wave Force Measurements	51
Vertical Regular Wave Force Measurements.....	54
Wave Transmission and Reflection.....	57
Coefficient of Reflection	57
Coefficient of Transmission	60
Uncertainty Analysis of Model Test Data Collection.....	62
DISCUSSION OF RESULTS.....	69
Comparison of Theoretical and Experimentally Measured Forces on Model	
Submerged Breakwater	69
Prototype Scale Results.....	75
CONCLUSIONS AND RECOMMENDATIONS.....	78
REFERENCES.....	83
APPENDIX A. FORCE GAUGE CALIBRATION AND FORCE PLOT DATA.....	86
APPENDIX B. CONSTRUCTION AND MODEL TEST PHOTOS.....	95

LIST OF FIGURES

	Page
Figure 1. Photograph of model 10 ft submerged breakwaters	1
Figure 2. General profiles of emerged (left) and submerged (right) breakwaters.....	5
Figure 3. General sediment response for offshore detached breakwaters.....	6
Figure 4. Shallow water wave basin in the Haynes Coastal Engineering Laboratory.	12
Figure 5. Complete submerged breakwater structure.....	14
Figure 6. End and side view drawings of model breakwater structure.	15
Figure 7. Schematic of force gauge and support structure layout.....	17
Figure 8. Load cell basin floor attachment frame (left) Horizontal cable support (right).....	18
Figure 9. Wave absorber on south wall.....	19
Figure 10. Wave calibration stand with 3 wave gauges.....	21
Figure 11. Vertical 500 lb force gauge (left) and horizontal 5,000 lb submersible force gauge (right).....	23
Figure 12 - Data acquisition set-up on instrument carriage	25
Figure 13. Submerged breakwater with instrumentation and DAQ system on bridge.....	26
Figure 14. Plan view of 10 ft model breakwater support structure with instrumentation locations.	27
Figure 15. Positions and relative distances of wave gauges.....	32
Figure 16. Example of the area used for drag calculation of one longitudinal bar.	36
Figure 17. Drag Coefficient vs. Reynolds Number (Vennard and Street 1982).....	38
Figure 18. Theoretical calculation results for model breakwater horizontal forcing	40
Figure 19. Theoretical calculation results for model breakwater vertical forcing.	40

	Page
Figure 20. Drawing of model 10 ft breakwater support structure and force gauges.	42
Figure 21. Irregular wave maximum total horizontal force.	44
Figure 22. Irregular wave minimum total horizontal force.	45
Figure 23. Irregular wave maximum total vertical force.....	47
Figure 24. Irregular wave minimum total vertical force.	48
Figure 25. Irregular wave peak upward forces on the front and rear of the breakwater.	49
Figure 26. Irregular wave peak downward forces on the front and rear of the breakwater.	49
Figure 27. Horizontal total force superposed on wave elevation for test number 18.....	50
Figure 28. Regular wave maximum total horizontal force.....	52
Figure 29. Regular wave minimum total horizontal force.	53
Figure 30. Regular wave maximum total vertical force.....	55
Figure 31. Regular wave minimum total vertical force.	55
Figure 32. Regular wave peak upward forces on the front and rear of the breakwater.	56
Figure 33. Regular wave peak downward forces on front and rear of the breakwater. ...	57
Figure 34. Total coefficient of reflection (C_{rt}) of 0° wave direction (Randall et al 2013).....	58
Figure 35. Total coefficient of reflection of -10° significant waves (Randall et al 2013).....	59
Figure 36. Coefficient of reflection for the model reef only (Randall et al 2013).	60
Figure 37. Coefficient of transmission of 0° waves (Randall et al 2013).	61
Figure 38. Coefficient of transmission of -10° waves.....	62

	Page
Figure 39. Comparison of minimum total horizontal force model test values with theoretical values.....	70
Figure 40. Comparison of maximum total horizontal force model test values with theoretical forces.	72
Figure 41. Comparison of minimum total vertical force model test values vs theoretical values.....	73
Figure 42. Comparison of maximum total vertical force model test values vs theoretical values.....	74
Figure 43. Common screw/auger anchor 66 in length with an 8 in diameter screw.	77
Figure 44. Vertical force gauge calibration (SN: 70300474).....	86
Figure 45. Vertical force gauge calibration (SN: 70309664).....	87
Figure 46. Vertical force gauge calibration (SN: 70300749).....	87
Figure 47. Vertical force gauge calibration (SN: 70335325).....	88
Figure 48. Horizontal force gauge calibration (left) 1,000-lb submersible and (right) 5,000-lb submersible.	88
Figure 49. Breakwater model being checked at Brazos Industries	95
Figure 50. Support frame construction.....	96
Figure 51. Support frame attachment plate (left) floor tie down (right)	96
Figure 52. Support frame with guide wires, without breakwater	97
Figure 53. Wave absorber on south wall.....	97
Figure 54. Installation of the breakwater (setting floor clearance)	98
Figure 55. Longitudinal spring plus overload wire in tripped position.....	99
Figure 56. Rear horizontal force reaction cables with supports	99
Figure 57. Front horizontal force reaction cable with force gauge and support	100
Figure 58. Longitudinal view of breakwater force test setup.....	100

	Page
Figure 59. Final force cable attachment point locations	101
Figure 60. Author Alex Knoll with final force test setup.....	101
Figure 61. During force testing of breakwater	102
Figure 62. 40 ft breakwater wave transmission reflection setup.....	102

LIST OF TABLES

	Page
Table 1. Tests without submerged breakwater in place.	9
Table 2. Force testing on 10 ft submerged breakwater irregular waves.	9
Table 3. Force testing on 10 ft submerged breakwater regular waves.	10
Table 4. Model and environmental conditions for selected 4:1 Froude scale.	14
Table 5. Instrumentation used in testing.	20
Table 6. Breakwater values used in force calculations.	37
Table 7. Hand calculation results for model breakwater forcing.	39
Table 8. Manufacturers reported accuracy of instruments used during testing.	63
Table 9. Uncertainty of force gauge measurements.	65
Table 10. Uncertainty of wave gauge measurements.	67
Table 11. Comparison of minimum and maximum error of calibrated force with actual value for a set voltage.	68
Table 12. Prototype and model controlling forces for a single anchor.	75
Table 13. Horizontal force gauge calibration (left) 1,000-lb submersible (right) 5,000-lb submersible.	89
Table 14. Force data used for irregular wave plots in main text (first row is period (s), second row is force (lb), second column is significant wave height and wave direction).	90
Table 15. Force data used for regular wave plots in main text (first row is period (s), second row is force (lb), second column is significant wave height and wave direction).	91
Table 16. Force data summary of all measurements (regular and irregular wave tests) for model and prototype scales.	92

INTRODUCTION

A submerged breakwater is one approach to mitigating beach erosion caused by waves and currents. Submerged breakwaters are able to provide protection to the shoreline without affecting the views along the coastline. The mesh submerged breakwater studied is a semi-cylinder structure constructed with 0.375 in steel rebar (#3) with a 6 in opening between the crossing rebars. It has overall dimensions of 13.9 ft outside diameter with the total height of 6.8 ft. The breakwater is proposed for installation in about 10 ft water depth along a coast line. The breakwater model used during testing was a 4:1 scale. The testing was conducted at the Haynes Coastal Engineering Laboratory at Texas A&M University. The laboratory has a 3D wave basin capable of generating the waves needed as well as the fabrication and data acquisition to complete the experiments. Figure 1 shows the model 10 ft breakwater in the wave basin that was used during the force testing.

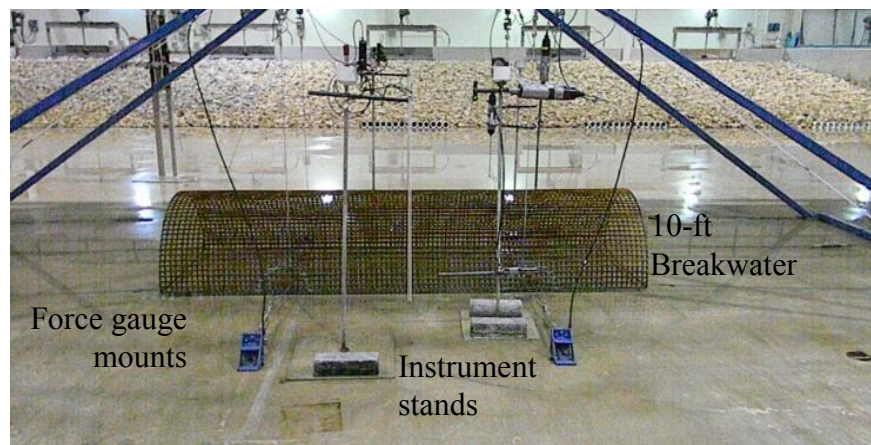


Figure 1. Photograph of model 10 ft submerged breakwaters

OBJECTIVES

The purpose of this physical modeling study was to test a 4:1 scale model of the submerged breakwater. The objectives of the testing was to measure the horizontal and vertical forces on a 10 ft section of the model submerged breakwater due to wave impact on model submerged breakwater. The drag force on the 10 ft section of submerged breakwater was also calculated using the theoretical wave velocity equations and drag law to find the force to compare the wave forces measured during the physical model tests. The theoretical wave equations used were Stokes 2nd Order and Airy Linear Wave theory. The comparison with the model tests is to verify the accuracy of using the theoretical equations to be able to estimate the anchor loads needed to secure the breakwater to the seafloor.

LITERATURE REVIEW

The main coastal protection methods used for decades were sea walls, jetties, groins, dunes, beach nourishment, and offshore breakwaters. The USACE Shore Protection Manual (SPM) (USACE 1984) provides a detailed basis to engineer different structures for shore protection, as well as a background of methods that can be used to provide protection against the environment. Beach dunes were the last resort for shore protection during major storms, and would fail on occasion during larger storms. The dunes would naturally rebuild over years but during that period there was reduced protection. Beach nourishment is an ongoing process that has to be replenished periodically. Larger beaches provide more area for wave breaking, dissipating the energy trying to make it to onshore structures during large storms. Sea walls are vertical or slanted hard structures. These structures do not provide any protection to the beach itself. Both groins and jetties help prevent littoral drift of the longshore sediment transport. Groins are structures that are normally perpendicular to the coastline spaced along the length of the beach. Jetties are used for wave protection for harbor inlets as well as the prevention of longshore transport.

At the time of publication the USACE SPM in 1984 detached breakwaters were just starting to be developed and used. Offshore breakwaters had been used for navigational and harbor protection but not as much for beach shoreline protection. These shore parallel segmented emerged breakwaters were normally rubble mound structures;

however everything from sunken ships to concrete filled sacks had been used. The Japanese and Europeans had started to experiment with submerged breakwaters further offshore as well though.

In the late 1980's and early 1990's the Italians started to experiment with submerged breakwaters and reefs in comparison to the traditional emerged rubble mound breakwater (Tomasicchio 1996). The rubble mound breakwaters were constructed in the late 1970' to 1980's. The performance of the breakwater was very good for the beach, but to be used as a bathing beach, the Italians have strict rules and the water quality did not pass. This was due to the bacteria build up on the breakwaters themselves as well as the low amount of water circulation around the breakwaters. The quality was not dangerous, just over the very tight regulations in place. Therefore, reefs and submerged breakwaters were examined because the waves could pass over to ensure mixing while still providing shore protection to keep the beaches from eroding. It was found that both the reef and the submerged breakwater had a low environmental impact. The breakwater was found to provide the proper amount of mixing, captured sediment to provide a stable beach, and was low in cost. The reef design however did not provide as good of beach protection, because the waves would break causing turbulence in the land side area.

A project had been undertaken in the Dominican Republic using an artificial reef structure as a submerged breakwater in 1998. Harris (2003) published the results of the performance as of 2001. The reef was made up of "Reef Balls" that were approximately

4.5 ft diameter domes that have large holes throughout to make them porous and promote the growth of marine life. The distance from the mean sea level to the top of the breakwater was approximately 1.5 ft. Over the 4 year span the beach width increased by 33 to 43 ft whereas the unprotected shoreline had no change in width. This project shows the feasibility of a submerged breakwater and or reef system as a method of shore protection.

Figure 2 gives an overview of a general profile view of both an emerged standard detached offshore breakwater, and the submerged breakwater or sill. Depending on the application there may be only one breakwater structure or there may be a series of breakwaters as shown in Figure 3. Submerged sills are the entire lengths of the beach in some cases; this would not be done with breakwaters due to the formation of tombolo and the degradation of the water quality on the onshore side of the breakwater.

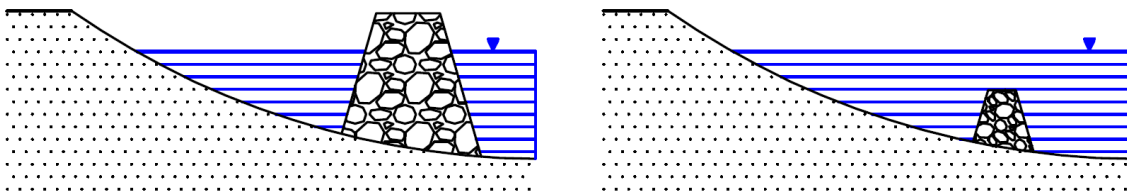


Figure 2. General profiles of emerged (left) and submerged (right) breakwaters

The responses of the beach profile as well as common notations are shown in Figure 3. Depending on the spacing and breakwater length and placement a feature known as a tombolo may form. This is when the sediment building on the beach reaches the

breakwater. Once a tombolo forms the longshore transport is interrupted causing potentially serious water circulation impacts.

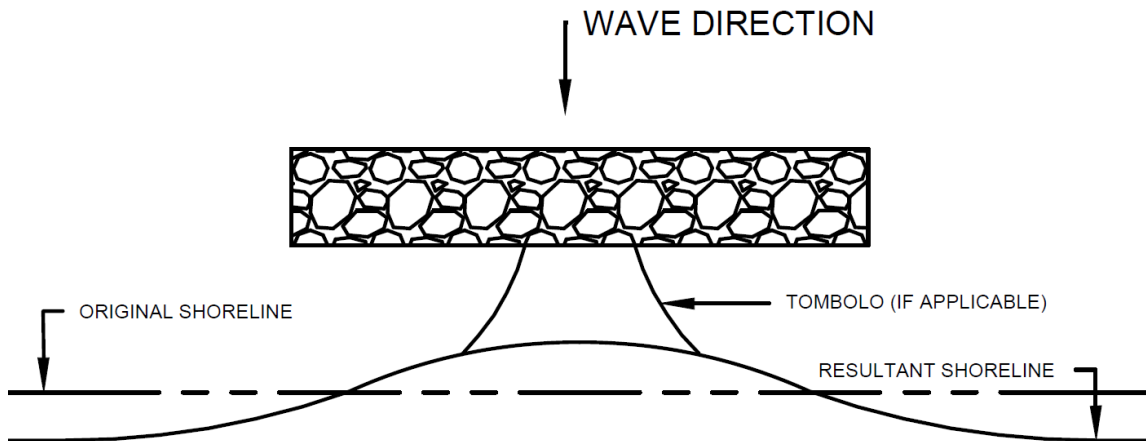


Figure 3. General sediment response for offshore detached breakwaters

Young et al. (2011) as well as the U.S. Army Corps of Engineers (USACE 1992, 2008) provide a good overview of different breakwaters and their performance, advantages and disadvantages. The submerged breakwater being examined in this research is always submerged therefore could also be considered a submerged sill. Submerged breakwaters and sills have become more popular due to the aesthetics compared to emergent breakwaters due to the un-interrupted offshore view. The submerged breakwaters also allow for better landward flow of water, improving the water quality in some cases. The submerged breakwaters have been used to improve local recreational activities as well. Some of the disadvantages of offshore breakwaters include the high cost of construction,

increased navigation hazards for boats as well as to people participating in recreational activities, increased difficulty of inspection, structure may not be high enough to significantly reduce wave activity or reduced seaward transport of sediment, and the limited use of submerged breakwaters and sills resulting in little experience for a design basis. The research and testing Young et al. (2011) found that the best for repelling wave energy is an emerged breakwater, then submerged vertical breakwater, and finally submerged semi-circular breakwater. The research also concluded submerged breakwaters have a smaller impact on irregular waves than regular waves, resulting in smaller reflection coefficients. Emerged breakwaters are still the most common offshore breakwater due to the performance over their submerged counterpart. The research also concluded that the semicircular breakwaters were more stable and less likely to fail than the vertical breakwaters under wave forcing. The breakwater being examined is a submerged semicircular breakwater; this means the wave forcing on the structure should be lower than other comparable breakwaters reducing the size of the anchoring system needed to secure the breakwater to the seabed. Without an adequate anchoring system the breakwater could be overturned and/or shift from the placement location.

Rambabu (2005) has compiled and completed several different models for theoretically analyzing submerged breakwaters. Most of this data is for trapezoidal impermeable breakwaters. The research on permeable breakwaters that have low permeability due to the small spaces in between the solids components of the breakwater. The breakwater research in this thesis will examine a half cylinder with a very porous structure.

TEST CASES FOR EXPERIMENT

The test plan consisted of 4 segments; gathering basin characteristics without any structures, 3 physical model tests and one computer model simulation. The 10 ft submerged breakwater force testing. Table 1 through Table 3 below details the wave conditions and directions used for each test setup. For the random wave generation the Joint North Sea Wave Project or JONSWAP wave spectrum was used. The JONSWAP spectrum uses a peak factor to modify the Pierson-Moskowitz spectrum. The peak factor (gamma- γ) allows for the tuning of the spectrum to different wave conditions around the world. This peak factor also better models the large sudden storms, such as hurricanes. JONSWAP is also becoming the most widely used spectrum from irregular wave laboratory testing (Sorensen 2006). The equations to calculate the spectral energy vs. frequency are listed below (Goda 1985).

$$S(f) = \alpha H_{1/3}^2 T_p^{-4} f^{-5} e^{-1.25(T_p f)^{-4}} \gamma e^{\frac{-(T_p f - 1)^2}{(2\sigma)^2}} \quad (1)$$

$$\alpha = \frac{0.0624}{0.230 + 0.0336\gamma - 0.185(1.9 + \gamma)^{-1}} \quad (2)$$

$$\sigma = \begin{cases} \sigma_a & f \leq f_p \\ \sigma_b & f \geq f_p \end{cases} \quad (3)$$

$$\gamma = 1 \sim 7 \text{ (mean of 3.3)} \quad (4)$$

$$\sigma_a = 0.07, \quad \sigma_b = 0.09 \quad (5, 6)$$

Where $H_{1/3}$ equals the significant wave height, T_p equals the peak wave period, and f is the frequency examined in Hz.

Table 1. Tests without submerged breakwater in place.

Test Number	Peak Wave Period (sec)	Significant Wave Height (feet)	Wave Direction (degrees)
1	2.0	0.75	0
2	2.0	1.0	0
3	2.5	0.75	0
4	2.5	1.0	0
5	3.0	0.75	0
6	3.0	1.0	0
7	2.0	0.75	-10
8	2.0	1.0	-10
9	2.5	0.75	-10
10	2.5	1.0	-10
11	3.0	0.75	-10
12	3.0	1.0	-10

Table 2. Force testing on 10 ft submerged breakwater irregular waves.

Test Number	Peak Wave Period (sec)	Significant Wave Height (feet)	Wave Direction (degrees)
13	2.0	0.75	0
14	2.0	1.0	0
15	2.5	0.75	0
16	2.5	1.0	0
17	3.0	0.75	0
18	3.0	1.0	0
19	2.0	0.75	-10
20	2.0	1.0	-10
21	2.5	0.75	-10
22	2.5	1.0	-10
23	3.0	0.75	-10
24	3.0	1.0	-10

Table 3. Force testing on 10 ft submerged breakwater regular waves.

Test Number	Peak Wave Period (sec)	Significant Wave Height (feet)	Wave Direction (degrees)
1-reg	2.0	0.75	0
2-reg	2.25	0.75	0
3-reg	2.5	0.75	0
4-reg	2.75	0.75	0
5-reg	3.0	0.75	0
6-reg	2.0	1.0	0
7-reg	2.25	1.0	0
8-reg	2.5	1.0	0
9-reg	2.75	1.0	0
10-reg	3.0	1.0	0

EXPERIMENT SET UP

Test Facility

The Haynes Coastal Engineering Laboratory in the Ocean Engineering Program of the Zachry Department of Civil Engineering at Texas A&M University houses a shallow water wave basin 120 ft long, 75 ft wide, and 4 ft deep. The design maximum operating depth for the 48 paddle wave generator is 3.3 ft, and the maximum irregular wave height is 1.2 ft. The maximum and minimum wave periods are 0.5 sec to 5.0 sec depending on the wave heights. The wave propagation direction is between 30 degrees plus or minus to the normal direction to the wave maker. A photograph of the shallow water basin and instrument carriage with the wave progressing in the -10 degree direction is shown in Figure 4 below. A 3 ton overhead crane spans the width and length of the laboratory for lifting models from the shop area to the basin. There is a large overhead door (14 ft high and 24.5 ft wide) located at the rear loading dock, and a 2 ton forklift and bobcat front end loader are used to move materials and models in and out of the laboratory. There are welding, electronics, and manufacturing shops to build models, equipment, and instrumentation setups.



Figure 4. Shallow water wave basin in the Haynes Coastal Engineering Laboratory.

Breakwater Model

The horizontal and vertical forces on the submerged breakwater were examined for different wave conditions. The test setup consisted of 6 force gauges (2 horizontal, 4 vertical), a support frame, 4 acoustic Doppler velocimeters (ADV), 5 wave capacitance gauges (WG), and a 10 ft section of breakwater structure. The force and wave gauges were connected to a 16-channel Lab View, National Instruments data acquisition system (DAQ). The ADVs are connected to the Nortek and SonTek software installed on separate computers. The ADVs were synchronized to start recording data at the same time as the force and wave gauges.

Model testing has been conducted for decades. Therefore, there are lots of data on model scaling parameters and gauge placement. The closer to prototype scale is to the model the less of an impact due to un-scalable effects. The model scaling used was a 4:1 scale; this was the largest model that would fit in the basin, and the largest sea state that was able to be generated. The model was scaled using Froude number (Fr) similarity between prototype and model (Hughes 1993). The Froude number is defined as

$$Fr = \frac{V}{\sqrt{gL}} \quad (7)$$

where V is the velocity, g is gravitational acceleration, and L is the length. For Froude scaling, the time scale is the square root of the geometric model scale, 4:1. Therefore, the time scale in the model is 2 times smaller than in the prototype. Using Froude scaling, the force scale is the cube of the geometric scale. Therefore, the force measured in the model tests are multiplied by 4^3 or 64 to get the prototype forces.

Using Froude scaling the 4:1 scale model submerged breakwater length is 10 ft, and the diameter is 3.37 ft to the center of the curved rebar. The opening between the rebars is 1.28 in by 1.28 in (center to center) with the actual opening being 0.9 in by 0.9 in. The water depth in the wave basin is 2.5 ft. A comparison of the prototype breakwater and the scale model breakwater is tabulated in Table 4. Figure 6 on the next page shows the CAD drawings of the breakwater structure with dimensions. The breakwater structures

were constructed by Brazos Industries in the College Station area. The final completed breakwater is shown in Figure 5.



Figure 5. Complete submerged breakwater structure.

Table 4. Model and environmental conditions for selected 4:1 Froude scale.

Characteristic	Prototype	10 ft Model
	ft	ft
Geometric Scale	1:1	4:1
Length	40.00	10.00
Width	14.00	3.37
Height	7.00	1.69
Environmental Conditions		
Water depth	10.00	2.50
Sig. wave heights (min)	3.00	0.75
Sig. wave heights (max)	4.00	1.00
Wave period (min) (seconds)	4.0	2.0
Wave period (max) (seconds)	6.0	3.0

ITEM NO.	PART NUMBER	DESCRIPTION	QTY.
1	Curved	Rebar - 3/8 OD - 5.15'	95
2	Straight	Rebar - 3/8 OD - 10'-0.7"	50
3	Crossbeam	Rebar - 3/8 OD 3'-5"	3

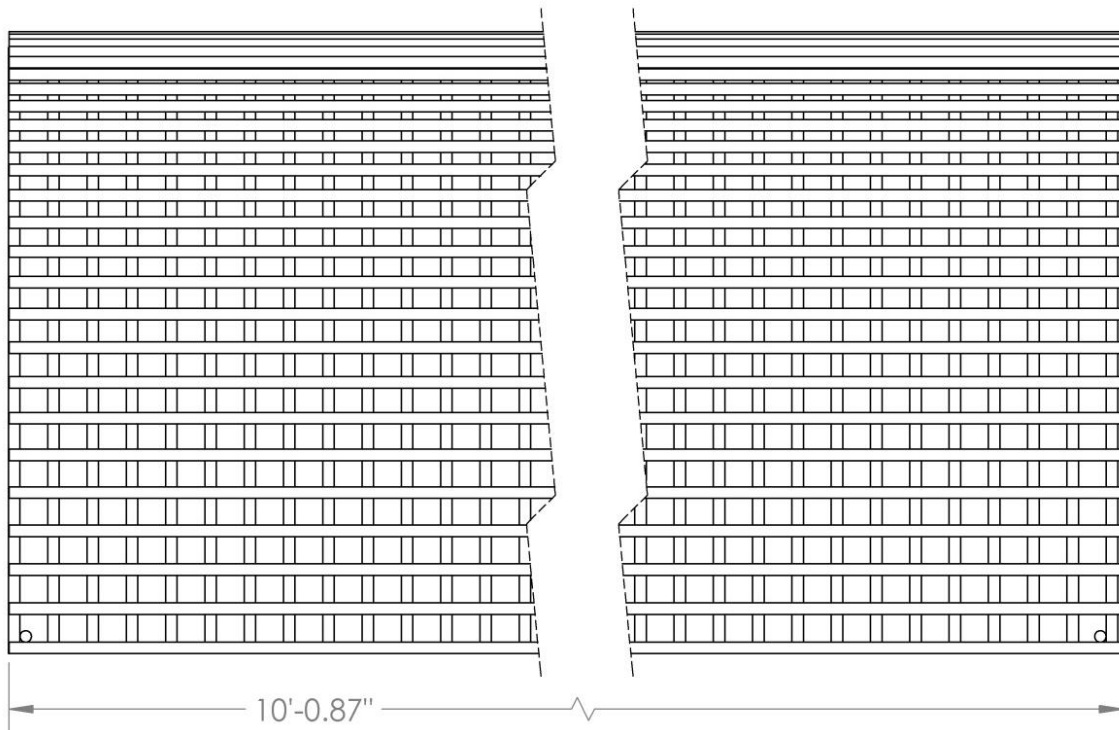
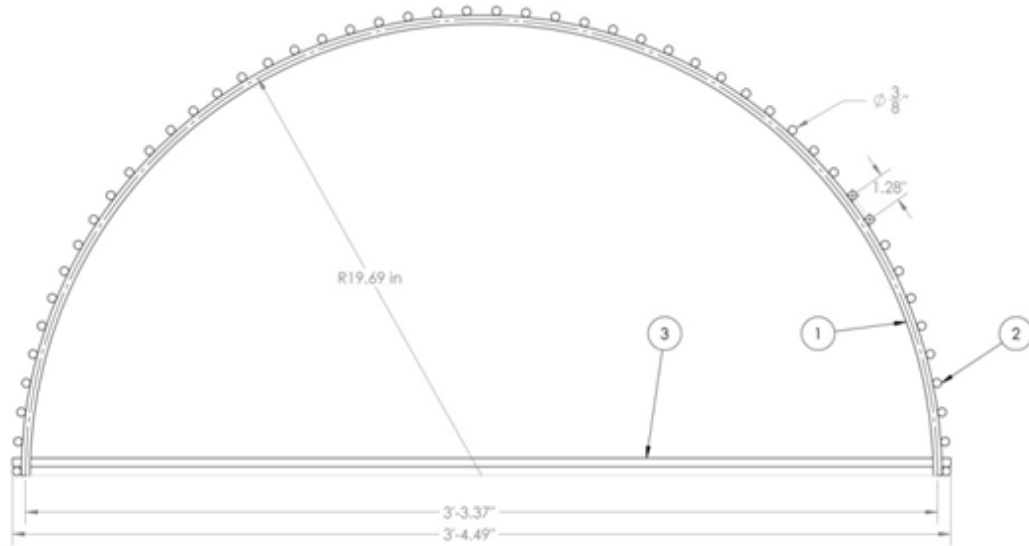


Figure 6. End and side view drawings of model breakwater structure.

Design of Model Support Structure for Force Measurements on 10 ft Breakwater

The 10 ft model breakwater was suspended from a metal tubular support structure during the force measurement testing. By suspending the model breakwater from the support structure and adding force gauges to the four vertical support cables, the vertical force at the four connection points was measured, and the friction between the breakwater structure and wave basin floor was eliminated. The horizontal load cells were located in the forward tie down cables. All of the securing cables had turnbuckles to adjust the length and tension. Structural analysis of the frame was conducted to find the deflections and stresses, and ensure the values were within operable ranges. It was found the structure was within allowable stresses but the deflections were out of desired ranges. To minimize the dynamics of the support frame, four guide wires were added and were brought to a high tension level to stiffen the frame. Without these guide wires, the frame deflection was too high and would have affected the test results. The legs of the frame were secured to the floor using U-bolts to connect to the tie downs in the basin floor, which eliminated the movement of the support frame its self. By having the guide wire cables tensioned and the support structure bolted to the basin floor, the structure was not able to offset, minimizing dynamic and gravity effects on the force measurements. In the longitudinal direction, cables with springs were installed to keep sway to a minimum. The longitudinal cables had an additional overload cable to limit total deflection to 1 in or less. There were small wires attached that have friction connectors that hold until the deflection reaches 1 in to allow us to check if the structure oscillated up to the 1 in limit

during the tests. Figure 7 shows a computer rendering of the force measurement test setup and the support structure in the wave basin.

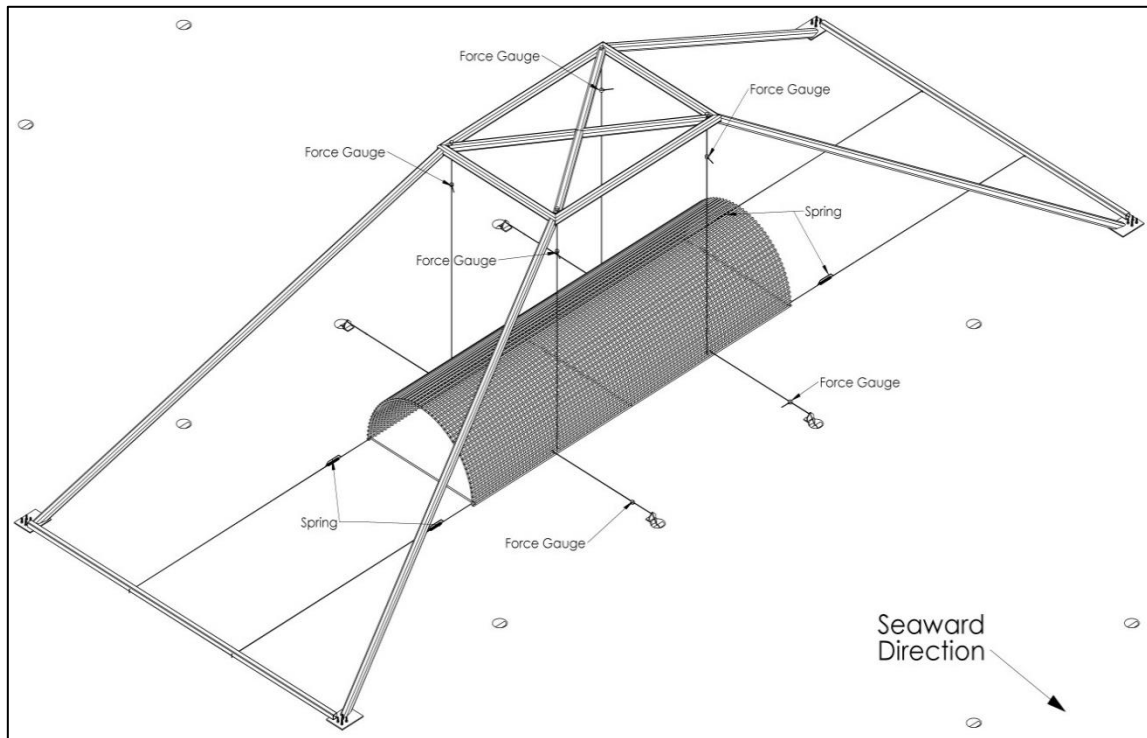


Figure 7. Schematic of force gauge and support structure layout

In the Figure 7 above the four guide line cables are not depicted. These cables were connected to padeyes on the support frame on the top four corners near the vertical cable padeyes. The cables were then run to tie downs in the basin floor and tensioned using turnbuckles. The forward two force gauges were attached to mounting frames u-bolted to the basin floor tie downs. The rear two horizontal cables were connected to the basin tie-downs that were then run over support structures to keep the cables in the horizontal plane only. These two structures are shown in Figure 8 on the next page.

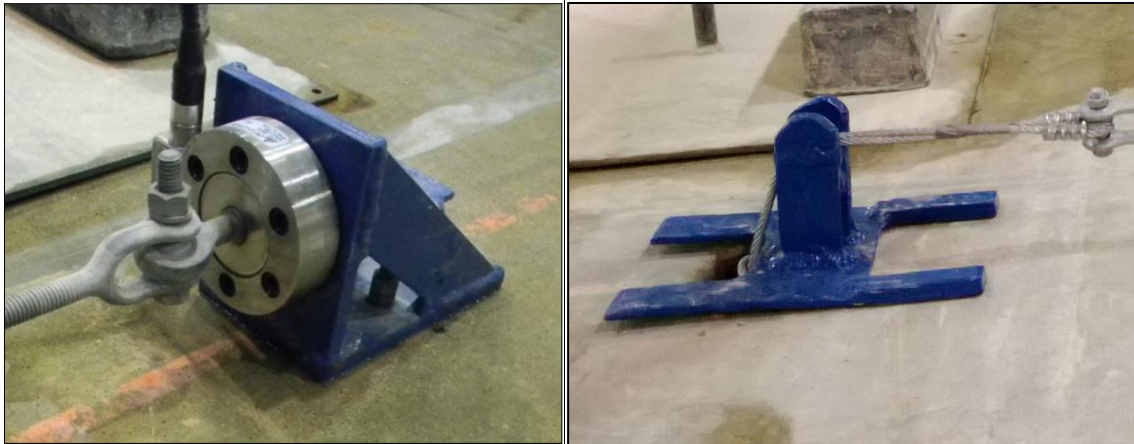


Figure 8. Load cell basin floor attachment frame (left) Horizontal cable support (right)

Wave Absorber

To reduce the reflection off of the side wall during directional (-10 degree) wave tests, a wave absorber shown in Figure 9 was constructed and installed along the south wall of the wave basin. The wave absorber is 48 ft long, 3 ft tall and 4 in thick of coated horse hair. Previous testing of the -10 degree wave files for the project showed some reflection off the bare walls and thus, the wave absorber was installed to minimize these wave reflections. The horse hair absorption material was secured to the south wall using fencing as well as custom clamps attached to the basin bridge rails. These clamps and fencing removed all motion of the horse hair during testing, keeping it in the region of the highest wave energy.



Figure 9. Wave absorber on south wall.

Instrumentation and Data Acquisition

The instrumentation and accuracy of instruments used during the physical tests are tabulated in Table 5. Wave height and water levels are measured with capacitance wave gauges. Wave orbital velocities were measured with four Acoustic Doppler Velocimeters (ADV). Loads on the 10 ft breakwater were measured using six load cells. The following subsections detail the different instruments, calibration procedures and locations of the instrumentation.

Table 5. Instrumentation used in testing.

Quantity	Instrument or Equipment Name
3	Nortek Vectrino acoustic Doppler current meters (3D)
1	SonTek acoustic Doppler current meter (2D)
5 + 1	Haynes Laboratory capacitance wave gauges
1	Omega submersible load cell (5000 lb)
1	Omega submersible load cell (1000 lb)
4	Omega load cell (500 lb)
1	National Instruments 16 channel acquisition system using Lab View

Capacitance Wave Gauge Data and Calibration

The 36 in long capacitance type wave gauges were calibrated at the beginning of each testing day. A motorized calibration stand shown in Figure 10 was used for calibration. The six wave gauges were attached to the calibration stand, and the data cables attached and connected to the Lab View 16 channel data acquisition system during each calibration. Five of the gauges were used to measure the reflection and transmission coefficients. The sixth gauge was an extra to replace one of the five if there was a malfunction without having to recalibrate all of the gauges in the basin during the tests. The calibration stand is automatically controlled and selects 5 water levels based on the input water level in the wave basin. The water level in the wave basin was checked by using the average reading from the water level gauges on the front of each wave paddle. The average water level is displayed on the wave generator computer. The desired water

level of 2.5 ft is adjusted by adding or draining water from the basin. A five point calibration technique was used, and the slope and intercept of a linear line were determined. The resulting calibration curve was applied to the recorded wave data to obtain the wave heights.

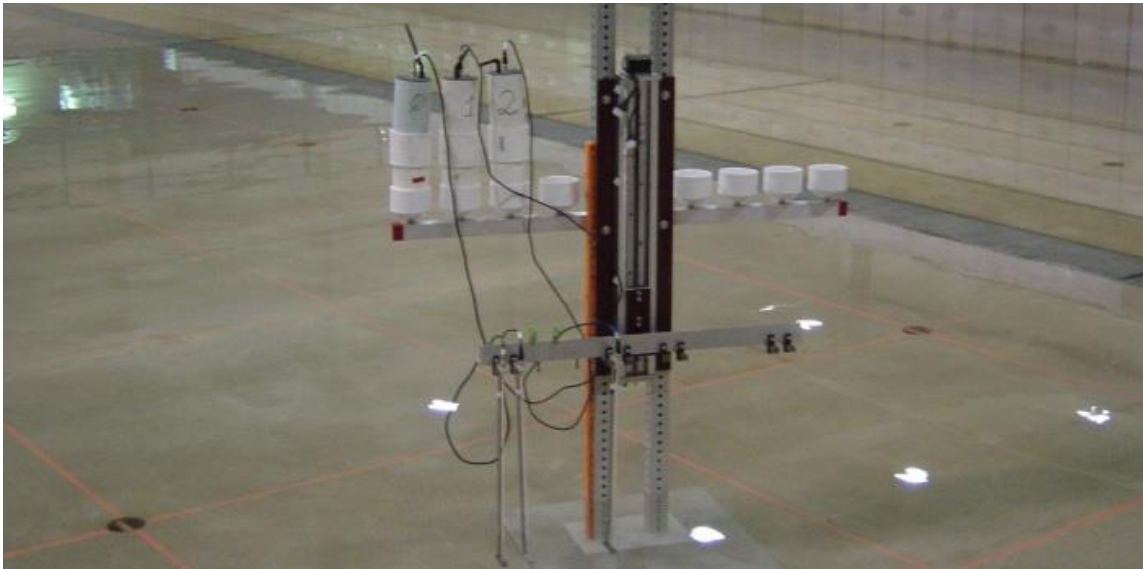


Figure 10. Wave calibration stand with 3 wave gauges.

After the calibration was completed, the wave gauges were removed from the calibration stand and placed on their corresponding wave gauge stands in the wave basin. For these tests, three wave gauges are lined up perpendicular to the breakwater and at a known distance based on the largest wave length in the test sequence. The distance from the wave maker to the first wave gauge is approximately one wave length to reduce the effect from the evanescent wave created by the wave maker during wave generation. The

three gauge set was used to determine wave conditions in the basin and to evaluate the coefficient of reflection based on procedures of Mansard and Funke (1980).

Probe spacing is important to properly capture wave reflection. Mansard and Funke (1980) developed equations to determine the location of the gauges. According to the procedures they defined, the distance from the wave maker to the first wave gauge (WG01) and distance from the third wave gauge (WG03) to the edge of the breakwater was approximately one wave length. The distance between the first wave gauge (WG01) and the second wave gauge (WG02) and the distance between the first wave gauge and the third wave gauge (WG03) were $1/10$ and $1/4$ of the largest wave length in the test sequence, respectively.

Load Cells

The force gauges were calibrated before being installed. The gauges were secured to the forklift, and a pallet was connected to hold the lead bricks during the calibration. The lead bricks were weighed and the weight was recorded on each brick. The lead bricks ranged in weight from 48-58 lbs. As bricks were loaded onto the suspended pallet, the weights and voltage were recorded. The weights were then removed one by one and the weights and voltage were recorded. Figure 11 shows how the vertical and horizontal gauges were installed in the basin. The 500 lb capacity vertical load cells were calibrated

from 0-486 lb. The 1,000 lb submersible force gauge was calibrated from 0-982 lb. The 5,000 lb submersible force gauge was calibrated from 0-1,094 lb.

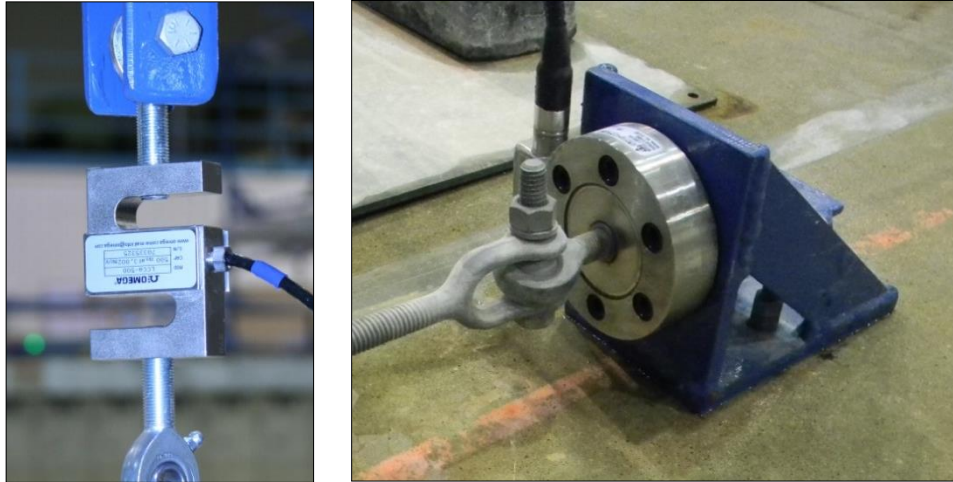


Figure 11. Vertical 500 lb force gauge (left) and horizontal 5,000 lb submersible force gauge (right).

Acoustic Doppler Velocimeters

Three Nortek and one SonTek acoustic Doppler velocimeters (ADV) were used to measure the orbital wave velocities in the wave basin. The ADV is calibrated by the manufacturer and no additional calibration procedures are used. The ADVs are attached to weighted stands and the measuring point of all the ADVs were placed 12 in above the wave basin floor. The three Nortek ADVs are 3-dimensional probes and the one SonTek ADV is a 2-dimensional probe. The SonTek ADV was used as the control along basin velocity measurement at the north end of the breakwater and was centered on the breakwater centerline. The manufacturers stated accuracy is ± 0.5 cm/s for the Nortek

ADV and ± 1 cm/s for the SonTek ADVs. All four of the ADVs were synced to the wave probe DAQ system using a pulse along a wire generated by the Labview wave height recording program to ensure the data timestamps were concurrent across all files.

Data Acquisition System

The data acquisition system consisted of 4 computers, a 16-channel analog acquisition card, and a custom Labview program to calibrate the wave gauges and record up to 40 channels of data. The SonTek ADV as well as one of the Nortek ADVs requires their own computer to record the velocities. The other two Nortek ADVs share one computer. The last computer in the data acquisition system on the bridge was the computer that runs the Labview program. All 16 channels of wave gauge and force data were recorded at the same time through the program. The Labview program also had the ability to send out a sync signal. This signal synced all 4 computers to start data recording at the same time, guaranteeing the data recording was synced across all of the computers and files. Figure 12 shows the bridge data acquisition system along with the location of the computer systems during testing.

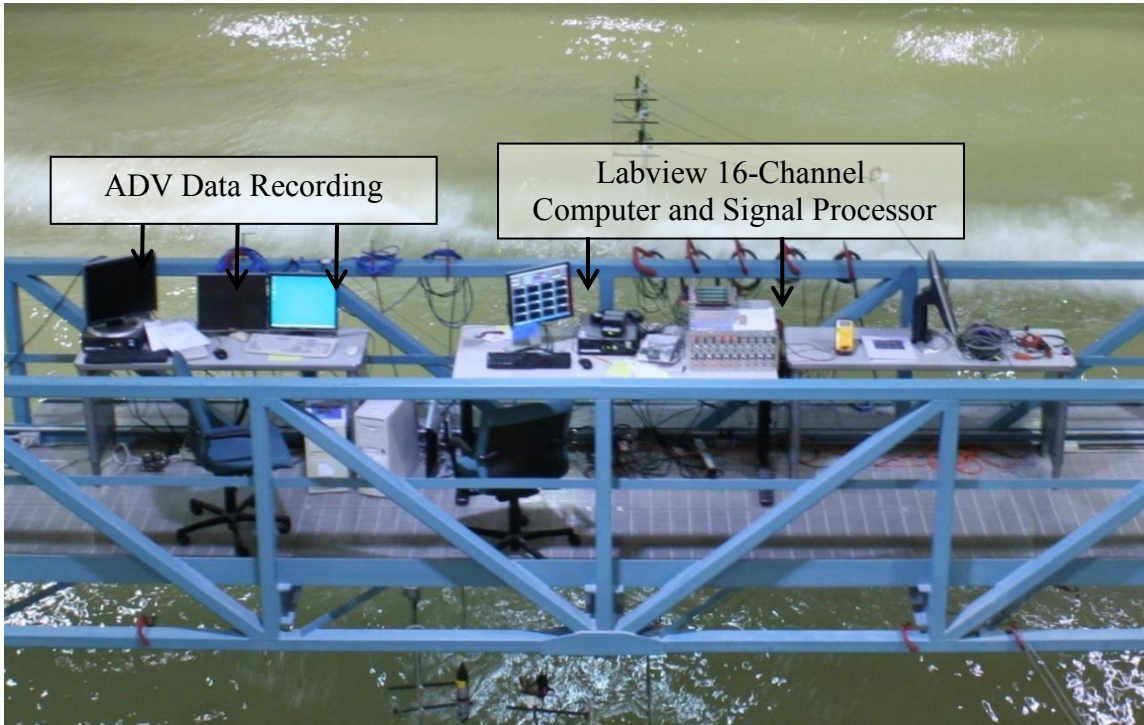


Figure 12 - Data acquisition set-up on instrument carriage

Location of Instrumentation

The basin layout and location of the wave gauges and acoustic Doppler velocimeters in relation to the model submerged breakwater are shown for the 10 ft breakwater. The wave gauges WG01, WG02 and WG03 are centered on the breakwater and were used to measure the reflection coefficient. The incident wave gauge (WG04) is located one diameter from the front edge of the breakwater (wave generator side). The transmitted wave gauge (WG05) is located one diameter from the edge of the breakwater on the beach side. Figure 13 shows the model setup with instrumentation before the water is added to the basin. The CAD drawing depicting the basin and locations of the instruments is shown in Figure 14.



Figure 13. Submerged breakwater with instrumentation and DAQ system on bridge.

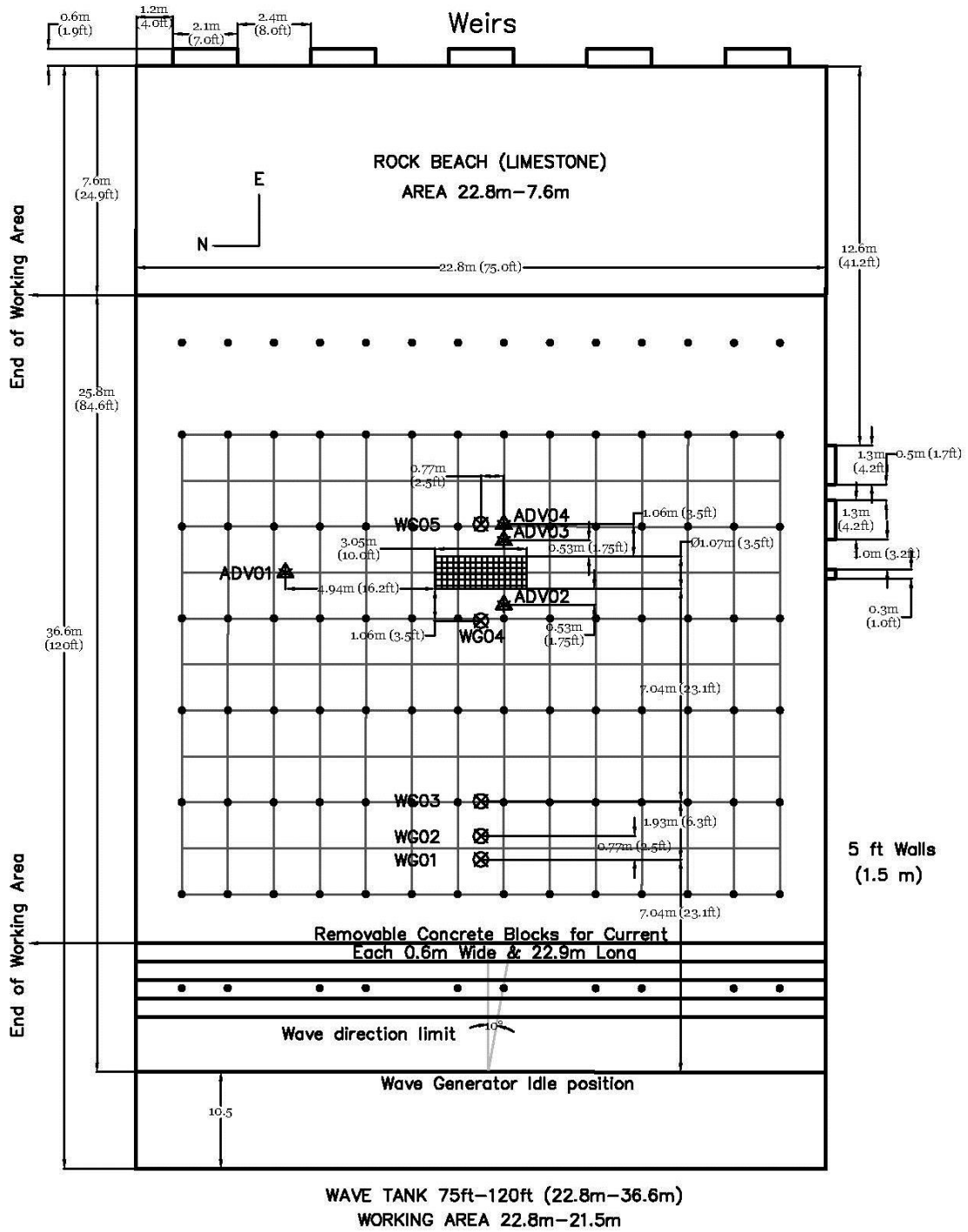


Figure 14. Plan view of 10 ft model breakwater support structure with instrumentation locations.

PROCEDURES AND THEORY

Experimentation Procedures

The first phase of the project was the test preparation. During this phase the model, test frame, and instrumentation stands were built. The data acquisition system was connected to all the instruments. After the system was operational, test data were gathered to ensure the system was properly synchronized for recording data. Once the test frame was constructed, it was installed into the basin. The breakwater was then hung from the test frame and secured while installing the load cells. The breakwater was then leveled and squared to the basin. The ADVs and wave gauges were then installed into their respective locations marked on the floor of the basin. The wave profiles were entered into the wave generator computer to generate the files needed to run the wave maker. The basin was then filled to the correct water level, and the wave maker and data systems were checked for functionality.

Phase two was the 10 ft breakwater force test. Each test morning the basin water level was checked and the wave gauges were calibrated according to the procedures in the previous section. The people responsible for each activity then took their place and waited for the cue to begin testing. Once a test was completed the data files were verified while waiting for the basin to become calm to not affect the results of the next test. This procedure was then repeated for all of the tests to be completed that day. Once all data

collection was completed it was copied to two hard drives in case of failure of a drive.

The data was then analyzed to determine if any tests must be rerun the following day.

The final phase was processing all of the data. This included converting the signals received by the DAQ system into forces and deflections, calculating wave transmission coefficients, and documenting the results.

DATA PROCESSING PROCEDURES

Force Data

To process the force data, the data was converted from volts to pound force using the calibration curve for each gauge. Since the raw data had noise the data was smoothed using several techniques, the different techniques were compared to determine the best method without compromising the data. The main method that was used was time averaging, different amounts of time steps and weighted averages were considered. Once the data were prepared the two horizontal gauges were summed to find the total horizontal force on the breakwater. The front two vertical and rear two vertical gauges were summed to find the total uplift force on the front and back as the wave passed over the structure. The high tensions of the horizontal cables allowed for the examination of both the push and pull horizontal forces. The cables connecting the model to the force gauges were not able to handle compression, and since there are only force gauges on the seaward side of the model when the wave pulls the model back out to sea the cables could become slack. Once the cables became slack the total minimum horizontal force was not be able to be determined. The mean tension in the cables was removed from the force time trace, and then the maximum and minimum values were determined.

Wave Transmission and Reflection

Position of Wave Gauges

For the no breakwater and 10 ft breakwater tests, there were five wave gauges used for reflection and transmission analysis. The first three wave gauges were used for evaluating the wave coefficient of reflection. These wave gauges were inline and perpendicular to the breakwater at a known distance according to the largest wave length in the test sequence. According to the procedures of Mansard and Funke (1980), the distance from the wave maker to the first wave gauge (WG01) and distance from the third wave gauge (WG03) to the edge of the breakwater is approximately one wave length. The distance between the first wave gauge (WG01) and the second wave gauge (WG2) and the distance between the first wave gauge and the third wave gauge (WG03) is 1/10 and 1/4 of the largest wave length in the test sequence, respectively.

The wave lengths for the 1 ft significant wave height with a peak period of 2 s, 2.5 s, and 3 s are 15.64 ft, 20.58 ft, and 25.38 ft, respectively. The wave lengths were evaluated using

$$L = \frac{g}{2\pi} T^2 \tanh \frac{2\pi h}{L} \quad (8)$$

where L is the wave length, g is gravitational acceleration, and h is water depth, which is 2.5 ft. The wave gauges were not moved for the different wave tests.

In order to evaluate the wave transmission coefficients through the model breakwater, two more wave gauges were placed in line with the first three wave gauges used for the reflection analysis, and positioned in front of and behind the breakwater. The distance from the fourth wave gauge (WG04) to the front edge of the breakwater and the distance from the back edge of the breakwater to the fifth wave gauge (WG05) were both equal to one breakwater diameter. The distance between WG05 and WG06 was one breakwater radius. The side view of the positions of these wave gauges are illustrated in Figure 15.

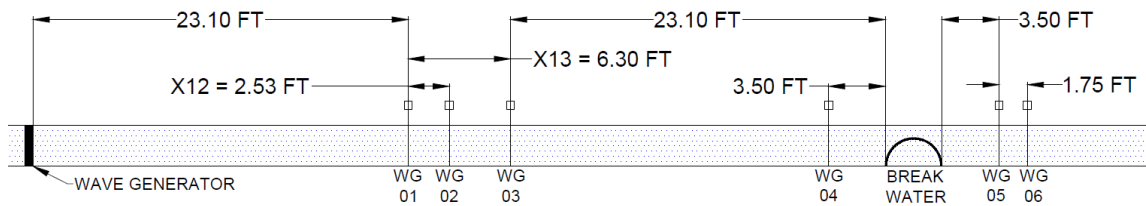


Figure 15. Positions and relative distances of wave gauges

Wave Transmission and Reflection

The methodologies to calculate the transmission and reflections coefficients are from the model test report submitted to TGLO (Randall et al 2013). The total coefficients of wave reflection (C_{rt}) were derived from the data acquired by the first three wave gauges

(WG01, WG02 and WG03). The data recorded by these wave gauges was processed and the spectral energy was calculated. The energies were then compared to the spectral energy of the generated waves to obtain the total system reflection coefficient. After computing the reflection coefficient of the total system (beach and breakwater), the reflection coefficient of the model breakwater only (C_{rr}) can be approximated using equation 9

$$C_{rt} = C_{rr} + (1 - C_{rr})^2 C_{rb} \quad (9)$$

where C_{rb} is the coefficient of reflection of beach with no breakwater in place and C_{rt} is the coefficient of reflection for beach with the breakwater in place (Mouraenko 2013). The coefficient of reflection for breakwater alone was determined by solving the quadratic equation using equation 10

$$C_{rr} = \frac{\sqrt{4 \cdot C_{rt} \cdot C_{rb} - 4 \cdot C_{rb} + 1} + 2 \cdot C_{rb} - 1}{2 \cdot C_{rb}} \quad (10)$$

where C_{rb} is the coefficient of reflection of beach with no breakwater in place and C_{rt} is the coefficient of reflection for beach with the breakwater in place.

Coefficients of transmission (C_{t1}) were evaluated by dividing the significant wave height measured by the wave gauges positioned in front and behind the breakwater, namely the significant wave height measured with WG05 divided by the WG04 measurement. The second coefficient of transmission was determined by dividing the significant wave height from WG06 by WG04, which is denoted as C_{t2} .

THEORETICAL WAVE FORCING

To calculate the forcing on the breakwater both the Airy Wave Theory and Stokes 2nd Order Theory were used along with the drag law. From Dean and Dalrymple (1991) the orbital particle velocities for waves were determined using the formulations for both Airy and Stokes second order wave theory. From these equations the horizontal, which is the controlling velocity direction, velocities were determined, including the second order effects that increase the velocity due to shallow water effects. The first order horizontal velocity equation is:

$$u = \frac{H}{2} \sigma \frac{\cosh(k(h+z))}{\sinh(kh)} \cos(kx - \sigma t) \quad (11)$$

The second order horizontal velocity equation is:

$$u = \frac{H}{2} \frac{gk}{\sigma} \frac{\cosh(k(h+z))}{\sinh(kh)} \cos(kx - \sigma t) + \frac{3}{16} H^2 \sigma k \frac{\cosh(2k(h+z))}{\sinh^4(kh)} \cos(2(kx - \sigma t)) \quad (12)$$

The first order vertical velocity equation is:

$$v = \frac{H}{2} \sigma \frac{\sinh(k(h+z))}{\sinh(kh)} \sin(kx - \sigma t) \quad (13)$$

The second order vertical velocity equation is:

$$v = \frac{H}{2} \frac{gk}{\sigma} \frac{\sinh(k(h+z))}{\sinh(kh)} \sin(kx - \sigma t) + \frac{3}{16} H^2 \sigma k \frac{\sinh(2k(h+z))}{\sinh^4(kh)} \sin(2(kx - \sigma t)) \quad (14)$$

where:

$$\sigma^2 = gk \tanh kh \quad (15)$$

These calculated velocities will then be combined with the drag coefficients and drag force equations in Randall (2010). The drag force equation used is

$$F = \frac{1}{2} C_d A \rho u |u| \quad (16)$$

The expected forcing on the breakwater structure can be estimated using this method.

The breakwater was split into 50 sections, one section for each of the longitudinal bars around the breakwater. Each section also includes the small parts of each of the 95 curved bars that are adjacent to each of the straight longitudinal bars. An example of one of these areas is shown in Figure 16 below; the overall breakwater is shown with the individual calculated area shaded maroon. The centroid locations were calculated to include in the calculations to account for the different incident velocities over the breakwater at the same time step. The forces for each area were then summed to obtain

the total forcing on the breakwater. The calculations were then repeated for a range of times to get a time trace of the vertical and horizontal forces on the breakwater to find the minimum and maximum forces. This procedure was then repeated for the different wave conditions that were tested. The values used to determine the forcing on the breakwater are listed in Table 6. The table is a printout from the spreadsheet that was developed to simulate the forces on this breakwater over time.

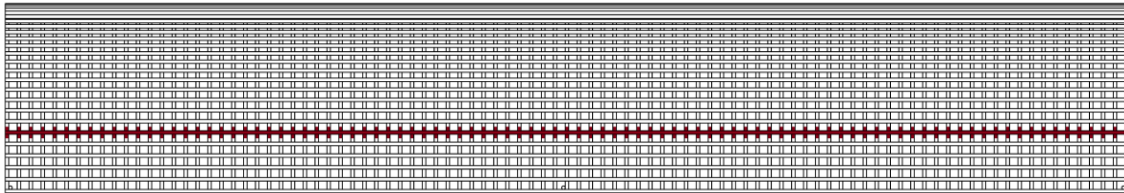


Figure 16. Example of the area used for drag calculation of one longitudinal bar.

Table 6. Breakwater values used in force calculations.

			#	x	z	h-x	h-y	Area-x	Area-y	Cd_x	Cd_y
Diameter	39.75	in	1	19.875	0.000	0.902	0.000	61.076	45.000	1.200	0.500
Length	120.00	in	2	19.834	1.273	0.901	0.058	77.118	46.030	1.198	0.500
Quantity	50		3	19.712	2.542	0.895	0.115	76.986	48.086	1.190	0.500
Delta Angle	3.67	deg	4	19.508	3.799	0.886	0.173	76.723	50.129	1.178	0.500
Water Depth	30	in	5	19.225	5.041	0.873	0.229	76.329	52.151	1.161	0.500
d_bar	0.375	in	6	18.862	6.263	0.857	0.284	75.807	54.143	1.139	0.500
			7	18.422	7.458	0.837	0.339	75.158	56.098	1.112	0.500
h_inbetween	0.902	in	8	17.907	8.623	0.813	0.392	74.385	58.008	1.081	0.500
# verticals	95		9	17.317	9.753	0.786	0.443	73.491	59.864	1.046	0.500
			10	16.657	10.843	0.756	0.492	72.480	61.658	1.006	0.546
time step	0.05	sec	11	15.928	11.887	0.723	0.540	71.356	63.385	0.962	0.598
total time	30	sec	12	15.134	12.884	0.687	0.585	70.124	65.036	0.914	0.648
# iterations	600		13	14.277	13.827	0.648	0.628	68.789	66.604	0.862	0.696
			14	13.362	14.713	0.607	0.668	67.356	68.084	0.807	0.740
Cd x base value	1.20		15	12.392	15.539	0.563	0.706	65.831	69.469	0.748	0.782
Cd y base value	1.00		16	11.371	16.301	0.516	0.740	64.220	70.753	0.687	0.820
			17	10.303	16.996	0.468	0.772	62.531	71.932	0.622	0.855
			18	9.193	17.621	0.417	0.800	60.769	73.000	0.555	0.887
			19	8.045	18.174	0.365	0.825	58.943	73.953	0.500	0.914
			20	6.864	18.652	0.312	0.847	57.059	74.786	0.500	0.938
			21	5.655	19.054	0.257	0.865	55.126	75.498	0.500	0.959
			22	4.423	19.377	0.201	0.880	53.151	76.084	0.500	0.975
			23	3.172	19.620	0.144	0.891	51.143	76.542	0.500	0.987
			24	1.908	19.783	0.087	0.898	49.109	76.871	0.500	0.995
			25	0.637	19.865	0.029	0.902	47.059	77.069	0.500	0.999
			26	-0.637	19.865	0.029	0.902	47.059	77.069	0.500	0.999
			27	-1.908	19.783	0.087	0.898	49.109	76.871	0.500	0.995
			28	-3.172	19.620	0.144	0.891	51.143	76.542	0.500	0.987
			29	-4.423	19.377	0.201	0.880	53.151	76.084	0.500	0.975
			30	-5.655	19.054	0.257	0.865	55.126	75.498	0.500	0.959
			31	-6.864	18.652	0.312	0.847	57.059	74.786	0.500	0.938
			32	-8.045	18.174	0.365	0.825	58.943	73.953	0.500	0.914
			33	-9.193	17.621	0.417	0.800	60.769	73.000	0.555	0.887
			34	-10.303	16.996	0.468	0.772	62.531	71.932	0.622	0.855
			35	-11.371	16.301	0.516	0.740	64.220	70.753	0.687	0.820
			36	-12.392	15.539	0.563	0.706	65.831	69.469	0.748	0.782
			37	-13.362	14.713	0.607	0.668	67.356	68.084	0.807	0.740
			38	-14.277	13.827	0.648	0.628	68.789	66.604	0.862	0.696
			39	-15.134	12.884	0.687	0.585	70.124	65.036	0.914	0.648
			40	-15.928	11.887	0.723	0.540	71.356	63.385	0.962	0.598
			41	-16.657	10.843	0.756	0.492	72.480	61.658	1.006	0.546
			42	-17.317	9.753	0.786	0.443	73.491	59.864	1.046	0.500
			43	-17.907	8.623	0.813	0.392	74.385	58.008	1.081	0.500
			44	-18.422	7.458	0.837	0.339	75.158	56.098	1.112	0.500
			45	-18.862	6.263	0.857	0.284	75.807	54.143	1.139	0.500
			46	-19.225	5.041	0.873	0.229	76.329	52.151	1.161	0.500
			47	-19.508	3.799	0.886	0.173	76.723	50.129	1.178	0.500
			48	-19.712	2.542	0.895	0.115	76.986	48.086	1.190	0.500
			49	-19.834	1.273	0.901	0.058	77.118	46.030	1.198	0.500
			50	-19.875	0.000	0.902	0.000	61.076	45.000	1.200	0.500

Compute Time Series

The drag coefficient for the calculations was determined from Figure 17. The average Reynolds Number for the maximum horizontal wave velocity case is on the order of 10^4 to 10^5 , and is on the order of 10^3 to 10^4 for the maximum vertical wave velocity case. These values correspond with a drag coefficient of 1.2 for the horizontal force calculations and 1.0 for the vertical force calculations. The drag coefficients were then multiplied by $\sin(\Theta)$ or $\cos(\Theta)$, where Θ is the angle from horizontal to the center of the longitudinal bar, and the minimum allowable value was 0.5. This helped account for the reduction of drag force due to the proximity of the other bars in the flow path reducing the flow velocity.

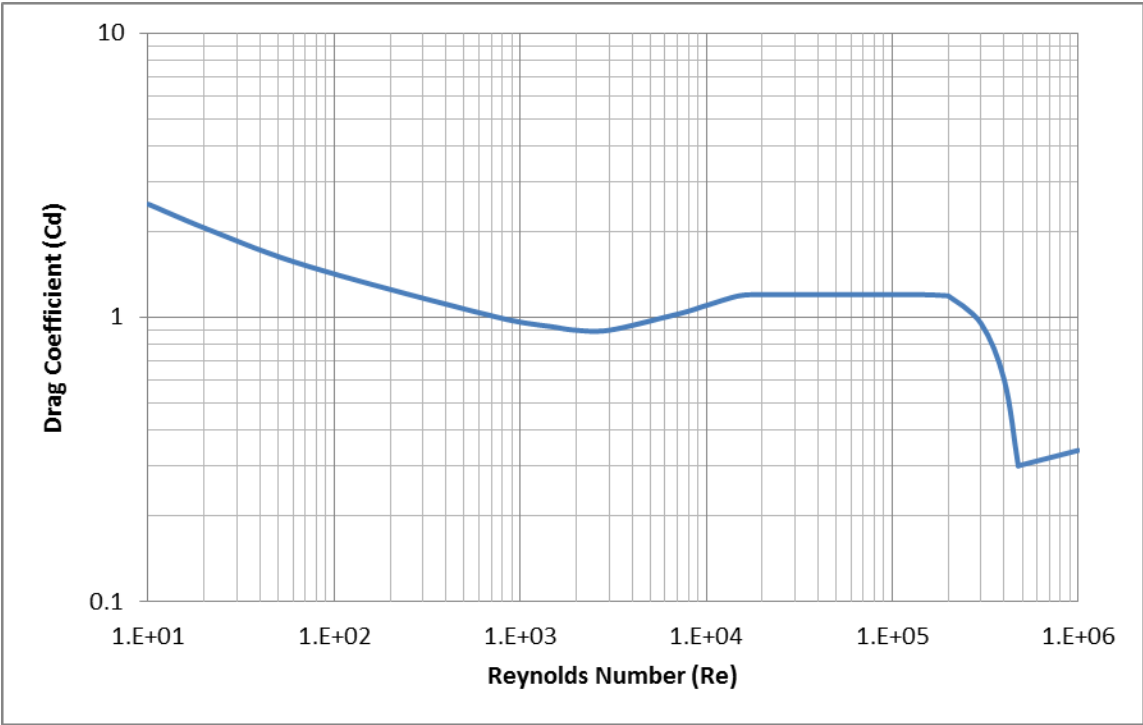


Figure 17. Drag Coefficient vs. Reynolds Number (Vennard and Street 1982)

The theoretical calculation force results for the breakwater model are detailed in Figure 18, Figure 19, and Table 7 on the next pages. These values were calculated using a macro in Excel that summed the forces using the drag law and the orbital velocities on each member. The macro then progressed one time step and repeated all of the drag equations. The 30 second time series was then analyzed to find the maximum and minimum forces for each of the wave calculation methods and directions. The plots are a visual representation of the data in Table 7 for the horizontal and vertical directions. The Airy wave theory results have the same magnitude for the positive and negative directions, whereas the Stokes 2nd Order has smaller reactions in the negative direction, this is due to the non-linear effects of the waves in intermediate to shallow water.

Table 7. Hand calculation results for model breakwater forcing.

Case	Fx - 2nd order (lbs)	Fx - Airy (lbs)	Fy - 2nd order (lbs)	Fy - Airy (lbs)
2.0 sec Max	18.9	16.9	5.0	8.1
0.75 ft Min	-15.0	-16.9	-5.0	-8.1
2.0 sec Max	34.8	30.0	9.5	14.3
1.0 ft Min	-25.6	-30.0	-9.5	-14.3
2.5 sec Max	28.7	22.5	4.4	8.1
0.75 ft Min	-17.1	-22.5	-4.4	-8.1
2.5 sec Max	55.1	40.0	8.8	14.5
1.0 ft Min	-27.5	-40.0	-8.8	-14.5
3.0 sec Max	39.0	26.0	4.2	8.2
0.75 ft Min	-15.6	-26.0	-4.2	-8.2
3.0 sec Max	78.1	46.1	9.2	14.6
1.0 ft Min	-23.7	-46.1	-9.2	-14.6

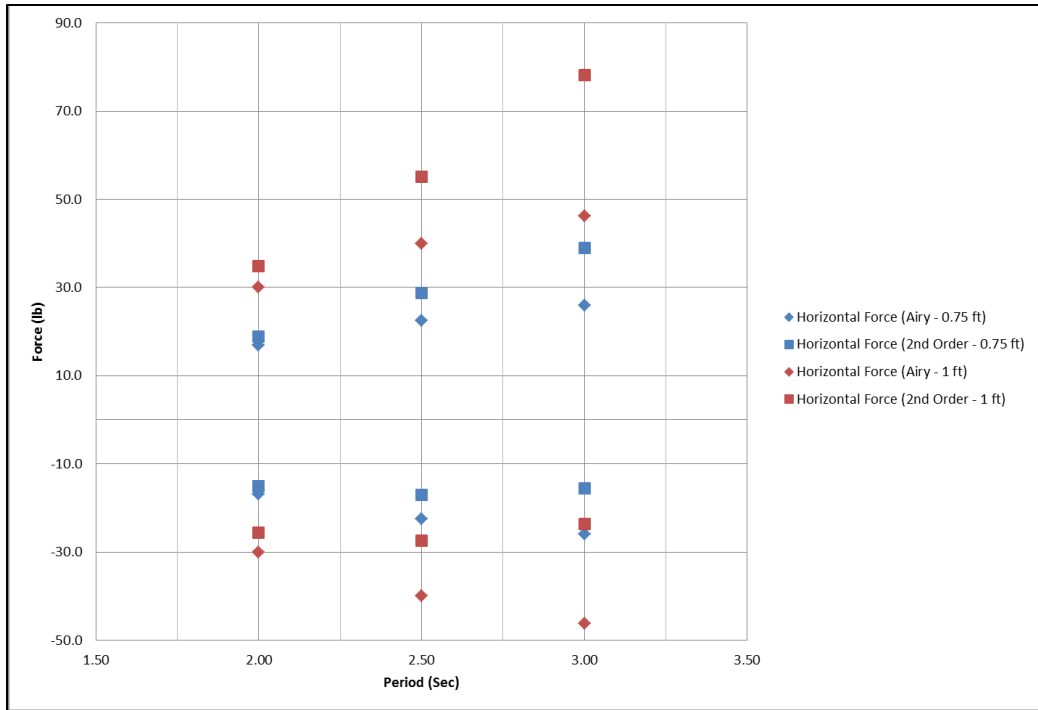


Figure 18. Theoretical calculation results for model breakwater horizontal forcing

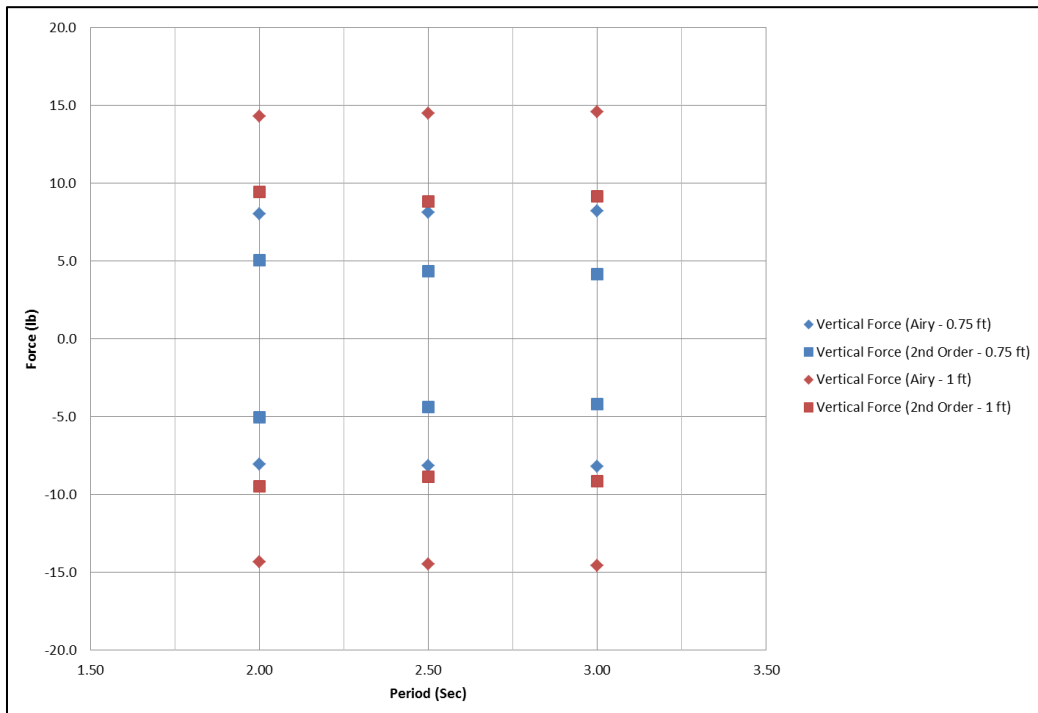


Figure 19. Theoretical calculation results for model breakwater vertical forcing.

MODEL TEST RESULTS

Horizontal and Vertical Force Measurements

The model 10 ft submerged rebar breakwater was supported by a tubular steel structure as shown in Figure 20. Two horizontal force gauges were attached to the breakwater at 2.5 ft either side of the perpendicular center line. Cables were attached to the opposite side of the breakwater and to the tie down points in the wave basin floor. These cables were connected with turnbuckles, and the turnbuckles were adjusted so that a tension of approximately 50 lb was applied. The support structure was bolted to the tie-down points in the wave basin floor using U-bolts. A 1000 lb gauge was used for one force gauge and a 5000 lb gauge was used for the other. The large force gauges were used because of the overestimation of the forces in the cables. These forces were estimated from the drag equations plus the pretension in the cables from the turnbuckles multiplied by a factor of safety to ensure the load cells would not be overloaded. These different size force gauges were used due to availability from the manufacture based on the testing time frame. The force gauges were calibrated and were accurate for the resultant force range. The 10 ft breakwater was suspended under the support structure, and the bottom of the breakwater was 1 in above the wave basin floor. Four vertical cables were attached to the breakwater and support structure. The vertical force gauges were connected in line with the cables and located so the gauges would not get submerged in the water. The vertical force gauges were rated at 500 lb.

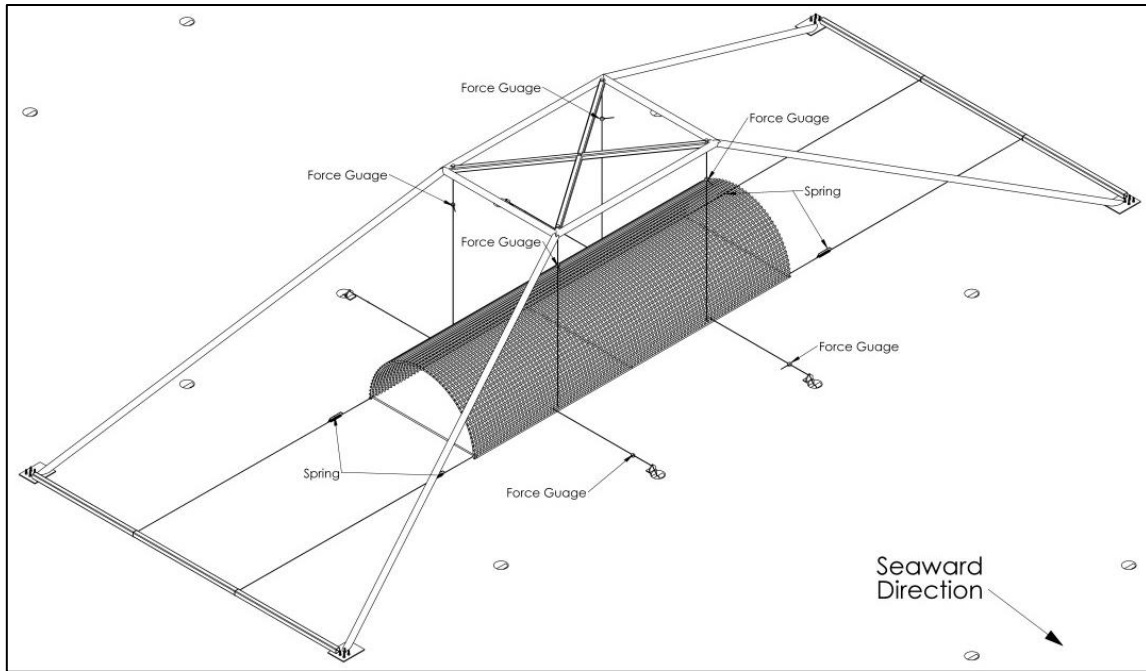


Figure 20. Drawing of model 10 ft breakwater support structure and force gauges.

The negative horizontal direction was in the seaward direction (toward the wave maker) and the positive direction was toward the beach. The positive vertical direction was upward. The weight of the breakwater created a negative force in the vertical force gauges. The force gauges were zeroed before each test, and thus, the zero reading represents the static equilibrium condition.

The weight of the model 10 ft breakwater in air is 372 lb. When the breakwater was hung from the support structure, the weight was determined using the output from the vertical load cells which included the weight of cables and connectors. The weight in air with all the cables is 385.6 lb and the in-water weight of the 10 ft breakwater is 337.7 lb. The buoyant force is the difference of these two readings which was 47.9 lb.

Horizontal Irregular Wave Force Measurements

The force measured with the horizontal force gauges was recorded by the data acquisition system at a sampling rate of 25 Hz. The wave maker generated the JONSWAP wave spectra for a significant wave height of 0.75 and 1.0 ft and peak wave periods of 2.0, 2.5, and 3.0 sec, and a peak enhancement factor (γ) of 3.3. The duration of each wave spectrum was 8 minutes and two directions (0 degree and -10 degree) were generated. The force, ADV and wave gauges were synchronized to start recording at the same time when the wave maker was actuated. The maximum forces generated by the wave orbital velocities were recorded, and the data file was searched to find the maximum force on each gauge and added together for the total maximum force. The force data used in this section for the plots is tabulated in Table 14 on page 90 in Appendix A.

The results for the total maximum horizontal force are illustrated in Figure 21. The lowest maximum horizontal forces occurred for the 2 sec peak period wave spectrum and ranged between 25 and 40 lb. The maximum horizontal forces increased almost linearly with increasing wave peak period. For the 3 sec peak period, the maximum horizontal forces ranged between 50 and 73 lb. The 1 ft significant wave height spectra resulted in higher forces than the 0.75 ft spectra as expected. When the waves were at a -10 degree angle to the breakwater the forces were slightly less by about 5 lb.

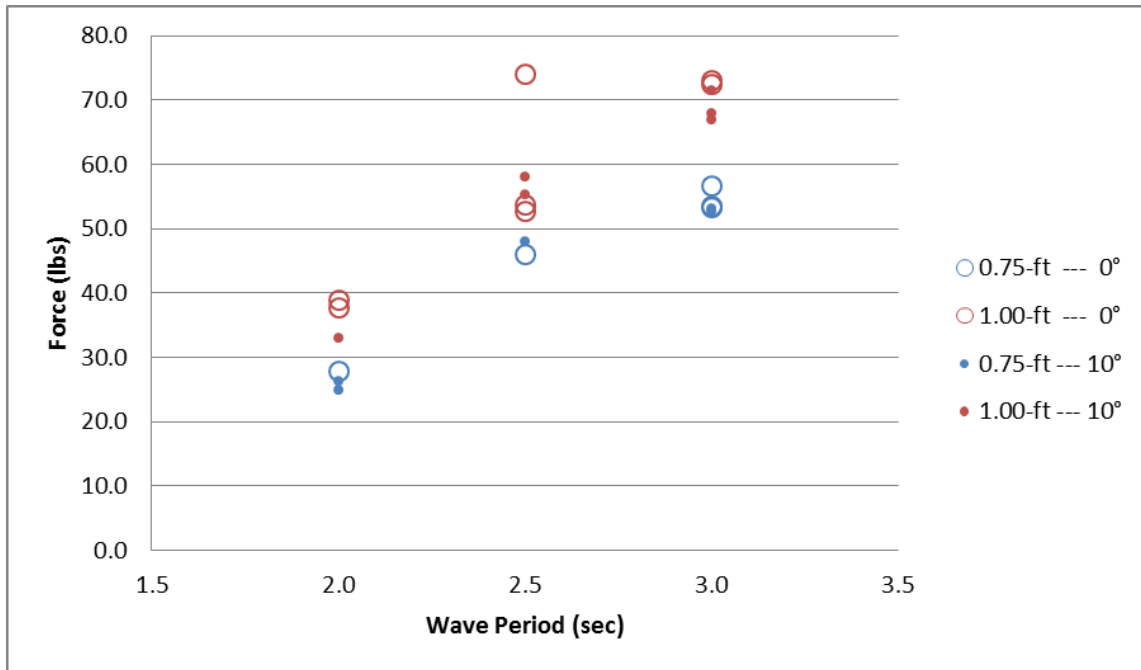


Figure 21. Irregular wave maximum total horizontal force.

Figure 22 shows the total minimum horizontal force as a function of the peak wave period and significant wave height. The force values are negative because the forces occur in the negative x-direction that is towards the wave maker. For the 2 sec peak period the model horizontal forces range between -27 and -40 lb. For 2.5 sec peak period, the model horizontal forces range between -34 and -41 lb, and the model horizontal forces for the 3 sec peak period are between -32 and -43 lb. The overall trend is for the negative horizontal force to increase slightly in magnitude with increasing peak wave period. Generally, the higher significant wave height produces larger forces, but the 2.5 sec peak period shows very little difference from the 3 sec period. In the case of the -10 degree direction, the 3 sec peak period shows the 0.75 ft significant wave height produces the largest model forces.

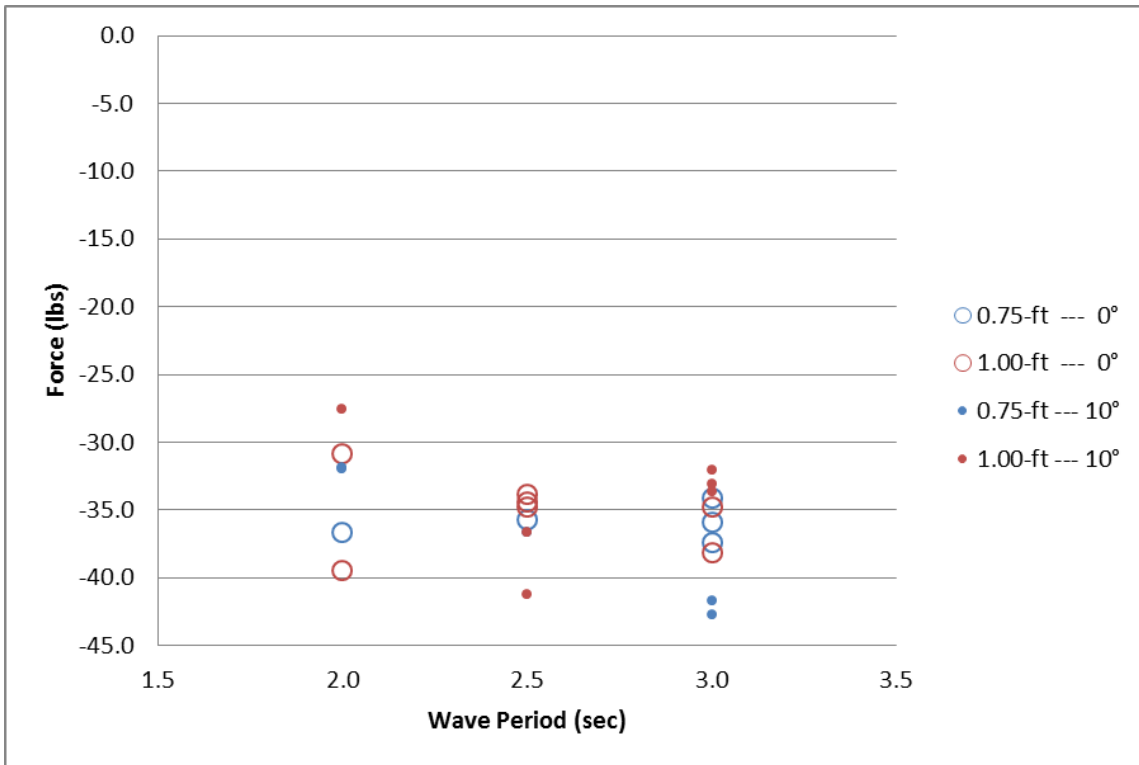


Figure 22. Irregular wave minimum total horizontal force.

The largest horizontal forces were measured in the direction of wave propagation toward the beach and increase nearly linearly with peak wave period. For the 2 sec peak wave period, the forces on the breakwater are approximately the same towards the beach and towards the wave maker. The 2.5 and 3.0 sec peak wave periods show the horizontal forces toward the beach are about 40% greater than toward the wave maker. The -10 degree direction of the waves shows only small differences in the forces. The forces generally increased with significant wave height by approximately 5 lb. As the wave passes through the breakwater, the force on the breakwater goes from a positive horizontal force to a negative horizontal force and thus the breakwater experiences an oscillating force due waves. This is important for the design of the mooring system that

must withstand an oscillating force. Some types of sands that are found offshore have a tendency to liquefy under cyclic loading; these sands require different anchors to mitigate the loss of holding capacity. To find out if this phenomena applies a sample of the sediment has to be taken into the laboratory to perform tests to determine the cyclic shear strength and modulus, pore generation pressure. These higher pore pressures cause the internal stresses of the soil to increase, decreasing the overall available shear stress for some soils and the strength reduction can be 20 to 30% (Moses and Rao 2007).

Vertical Irregular Wave Force Measurements

The total maximum vertical forces upward on the model 10 ft submerged rebar breakwater as a result of an 8 min duration JONSWAP wave spectra are illustrated in Figure 23. The model vertical forces range between 13 and 20 lb. The forces for the 2 sec and 3 sec peak period are grouped around 15 lb, while the 2.5 sec peak period shows a wider spread between 13 lb and 20 lb. The -10 degree directional waves generally show a slight increase in vertical force by 2 to 3 lb. The 1 ft significant wave height causes higher vertical forces than the 0.75 ft significant wave height by 2 to 4 lb. The total minimum vertical forces are illustrated in Figure 24. The forces are negative indicating the force is acting down or towards the wave basin floor. The downward vertical forces show a larger spread and range between -10 lb and -25 lb. The spread is larger for the 3 sec peak period than the 2 sec peak period waves. The average

downward force appears to be 5 lb larger than the vertical upward force. The 1 ft significant wave produces slightly larger downward forces than the forces produced with the 0.75 ft significant wave height. The -10 degree directional waves show slightly higher downward forces than the zero degree wave direction.

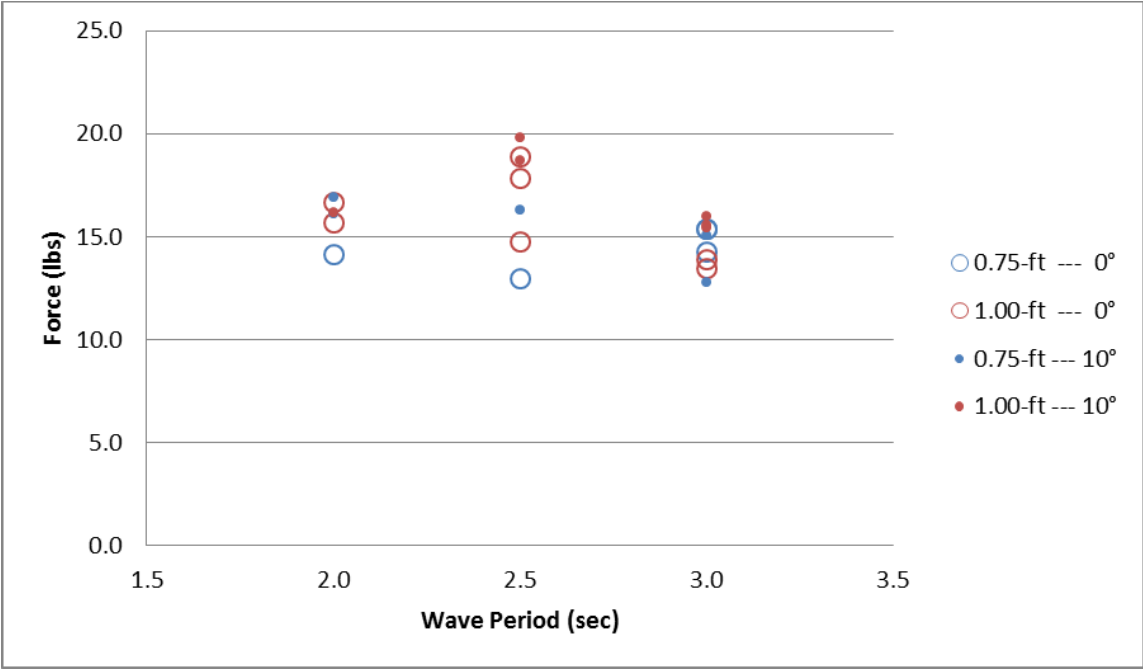


Figure 23. Irregular wave maximum total vertical force.

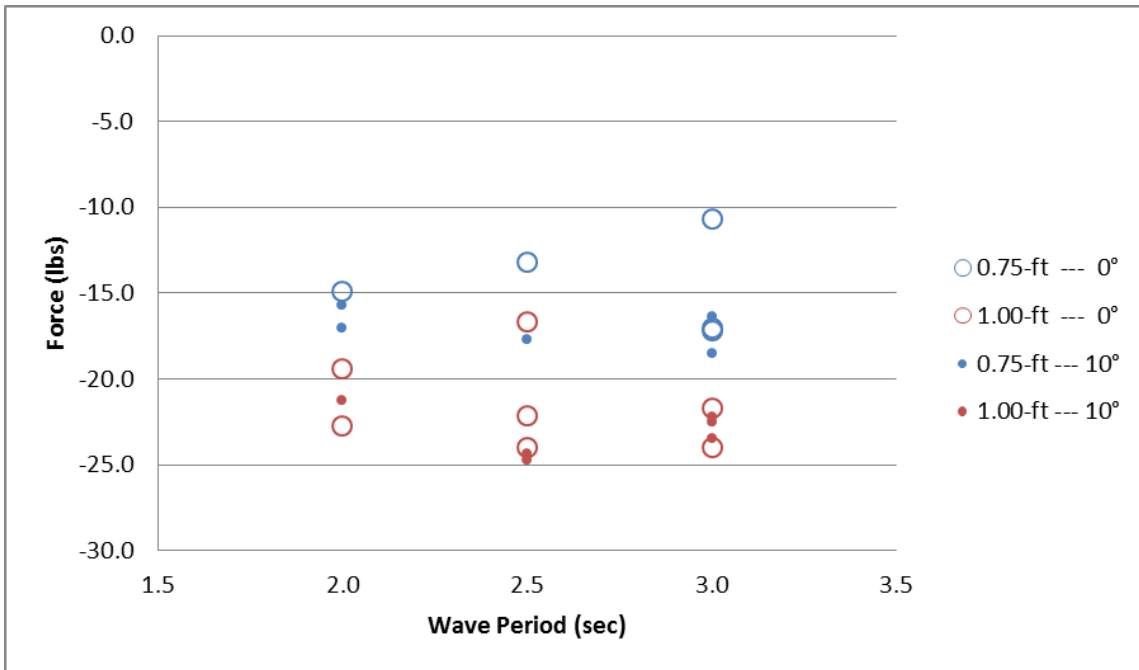


Figure 24. Irregular wave minimum total vertical force.

The positive (maximum) and negative (minimum) vertical forces on the front (wave maker) and rear (beach) of the 10 ft submerged breakwater are shown in Figure 25 and Figure 26, respectively. The measured forces and the coordinates of the attachment points can be used to determine the overturning moment. The positive (upward) forces on the beach side of the breakwater are larger than the upward forces acting on the wave maker side by a factor of 2 (e.g. 13 lb average rear and 6 lb average front). The spread is larger for the 2.5 and 3 sec peak wave period with values ranging from 5 lb to 17 lb. The downward forces shown in Figure 26 range from -7 lb to -24 lb and the spread for 2 sec peak period is from -7 lb to -15 lb while it is -7 to 24 lb for the 3.0 sec peak period. The average downward forces on the rear (beach) side are -10 lb and on the front (wave maker) side the average downward force is -20 lb.

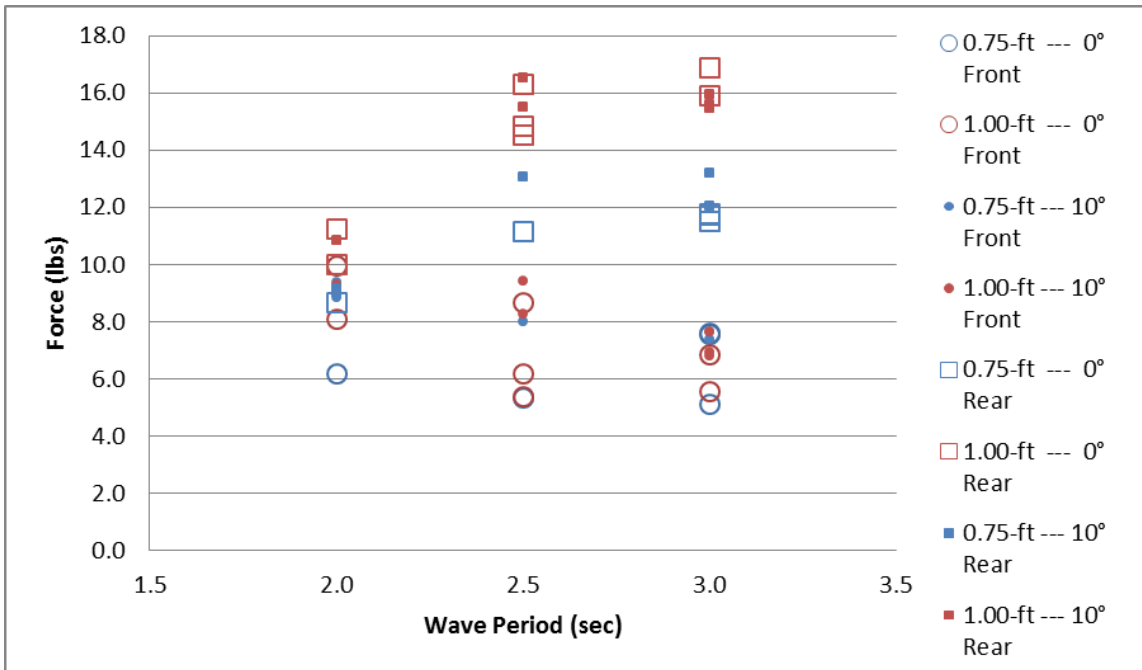


Figure 25. Irregular wave peak upward forces on the front and rear of the breakwater.

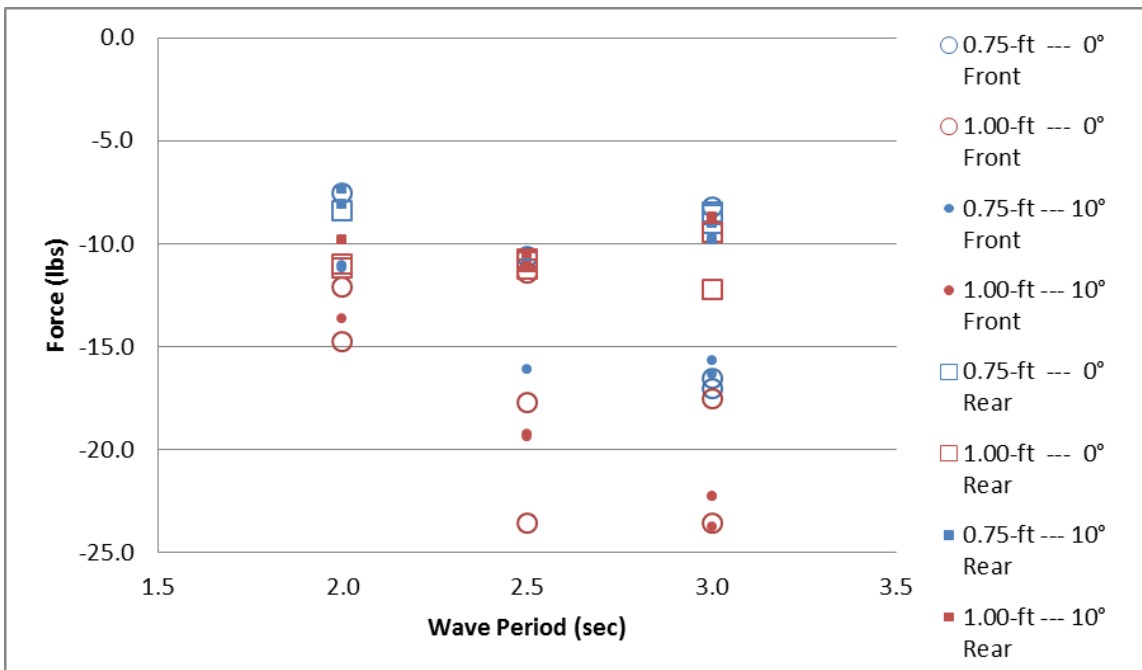


Figure 26. Irregular wave peak downward forces on the front and rear of the breakwater.

The positive horizontal force is plotted along with the wave elevation data for test 18 in Figure 27. Test number 18 was an 8 min duration JONSWAP spectra with the significant wave height of 1 ft and peak period of 3 sec. The wave direction is perpendicular to the 10 ft breakwater. The wave data were recorded from the incident wave gauge located one breakwater diameter from the front of the breakwater. Figure 27 shows the maximum wave elevation preceding the maximum horizontal force as expected. The maximum force and maximum wave elevation are coincident if the wave celerity is used to adjust for the separation distance between the wave gauge and the breakwater.

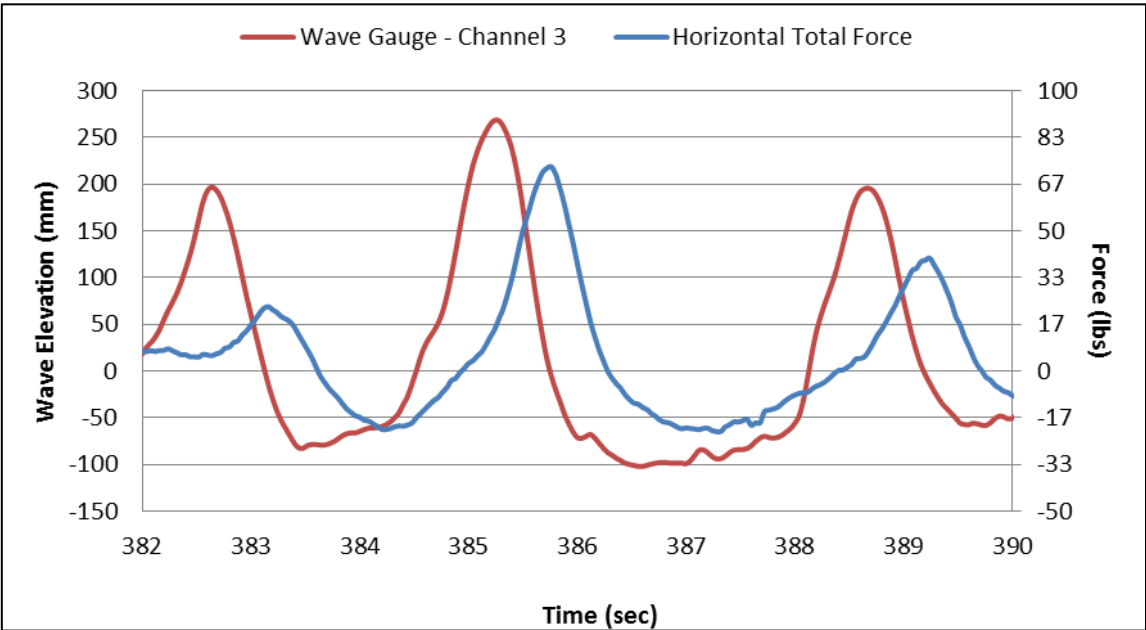


Figure 27. Horizontal total force superposed on wave elevation for test number 18.

Horizontal Regular Wave Force Measurements

The force measured with the horizontal force gauges was recorded by the data acquisition system at a sampling rate of 25 Hz. The wave maker generated the JONSWAP wave spectra for a significant wave height of 0.75 and 1.0 ft and peak wave periods of 2, 2.5, and 3 sec. The duration of each wave spectrum was 8 minutes and two directions (0 degree and -10 degree) were generated. The force, ADV and wave gauges were synchronized to start recording at the same time when the wave maker was actuated. The maximum forces generated by the wave orbital velocities were recorded, and the data file was searched to find the maximum force on each gauge and added together for the total maximum force. The force data used in this section for the plots is tabulated in Table 15 on page 91 in Appendix A.

The results for the total maximum horizontal force are illustrated in Figure 28. The lowest maximum horizontal forces occurred for the 2 sec peak period wave spectrum and ranged between 23 and 41 lb. The maximum horizontal forces increased almost linearly with increasing wave peak period. For the 3 sec period, the maximum horizontal forces ranged between 33 and 63 lb. The 1 ft wave height spectra resulted in higher forces than the 0.75 ft spectra as expected.

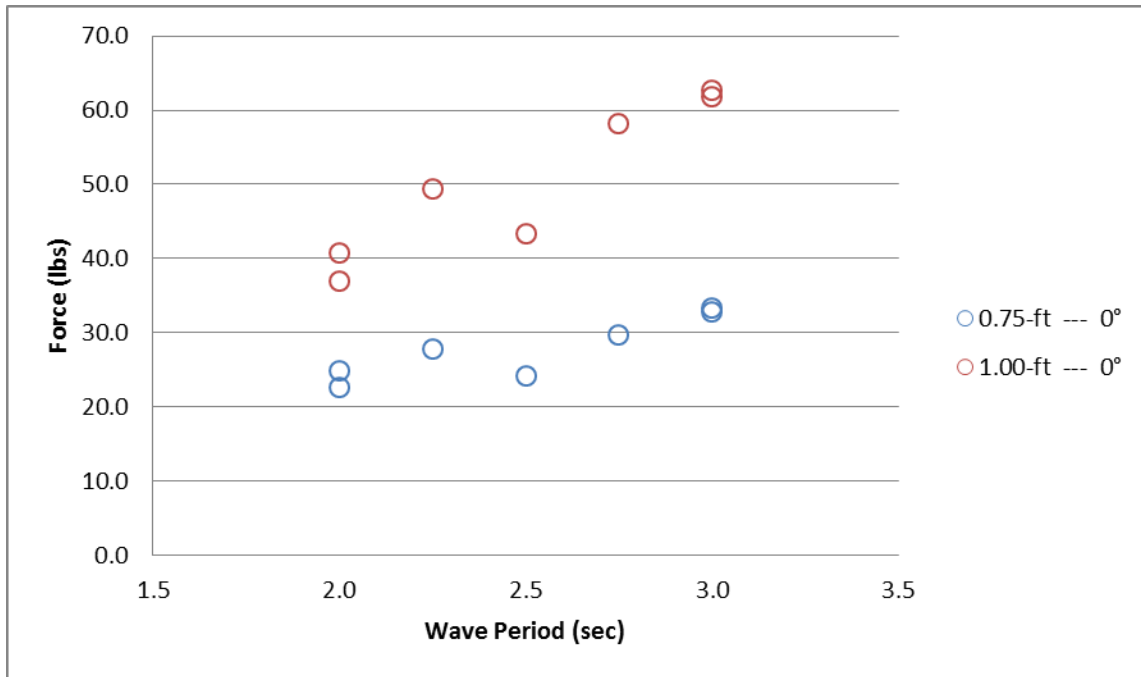


Figure 28. Regular wave maximum total horizontal force.

Figure 29 shows the total minimum horizontal force as a function of the wave period and wave height. The force values are negative because the forces occur in the negative x-direction that is towards the wave maker. For the 2 sec period the model horizontal forces range between -20 and -40 lb. For the model horizontal forces for the 3 sec peak period are between -23 and -44 lb. The overall trend is for the negative horizontal force to increase slightly in magnitude with increasing peak wave period. The higher wave height produces larger forces, however the minimum total force decreases slightly from 2 to 2.75 sec for both the 0.75 and 1.0 ft wave heights. The 3 sec wave period cases have the highest overall magnitude.

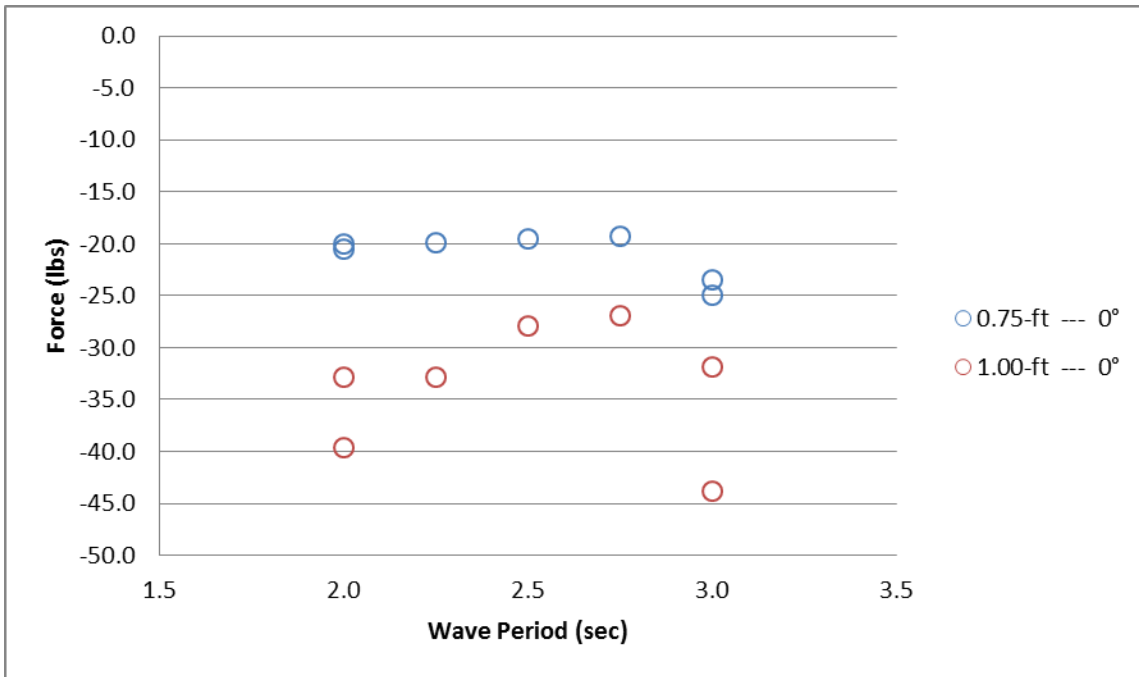


Figure 29. Regular wave minimum total horizontal force.

The largest horizontal forces were measured in the direction of wave propagation toward the beach and increase nearly linearly with peak wave period. For the 2 sec peak period, the forces on the breakwater are approximately the same towards the beach and towards the wave maker. The 3.0 sec periods show the horizontal forces toward the beach are about 50% greater than toward the wave maker. The horizontal forces towards the beach increased with significant wave height by approximately 15 lbs for the 2 sec period and the difference generally linearly increasing to 30 lbs for the 3 sec period case. As the wave passes through the breakwater, the force on the breakwater goes from a positive horizontal force to a negative horizontal force and thus the breakwater experiences an oscillating force due waves. This is important for the design of the mooring system that must withstand an oscillating force. Some types of sands that are found offshore have a

tendency to liquefy under cyclic loading; these sands require different anchors to mitigate the loss of holding capacity.

Vertical Regular Wave Force Measurements

The total maximum vertical forces upward on the model 10 ft submerged rebar breakwater as a result of a 3 min regular wave is illustrated in Figure 30. The model vertical forces range between 6 and 17 lb. The forces for the 2 sec period is grouped around 17 lb and 9 lb for the 1.0 ft and 0.75 ft wave heights respectively, while the 3.0 sec period has a lower magnitude between 11 lb and 6 lb for the 1.0 ft and 0.75 ft wave heights respectively. The 1 ft wave height causes higher vertical forces than the 0.75 ft wave height by 6 to 8 lb. The total minimum vertical forces are illustrated in Figure 31. The forces are negative indicating the force is acting down or towards the wave basin floor. The downward vertical forces show a range between -8 lb and -19 lb. The spread between the .075 ft and 1.0 ft waves is approximately the same for all of the wave periods. The average downward force appears to be 2 lb less in magnitude than the vertical upward force. The 1 ft significant wave produces larger uplift forces than the forces produced with the 0.75 ft significant wave height. However, similar to the maximum vertical forces, as the period of the wave increases the magnitude of the resultant force decreases.

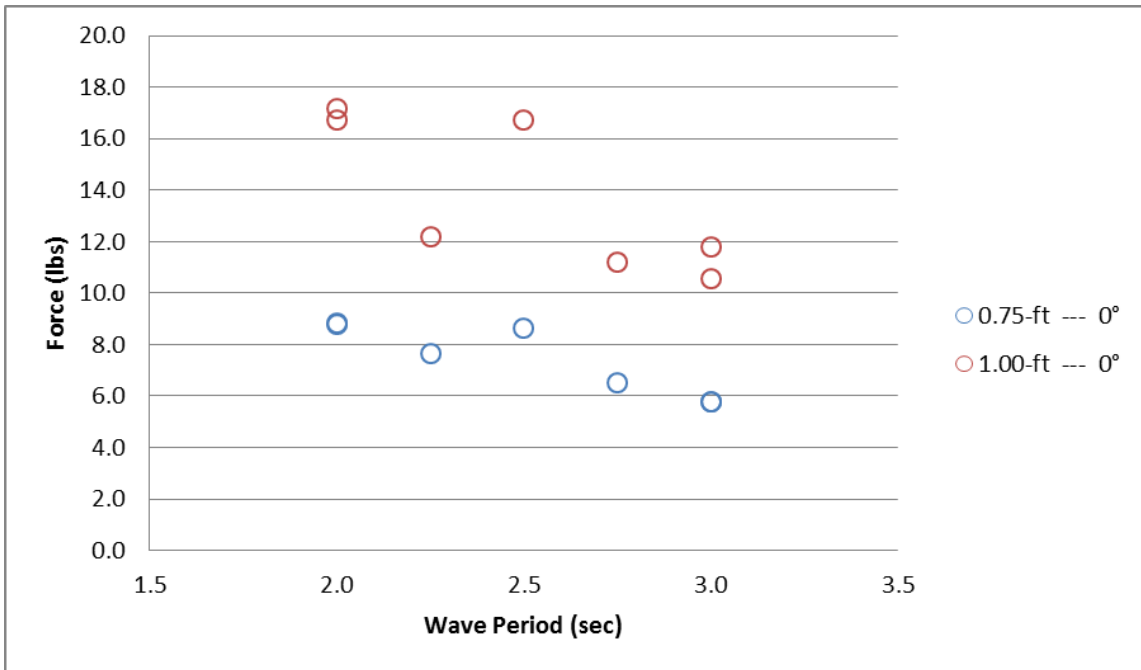


Figure 30. Regular wave maximum total vertical force.

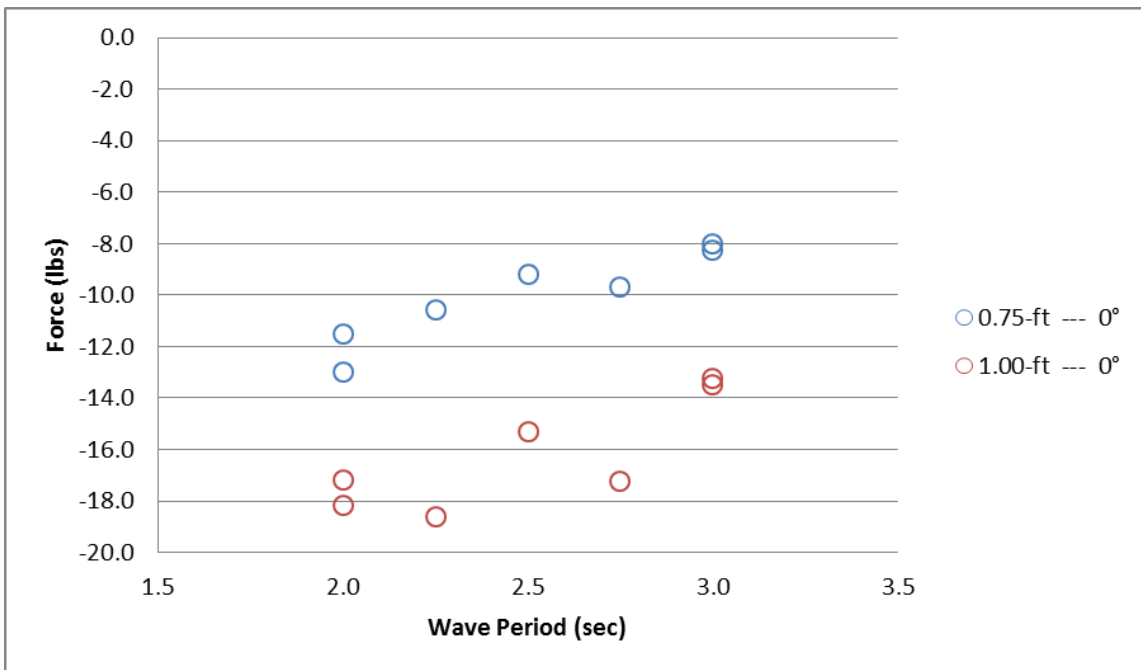


Figure 31. Regular wave minimum total vertical force.

The positive (maximum) and negative (minimum) vertical forces on the front (wave maker) and rear (beach) of the 10 ft submerged breakwater are shown in Figure 32 and Figure 33, respectively. The measured forces and the coordinates of the attachment points can be used to determine the overturning moment. The positive (upward) forces on the beach side of the breakwater are larger than the upward forces acting on the wave maker side by a factor of 1.5 to 2.7. The spread generally increases as the wave period increases. The downward forces shown in Figure 33 range from -4 lb to -19 lb and the spread for 2 sec period wave is from -5 lb to -14 lb while it is -5 to -19 lb for the 3.0 sec period wave. The average upward forces on the rear (beach) side are 10.2 lb and on the front (wave maker) side the average upward force is 5.3 lb.

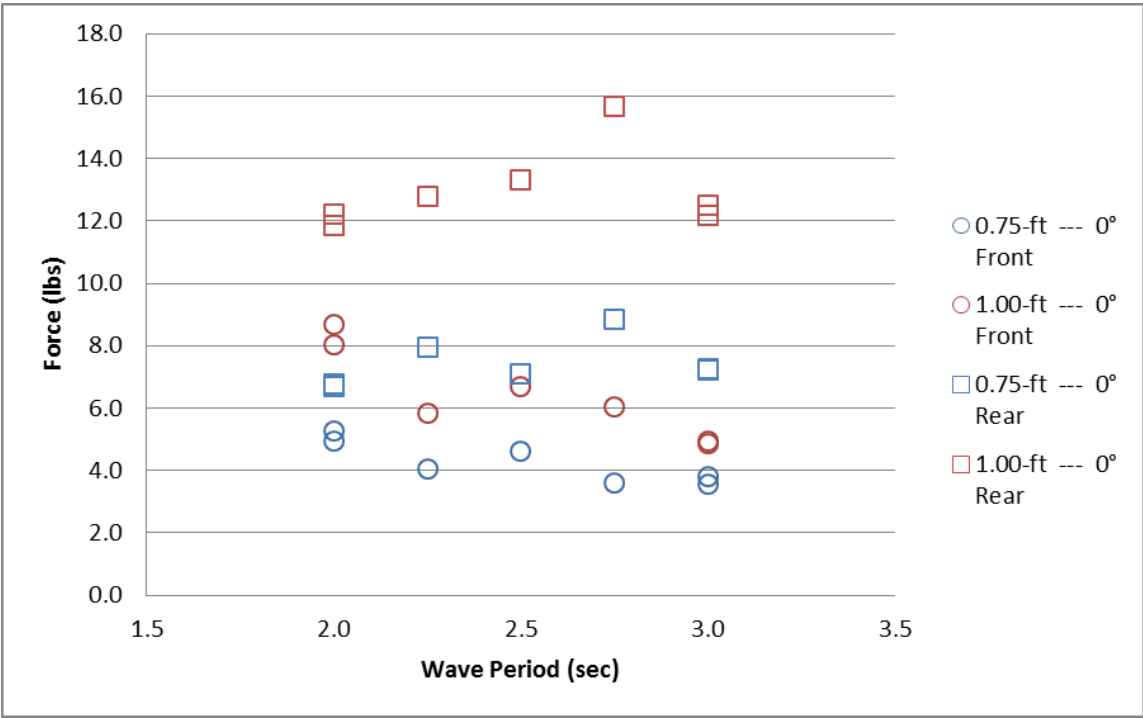


Figure 32. Regular wave peak upward forces on the front and rear of the breakwater.

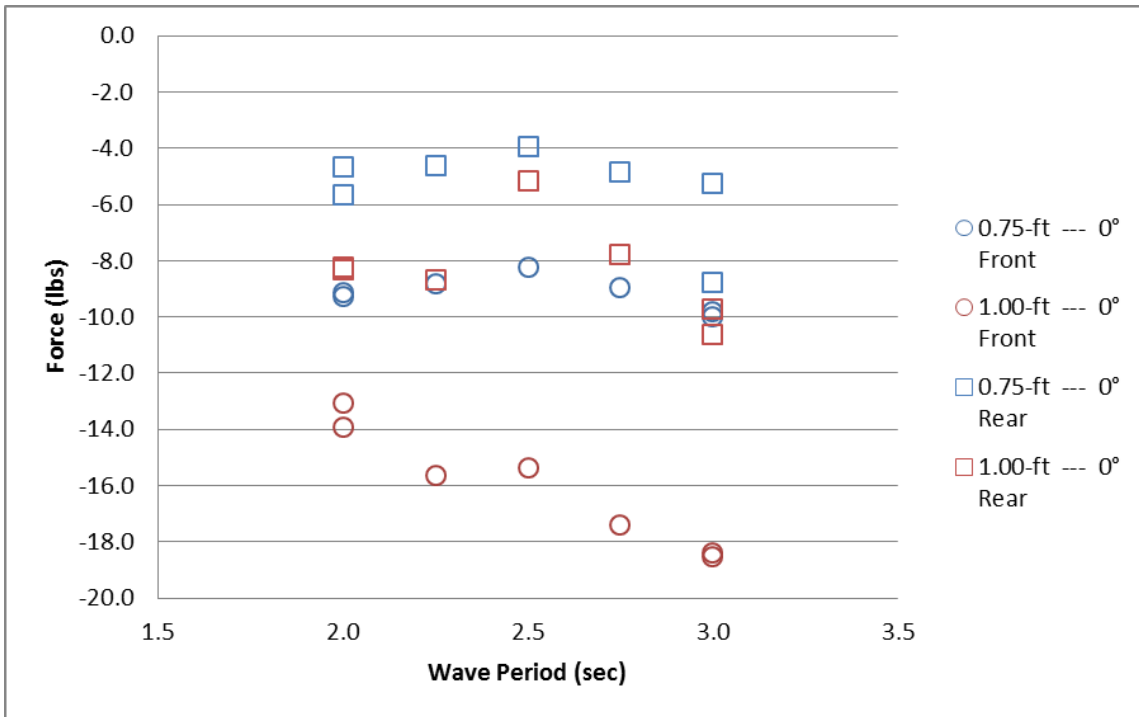


Figure 33. Regular wave peak downward forces on front and rear of the breakwater.

Wave Transmission and Reflection

Coefficient of Reflection

The total coefficients of wave reflection (C_{rt}) were derived from the data acquired by the first three wave gauges (WG01, WG02 and WG03). There were 12 tests with several repeats for wave spectra with 1 ft and 0.75 ft significant wave heights, wave peak periods of 2 s, 2.5 s, and 3 s, and wave directions of 0° and -10° for each configuration of no reef, 10 ft breakwater, and 40 ft breakwater. The 40 ft breakwater case did not

contain any force data and was used for wave transmission and reflection analysis. Therefore it is not included in any other part of this thesis. These values were calculated as part of the Texas Land Grant Office model test report (Randall et al 2013). The breakwater was referred to as a reef in the report.

The percentage relationships of these reflection coefficients for 0° and -10° cases are shown in Figure 34 and Figure 35, respectively. For these two bar charts, the color blue, red and green represents irregular waves with peak periods of 2.0 s, 2.5 s, and 3.0 s, respectively. The orange line with a square marker represents the mean value of the reflection coefficients.

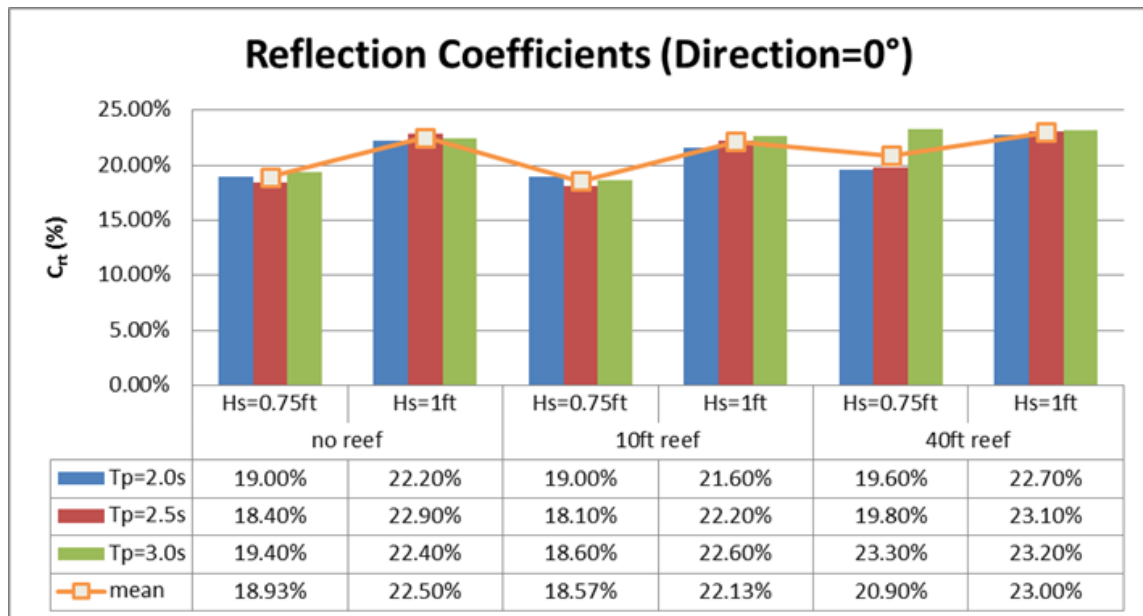


Figure 34. Total coefficient of reflection (C_{rt}) of 0° wave direction (Randall et al 2013).

Based on the data plotted in Figure 34 for the 0° wave direction, the mean values indicate that the coefficients of reflection for 1 ft significant waves are higher than that of 0.75 ft significant wave height waves for the same reef conditions. The reflection coefficient values are approximately 19% and 22.5% respectively, and the difference is 3.5%. The 40 ft reef has a slightly higher mean value for the coefficient of reflection than that of 10 ft reef, but the differences between them are small (<2%). For -10° directional waves, the mean values of coefficient of reflection in Figure 35 show that the reflection coefficients for the 1ft significant waves are approximately 4% higher than that for the 0.75 ft significant waves for each reef condition.

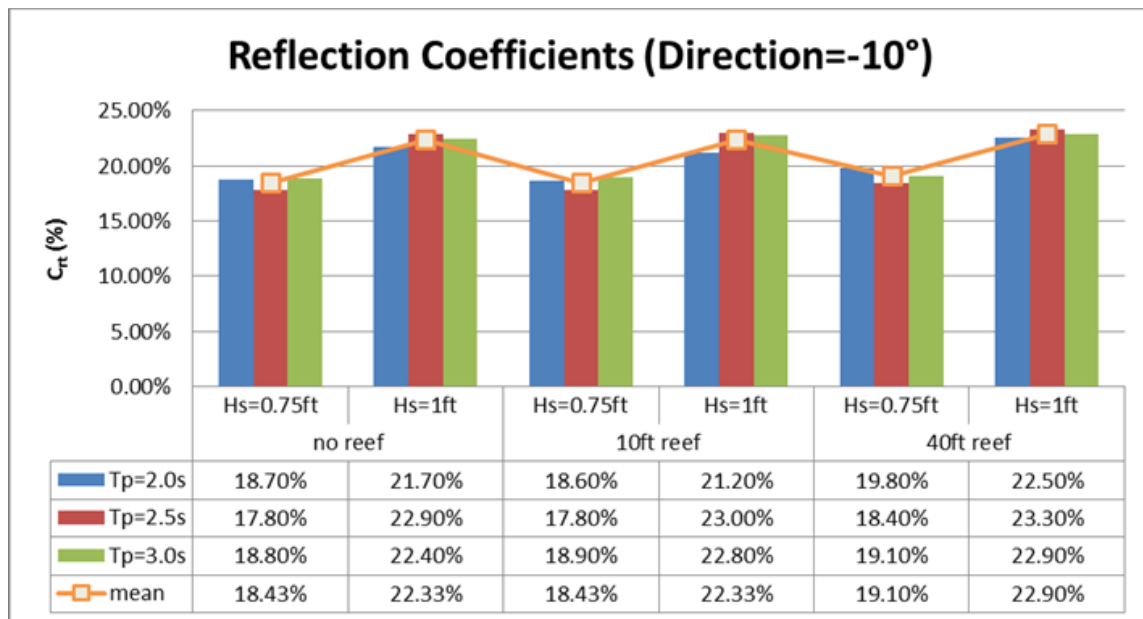


Figure 35. Total coefficient of reflection of -10° significant waves (Randall et al 2013).

Removing the reflection of the beach from the results the reflection of the 40 ft breakwater only becomes only 1% on average. This is show in Figure 36. These low

reflections are consistent with the force results. The low forces show that there is little energy being imparted on the breakwater from the waves. Therefore there is only a small amount of energy that can be reflected. If the reflection was higher the force would be much greater.

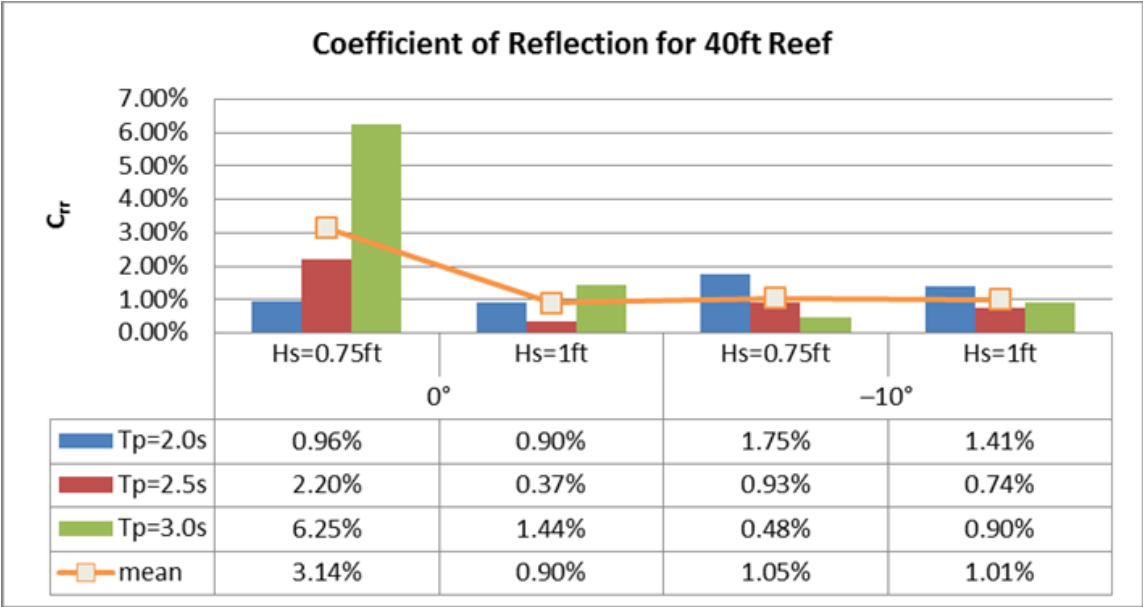


Figure 36. Coefficient of reflection for the model reef only (Randall et al 2013).

Coefficient of Transmission

Coefficients of transmission (C_{t1}) are evaluated by dividing the significant wave height measured by the wave gauges positioned in front and behind the reef, namely the significant wave height measured with WG05 divided by the WG04 measurement. These coefficients of transmission are illustrated in Figure 37 and Figure 38 for the 0°

wave direction and -10° wave direction, respectively. For the 40 ft reef, one additional wave gauge (WG06) was used for computing a second wave transmission coefficient. The second coefficient of transmission was determined by dividing the significant wave height from WG06 by WG04, which is denoted as C_{t2} . For the 0° wave direction, Figure 37 shows the coefficients of transmission (C_{t1}) are approximately 96%. For the -10° wave, Figure 38 shows the coefficients of transmission are generally near 96% for waves with periods of 2.5 sec and 3.0 sec. These high transmission coefficients show the majority of the energy is passing through the breakwater. If the value was close to the 0.7 that is preferred the forces would be much higher and therefore need higher capacity anchors. The shoreline would also be protected. At the levels of transmission for the model the breakwater would not help the beach retain sand.

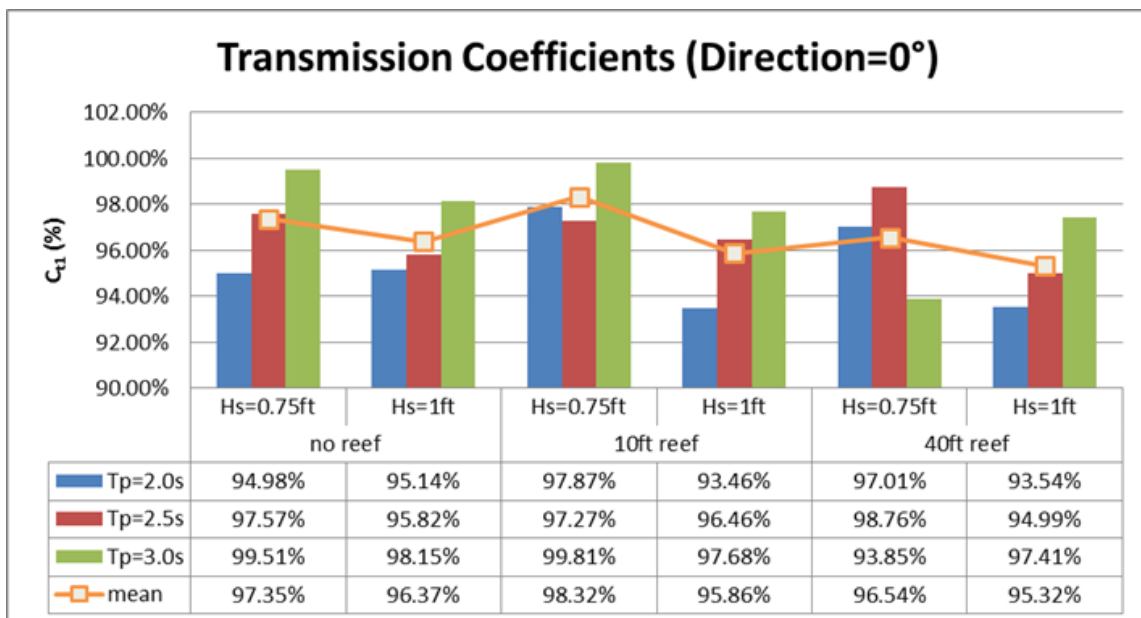


Figure 37. Coefficient of transmission of 0° waves (Randall et al 2013).

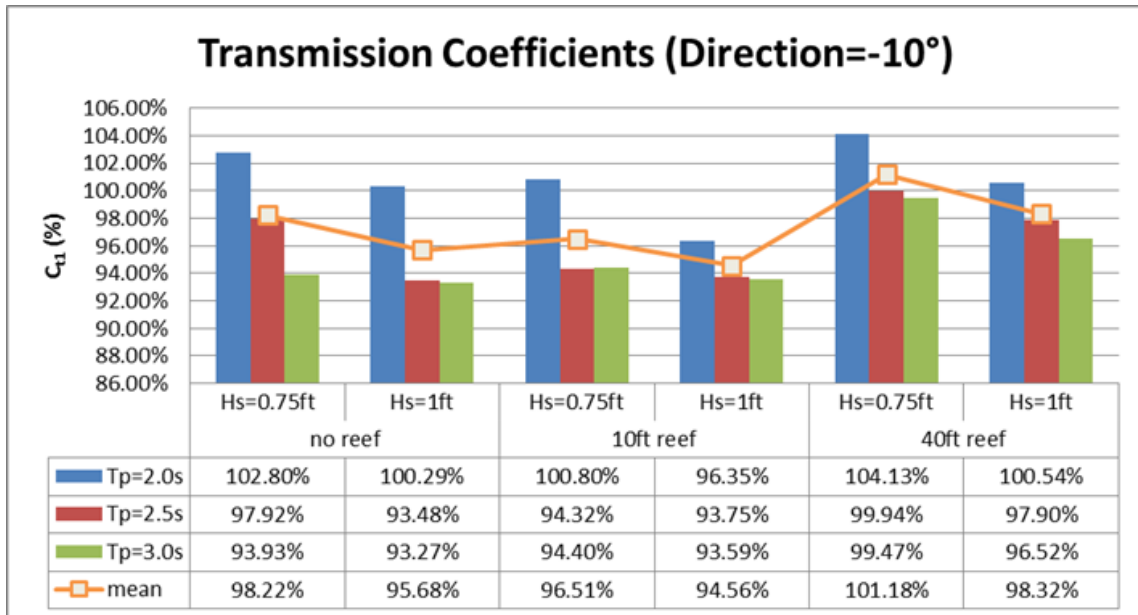


Figure 38. Coefficient of transmission of -10° waves.

Uncertainty Analysis of Model Test Data Collection

As with any instrumentation and data collection there is some error. This section goes over the level of error for the different types of instrumentation used to collect the wave heights and forces. Using Holman's (1989) method the total uncertainty of the measurements during the data acquisition can be quantified. Holman's equation:

$$w_R = \left[\left(\frac{\partial R}{\partial x_1} w_1 \right)^2 + \left(\frac{\partial R}{\partial x_2} w_2 \right)^2 + \dots + \left(\frac{\partial R}{\partial x_n} w_n \right)^2 \right]^{1/2} \quad (17)$$

where w_R is the total uncertainty in the result, $w_1, w_2 \dots w_n$ are the uncertainties in each of the independent variables, and R is a function of the independent variables to obtain the results. The w_n values for each type of gauge used during the experiments are listed on the next page in Table 8. The ADVs do not have any other effects therefore the uncertainty of the measurement (w_R) is equal to the w_n value listed in Table 8 above, which is ± 1.0 cm/s and ± 0.5 cm/s for the two different types of ADVs. The force gauge calibration was conducted using ~ 50 lb lead bricks that had been weighed. However during the recoding of the weights when creating the calibration curves the decimals were dropped. Therefore the weights for calibration had an error ($w_{weights}$) of ± 0.5 lb. This error also must be included in the uncertainty analysis. When measuring the voltage to create the calibration curve a multimeter was used, the error of the voltage reading $\pm 0.5\%$ FSO.

Table 8. Manufacturers reported accuracy of instruments used during testing.

Instrument or Equipment Name	Accuracy (w_n)
Nortek Vectrino acoustic Doppler current meters (3D)	± 0.5 cm/s
SonTek acoustic Doppler current meter (2D)	± 1.0 cm/s
Haynes Laboratory capacitance wave gauges	± 3.3 mm
Omega submersible load cell (5000 lb)	$\pm 0.2\%$ FSO
Omega submersible load cell (1000 lb)	$\pm 0.2\%$ FSO
Omega load cell (500 lb)	$\pm 0.03\%$ FSO
National Instruments 16 channel acquisition system using Lab View	± 3.23 mV
2310 Signal Processor – Excitation (Noise + Accuracy)	± 0.64 mV
2310 Signal Processor – Gain (Noise)	$\pm 0.5\%$

For the 1000 and 5000 lb load cells this is equal to $\pm 0.2\%$ full scale operating (FSO) value which is 2 lb and 10 lb respectively. For the 500 lb load cell the uncertainty is $\pm 0.03\%$ FSO which equal to 0.15 lb. For the combination of load cells which was used to find the total horizontal force and the front, rear and total vertical forces, the uncertainty from each of the gauges must be included.

There are two sources of uncertainty, one during the creation of the calibration curve and one during data acquisition. The total uncertainty is a combination of these two. The terms including voltage must be converted to a force to be able to get a single uncertainty for the force measurement. This is done by finding $\frac{\partial V}{\partial F}$ of the calibration curve equation. The uncertainty calculations for the force gauges are shown in Table 9.

$$w_{V_{tot}} = \left[\left(\frac{\partial}{\partial V} w_{SP_Ex} \right)^2 + \left(\frac{\partial Gain}{\partial V} w_{SP_Gain} \right)^2 + \left(\frac{\partial}{\partial V} w_{SP_Ex} \right)^2 + \left(\frac{\partial}{\partial V} w_{multimeter} \right)^2 \right]_{Cal}^{1/2} + \left[\left(\frac{\partial}{\partial V} w_{SP_Ex} \right)^2 + \left(\frac{\partial Gain}{\partial V} w_{SP_Gain} \right)^2 + \left(\frac{\partial}{\partial V} w_{SP_Ex} \right)^2 + \left(\frac{\partial}{\partial V} w_{NI_DAQ} \right)^2 \right]_{DAQ}^{1/2} \quad (18)$$

$$w_{F_{tot}} = \left[\left(\frac{\partial}{\partial V} w_{F_Cali} \right)^2 + \left(\frac{\partial}{\partial Force} w_{FG} \right)^2 \right]_{Cal}^{1/2} + \left[\left(\frac{\partial}{\partial Force} w_{FG} \right)^2 \right]_{DAQ}^{1/2} \quad (19)$$

$$w_{force\ gauge\ total} = \left[\left(\frac{\partial V}{\partial F} w_{V_{tot}} \right)^2 + \left(\frac{\partial}{\partial Force} w_{F_{tot}} \right)^2 \right]^{1/2} \quad (20)$$

Where $\frac{\partial Gain}{\partial V} = (1\mu V * Gain)$, $\frac{\partial V}{\partial F} = (force\ gauge\ calibration\ curve\ slope)$, and $\frac{\partial Height}{\partial V} = (wave\ gauge\ calibration\ curve\ slope)$. The minimum and maximum values are based on the lowest and highest slopes of all the calibration curves calculated during testing. The wave gauges are calculated using the same method, and the results are tabulated in Table 10.

$$W_{wave\ gauges\ total} = \left[\left(\frac{\partial Height}{\partial V} w_{WG_V} \right)^2 + \left(\frac{\partial}{\partial Height} w_{WG} \right)^2 \right]_{Cal}^{1/2} + \left[\left(\frac{\partial Height}{\partial V} w_{WG_V} \right)^2 + \left(\frac{\partial}{\partial Height} w_{WG} \right)^2 \right]_{DAQ}^{1/2} \quad (21)$$

Table 9. Uncertainty of force gauge measurements.

Total Voltage W Calculations	Calibration						
	Signal Processor - Excitation		Signal Processor - Gain			Multimeter	
	d/dVolt	W (%)	Gain	dGain/dVolt	W (%)	d/dVolt	W (%)
1k lb (Force)	1.000	0.064%	320	0.00032	1.00%	1.000	0.50%
5k lb (Force)	1.000	0.064%	610	0.00061	1.00%	1.000	0.50%
500 lb min (Force)	1.000	0.064%	300	0.00030	1.00%	1.000	0.50%
500 lb max (Force)	1.000	0.064%	300	0.00030	1.00%	1.000	0.50%

Table 9 Continued

Total Voltage W Calculations	Data Acquisition						
	Signal Processor - Excitation		Signal Processor - Gain			NI DAQ	
	d/dVolt	W (%)	Gain	d/dVolt	W (%)	d/dVolt	W (%)
1k lb (Force)	1.000	0.064%	320	0.00032	1.00%	1.000	0.323%
5k lb (Force)	1.000	0.064%	610	0.00061	1.00%	1.000	0.323%
500 lb min (Force)	1.000	0.064%	300	0.00030	1.00%	1.000	0.323%
500 lb max (Force)	1.000	0.064%	300	0.00030	1.00%	1.000	0.323%

Total Force W Calculations	Calibration				Data Acquisition	
	Calibration Weight Error		Force Gauge Error		Force Gauge Error	
	d/dVolt	W (lb)	d/dForce (FSO - lb)	W (%)	d/dForce (FSO - lb)	W (%)
1k lb (Force)	1.000	0.500	1000	0.20%	1000	0.20%
5k lb (Force)	1.000	0.500	5000	0.20%	5000	0.20%
500 lb min (Force)	1.000	0.500	500	0.03%	500	0.03%
500 lb max (Force)	1.000	0.500	500	0.03%	500	0.03%

Total Uncertainty of Force Gauge Measurements	Total Voltage		Total Force		Total Force Uncertainty lb
	dVolt/dForce	W _{voltage} (V)	d/dForce	W _{force} (lb)	
1k lb (Force)	99.96	0.00602	1.000	2.872	2.935
5k lb (Force)	266.38	0.00602	1.000	14.151	14.242
500 lb min (Force)	54.86	0.00602	1.000	0.543	0.636
500 lb max (Force)	57.40	0.00602	1.000	0.543	0.644

Total Uncertainty of Multiple Force Gauges	Total Horizontal Force (lb)	Vertical front/rear Force (lb)	Total Vertical Force (lb)
Minimum	14.541	0.899	1.271
Maximum		0.910	1.288

Table 10. Uncertainty of wave gauge measurements.

Total Wave Gauge Height W Calculations	Calibration				Data Acquisition			
	NI DAQ		Wave Gauge		NI DAQ		Wave Gauge	
	$\frac{\partial Height}{\partial V}$	W (V)	$\frac{\partial}{\partial Height}$	W (mm)	$\frac{\partial Height}{\partial V}$	W (V)	$\frac{\partial}{\partial Height}$	W (mm)
Minimum	199.433	.00323	1.000	3.300	199.433	.00323	1.000	3.300
Maximum	277.470	.00323	1.000	3.300	277.470	.00323	1.000	3.300

Total Wave Gauge Uncertainty	
in	mm
0.187	4.755
0.190	4.836

The total horizontal force manufactures based uncertainty is equal to

$$w_R = [(W_{1k FG total})^2 + (W_{5k FG total})^2]^{1/2} \gg w_R = \pm 14.5 lb \quad (22)$$

For the total front or back vertical force manufactures based uncertainty is equal to

$$w_R = [2 * (W_{500 lb FG total min})^2]^{1/2} \gg \begin{matrix} w_{FG min} = \pm 0.90 lb \\ w_{FG max} = \pm 0.91 lb \end{matrix} \quad (23)$$

For the total vertical force manufactures based uncertainty is equal to

$$w_R = [4 * (W_{500 lb FG total max})^2]^{1/2} \gg \begin{matrix} w_{FG min} = \pm 1.27 lb \\ w_{FG max} = \pm 1.29 lb \end{matrix} \quad (24)$$

Looking at the voltage from a known applied load vs the expected value from the calibration curve for a particular voltage also gives an indication of the accuracy of the gauges as well as the calibration. The vertical load cells (500 lb force gauge) have a larger than expected error for this test, a range of -3.0 lb to +1.7 lb vs the ± 0.64 lb that

was calculated. The 1000 lb load cell had a greater error than expected, -6.0 lb to +4.0 lb vs ± 3.0 lb that was calculated. The 5,000 lb load cell performed better than anticipated with the range of error during calibration being -3.8 lb to +3.2 lb vs the ± 14.2 that was calculated. Table 11 below details the minimum and maximum of the errors of the force measurement based on the calibration curve minus the actual force applied to the load cell.

Table 11. Comparison of minimum and maximum error of calibrated force with actual value for a set voltage.

	1k Force (lb)	5k Force (lb)	500 Force (lb)	500 Force (lb)	500 Force (lb)	500 Force (lb)
Minimum	-6.01	-3.76	-0.58	-1.36	-3.02	-1.44
Maximum	3.95	3.20	1.12	1.16	1.69	0.84

DISCUSSION OF RESULTS

Comparison of Theoretical and Experimentally Measured Forces on Model Submerged Breakwater

The forcing on the submerged breakwater was calculated using wave theory and the drag law, as well as performing laboratory model tests. The purpose of the laboratory model tests was to conduct the experiments to determine the vertical and horizontal forces due to waves on the breakwater. The theoretical calculations were used to size the instrumentation needed and to verify the model force results by showing agreement of the order of the theoretical and model results. Also by having the ability to calculate the expected loads the breakwater which allows for correct sizing of the breakwater before the design is finalized. This reduces costs and wasted time, by reducing the probability of inadequate or over designed breakwaters. When comparing the theoretical forces to the measured forces the -10 degree case has the same values as the 0 degree case for the same wave height and period. This is due to the way the model was broken apart to calculate the areas and forces. The percent difference between the model and theory was found by taking the difference of the average model force and the theoretical force then dividing by the theoretical force.

The minimum horizontal forces generated by the 0.75 to 1.0 ft irregular and regular waves, as well as the theoretical values are shown in Figure 39. The second order

theoretical result for the 1.0 ft wave height under predicts the minimum wave force by a difference of 30% for the 2.0 second wave and by 58% for the 3.0 second wave. The Airy wave theory results better predict the minimum total horizontal forces. The Airy wave theory for the 1.0 ft wave height under predicted the minimum model wave force by a difference of 19% for the 2.0 second wave and over predicted by 19% for the 2.5 and 3.0 second wave. This is more conservative which is preferable when calculating the forces on the structure.

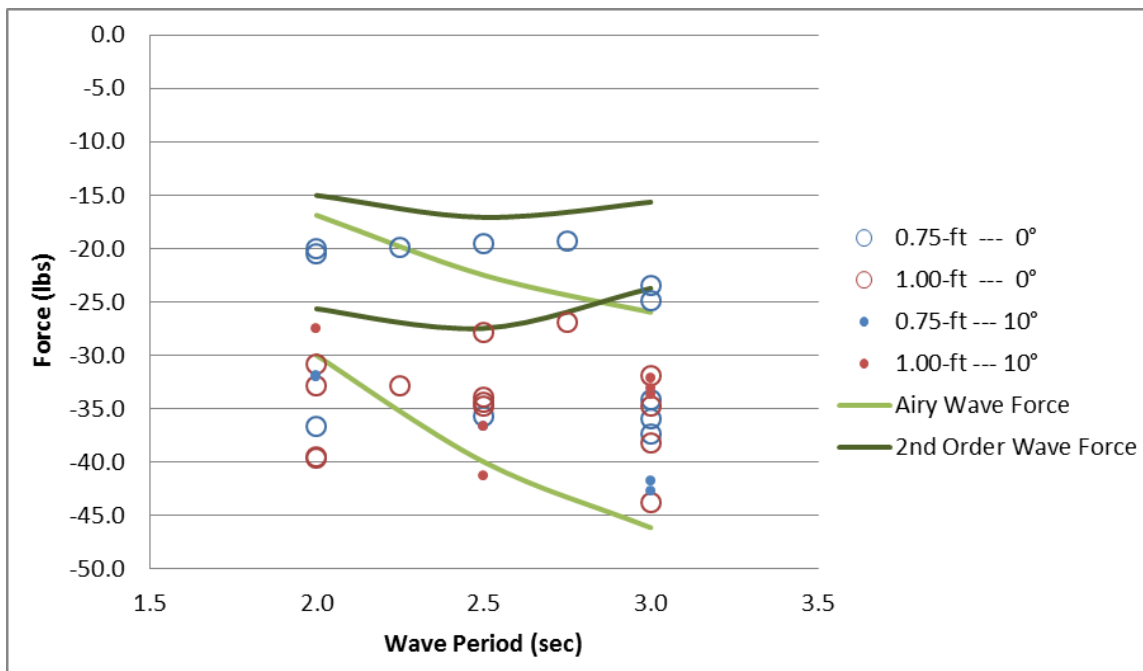


Figure 39. Comparison of minimum total horizontal force model test values with theoretical values.

For the maximum total horizontal forces, shown in Figure 40, the Airy wave theory under predicts the forces on the submersible breakwater. The results do follow the same trend as the model test data, for the 0.75 ft wave the Airy wave theory under predicts the

forces by a difference of 50% for the 2.0 sec wave and 77% for the 3.0 second wave. However these differences are inflated due to the irregular wave data, for the regular wave the Airy wave theory under predicts the differences in the force by approximately 25% for 2.0 sec and 3.0 sec waves. For the 1.0 ft max horizontal wave for case the Airy wave theoretical value under predicts the forces by a difference of 29% for the 2.0 sec wave and 47% for the 3.0 second wave. Using the 2nd order Stokes wave theory the differences of the resultant forces and theory are under predicted by 11% for the 1.0 ft 2.0 second wave and over predicted by 14% for the 3.0 second wave. This could be due to either the theory not properly representing the physics due to over simplification, or due to the physics of the wave basin not being the same as real world conditions. One difference between the basin and real world is the ratio of water depth to maximum wave height without breaking. In the basin the ratio of water depth to breaking wave height is at most 0.5, whereas in the field ratios of H/d is normally 0.78 (Dean and Dalrymple 1991) and is up to 0.9 (Sorensen 2006). The higher the ratio the larger the wave before breaking and dissipating energy, this leads to higher orbital velocities leading to higher forces on the submerged breakwater. These differences could also be due to the piling up of waves over the breakwater due to the irregular seas without breaking causing higher velocities, or a wave breaking right on the structure.

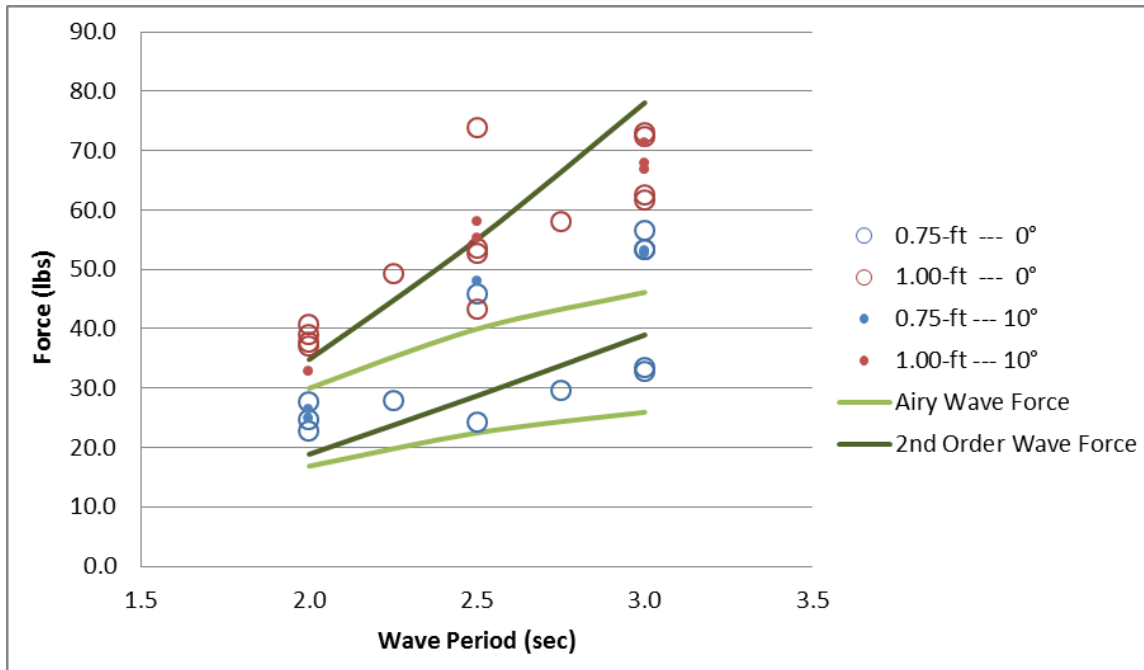


Figure 40. Comparison of maximum total horizontal force model test values with theoretical forces.

Both the minimum and maximum vertical forces obtained from the model testing do not line up with either Airy or 2nd order Stokes wave theory. Figure 41 shows the trend of the data to the theoretical is similar, however the values are under estimated. Airy wave theory does a little better job of estimating the forces on the structure but on average it still under predicts the values by a difference ranging between 40 and 60% for the 0.75 ft and ranging between 25 and 35% for the 1.0 ft wave cases. This greater downward force could be due to the modeling of the breakwater. The horizontal restraints were at the bottom of the breakwater therefore the horizontal force causes an overturning moment which increases the downward force on the back side of the breakwater from the current. With the non-linear shallow water waves the horizontal velocity is greater while the z velocity is approximately the same magnitude vs a deep water wave. This allows for the

uplift/downward force and overturning moment to coincide causing greater vertical forces than just forces due to the flow in the vertical direction.

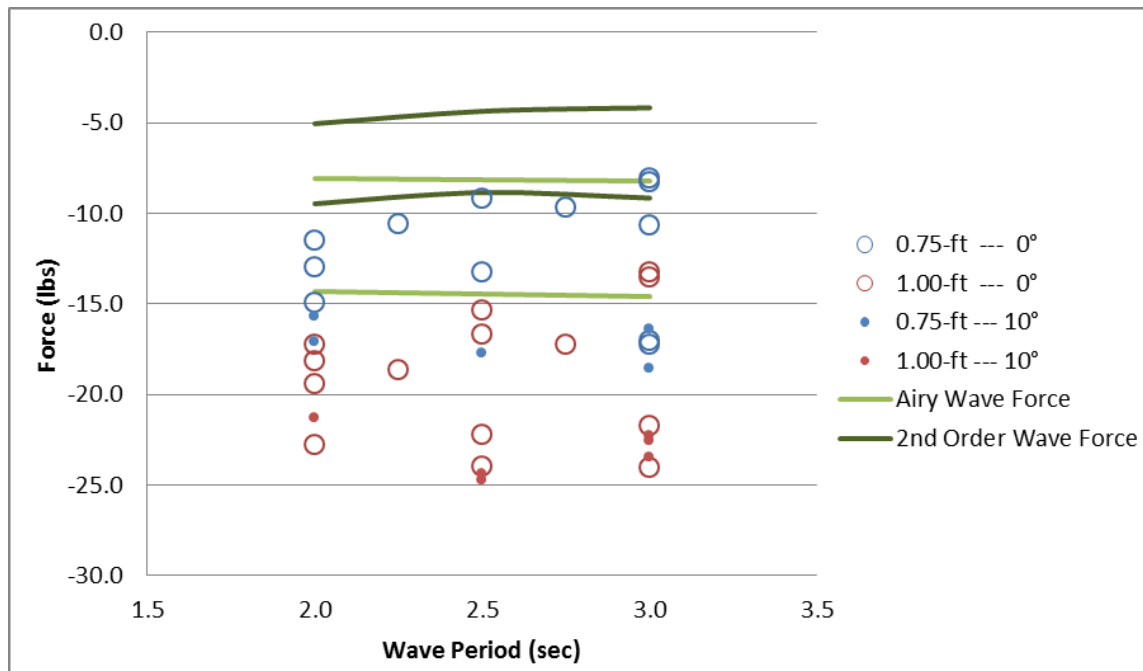


Figure 41. Comparison of minimum total vertical force model test values vs theoretical values.

The maximum vertical force results shown in Figure 42 have several issues. The trend of the 1.0 ft data from the model test does not match either the Airy or 2nd order wave theory. From the model test data the 2.5 second wave had the highest average load for both the 0.75 ft and 1.0 ft waves. However the theoretical data results had the 2.5 second wave with lower magnitude forces. The Airy wave theory is approximately the same as the regular wave results, a difference ranging from under predicting by 10% to over predicting by 30%, and under predicts the irregular wave results by a difference of 70%.

The vertical forces would also be increased due to the horizontal force causing an overturning moment increasing the vertical force.

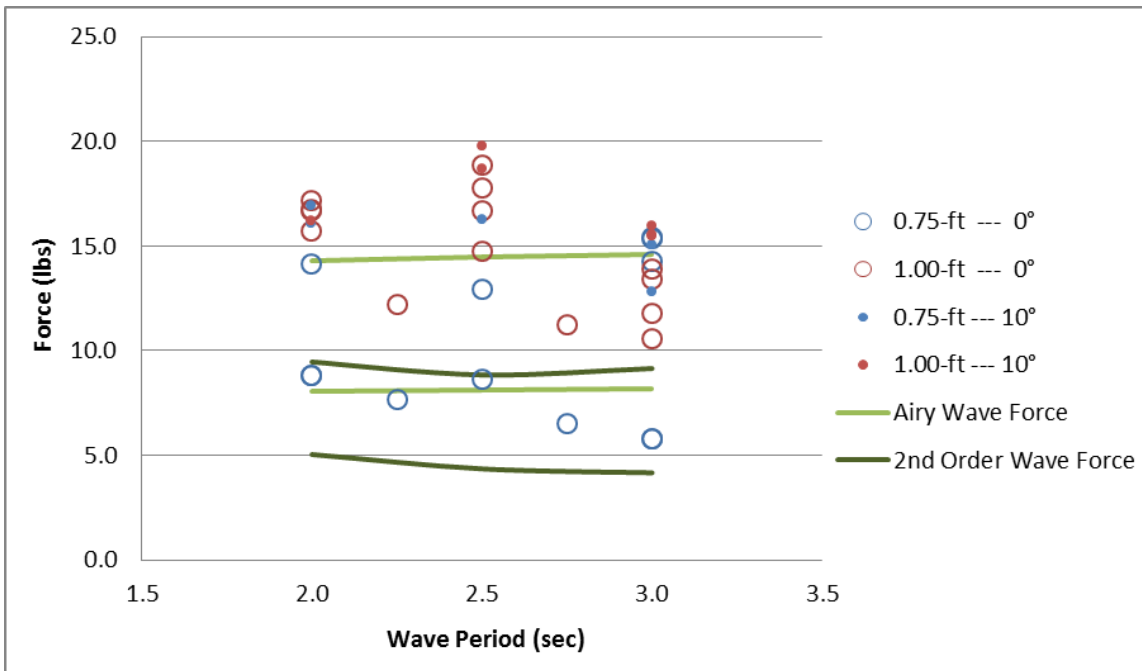


Figure 42. Comparison of maximum total vertical force model test values vs theoretical values.

Prototype Scale Results

To get the expected forces on the prototype the forces must be scaled using Froude scaling. The scale of the model that was tested to the prototype was 4:1. Using Froude scaling the ratio to obtain the prototype from the model is:

$$F_p = F_m * Scale^3 \quad (25)$$

Therefore the ratio of the prototype forces to the model forces is 4^3 which is equal to 64. Table 12 below details the highest magnitude force for each metocean criteria. All periods are included in the scope of each wave. The overall maximum expected load at the anchor without any factor of safety is 38 lb in shear and 9.9 lb of uplift force. This equates to 2,433 lb shear and 633 lb of uplift force.

Table 12. Prototype and model controlling forces for a single anchor.

All forces in pounds		0.75-ft 0°	1.00-ft 0°	0.75-ft 10°	1.00-ft 10°
Model	Max Horizontal	29.88	37.62	27.56	38.01
	Min Horizontal	-29.02	-36.56	-32.29	-25.90
	Max Vertical	6.58	8.54	7.63	9.89
	Min Vertical	-9.16	-12.72	-9.11	-11.96
Prototype	Max Horizontal	1912	2408	1764	2433
	Min Horizontal	-1858	-2340	-2067	-1658
	Max Vertical	421	546	488	633
	Min Vertical	-586	-814	-583	-765

A factor of safety of at least 2.0 is recommended for the anchor holding capacity. This is due to the possibility of a higher amount of marine growth than designed causing higher drag forces or the breakwater being snagged or struck by loose debris during a storm. The factor of safety should be even higher if there is not sufficient data of the sediments where the breakwaters are being installed. Using the FOS of 2.0 the prototype horizontal reaction force required is 4,866 lb and the uplift reaction is 1,266 lb.

Multiple types of anchors could be used to secure the breakwater. Clump anchors are normally inexpensive. The horizontal reaction is from the drag coefficient and normal force due to the weight of the anchor. When calculating the anchor weight required a normal friction coefficient is assumed to be 0.5 and the normal force must be reduced by the uplift force applied to the anchor. Therefore the minimum clump anchor weight per anchor for the breakwater is 11,000 lb. This is very heavy and large when considering there are 4 of these anchors per 40 ft segment of prototype breakwater. The better anchor solution may be a driven pile. The water depth is shallow enough a normal construction barge would be able to install the piles without special machinery. The piles would also take up less area around the breakwaters. However a sediment profile would have to be completed to accurately calculate the holding capacity with any confidence. The last type of anchor that would be feasible is a screw anchor, or auger shown in Figure 43.



Figure 43. Common screw/anchor 66 in length with an 8 in diameter screw.

From one vendor the minimum screw anchor required is a 66 in anchor. This anchor has a holding capacity of 11,000 lbs (GME Supply 2014). The screw is 8 inches in diameter. These are twisted into the sediment to gain holding capacity. Once again the soil profile and sediment type would have to be known to guarantee holding capacity.

It is important for the design of the mooring system that it must withstand an oscillating force. Some types of soils that are found offshore have a tendency to liquefy under cyclic loading; these sands require different anchors to mitigate the loss of holding capacity. The soils are not frequent however in certain regions around the world they are more common. To find out if this phenomena applies a sample of the sediment has to be taken into the laboratory to perform tests to determine the cyclic shear strength and modulus, pore generation pressure. These higher pore pressures cause the internal stresses of the soil to increase, which decreases the overall available shear stress, and for some soils, the strength reduction can be 20 to 30% (Moses and Rao 2007).

CONCLUSIONS AND RECOMMENDATIONS

The horizontal and vertical forces experienced by the 10 ft breakwater were measured with two horizontal force gauges and four vertical force gauges installed in cables that suspended the model 10 ft breakwater 1 in above the wave basin floor using a metal support structure. The JONSWAP wave spectrum and a regular sinusoidal wave were used during the testing. The lowest maximum horizontal forces occurred for the model 2.0 sec peak wave period and ranged between 23 and 41 lb, and the largest forces ranged between 33 and 73 lb for the 3.0 sec peak model wave period. The 1 ft significant wave height spectra resulted in higher forces than the 0.75 ft significant wave height spectra, and the -10 degree directional waves resulted in slightly smaller forces by about 5 lb. The minimum horizontal force values are negative because the forces occur in the negative x-direction that is towards the wave maker. The minimum horizontal forces ranged between -20 lb and -40 lb for the 2.0 sec peak wave period, -20 and -41 lb for the 2.5 sec peak wave period, and -24 and -44 lb for the 3.0 sec peak wave period. The overall trend is for the negative horizontal force to increase slightly in magnitude with increasing peak wave period. Generally, the higher significant wave height produces larger forces. However, in the case of the -10 degree direction, the 3.0 sec peak period shows the 0.75 significant wave height produces the largest forces. The largest horizontal forces were measured in the direction of wave propagation toward the beach and increased nearly linearly with peak wave period.

The total maximum vertical force range was between 13 and 20 lb. The forces for the 2.0 sec and 3.0 sec peak period are grouped around 15 lb, while the 2.5 s peak period shows a wider spread between 13 lb and 20 lb. The -10 degree directional waves generally show a slight increase in vertical force by 2 to 3 lb. The 1 ft significant wave height causes higher vertical forces than the 0.75 ft significant wave height by 2 to 4 lb. The total minimum vertical forces are negative indicating the force is acting downward or towards the wave basin floor. The downward vertical forces show a larger spread and range between -10 lb and -25 lb. The average downward force was 5 lb larger than the vertical upward force. The -10 degree directional waves show slightly higher downward forces than the zero degree wave direction. As the waves pass through the breakwater, the force on the breakwater goes from a positive horizontal force to a negative horizontal force, and thus the breakwater experiences an oscillating force due waves. A similar phenomena occurs in the vertical direction that creates an oscillatory upward and downward force on the breakwater.

The theoretical wave equations and drag law can be used to calculate with some accuracy the maximum horizontal forces on the breakwater using the 1st order (Airy) or 2nd order (Stokes) theoretical wave orbital velocity equations. There must be care taken in splitting apart the model to get an accurate representation of frontal area and location of the member to calculate the forces. The drag coefficients used were 1.2 for the horizontal forces and 1.0 for the vertical forces. These values are concurrent with the known experimental data from testing of flow over a long cylinder, which each rebar

longitudinal beam is. For the minimum horizontal force as well as the vertical forces the equations do not do a good job of estimating the forces. For the minimum horizontal force the average difference between the theoretical value and the measured was under predicted by approximately 50%. The highest minimum vertical force difference was ranging between 40 and 60% for the 0.75 ft and ranging between 25 and 35% for the 1.0 ft wave cases. For the highest maximum vertical force difference, the Airy wave theory is approximately the same as the regular wave results, a difference ranging from under predicting by 10% to over predicting by 30%, however it under predicts the irregular wave force results by a difference of 70%. This is due to the lack of inclusion of the overturning moment in the basic simplified drag equations for the vertical forces. The minimum horizontal force was based on the relaxation of the cables holding the breakwater and therefore there is more uncertainty. However, the Airy wave equations are able to predict the upper force magnitude for the longer wave periods. More work could be done to split the theoretical model further to better represent the actual physics and reactions based on the tie down locations to be used when implementing the breakwater.

The recommended anchor is based on the sediment profile of the installation location. Either a screw or auger anchors should be installed or piles should be driven. In either case the holding capacity should have a FOS of 2.0 or greater to account for additional unplanned growth of the breakwater, or accidental loading of the breakwater. Clump anchors are not recommended due to the large weight and size needed to properly secure

the breakwater. The clump anchor would have to be approximately 11,000 lb to resist the prototype horizontal reaction force of 4,866 lb, and the uplift reaction is 1,266 lb using a FOS of 2.0. Both piles and screw anchors would be a better choice. From one vendor the minimum screw anchor required is a 66 in anchor with a screw diameter of 8 in. This anchor has a holding capacity of 11,000 lb (GME Supply 2014) which is adequate. The sediment must be tested to find the mechanical properties to verify the holding capacity. The sediment should also be tested for liquefaction due to cyclic loading, and if liquefaction does occur the holding capacity could be reduced by 20% or more.

If more testing was to be done there are several lessons learned. The first lesson learned is to use load cells with the highest precision as reasonable. The calibration of the force gauges should have been accomplished with the calibration weights measured to more than one decimal point. By not including any decimals in the calibration there was a 1% error introduced that was not necessary. A second recommendation is to either be able to change the rebar diameter or somehow make the breakwater less porous. The breakwater had a very low effect on the transmission waves progressing through it. The transmission coefficients were very high (96%), and the reflection coefficients were very low (1%) on average. The low forces on the structure confirm there was not much resistance to the waves. These low coefficients show a negligible amount of energy was removed from the progressing waves. Another test would be to have a larger diameter breakwater or an oval cross-section breakwater to see how the height of the breakwater effects the energy

reduction of the system. Smaller force gauges are recommended for the horizontal force measurements. With smaller gauges the gain could be reduced which would reduce the noise of the data. The uncertainty analysis of the data collection showed the quality of the data was reasonable. The smaller load cells would improve the accuracy and uncertainty of the force measurements. The smaller the FSO range, the smaller the error of the gauge. For the instrumentation system used, the uncertainty was 14.5 lb for the total horizontal force, 1.3 lb for the total vertical force, and 0.190 in for the wave gauges. Using the calibration data, the uncertainty of the horizontal load cells resulted in a better value of approximately 3.7 to 6.0 lb. This is still high compared to some of the forces being measured that are in the range of 13 to 20 lb.

REFERENCES

- Dean, R. and Dalrymple, R. *Water Wave Mechanics for Engineers and Scientists*.
World Scientific: Hackensack, New Jersey, 1991
- GME Supply. (July 2014) *Screw Earth Ground Anchors*. Retrieved from
<http://www.gmesupply.com/wire-rope-guying/ground-anchors/66-galvanized-earth-screw-anchor>
- Goda, Y. *Random Seas and Design of Maritime Structures*, University of Tokyo
Press: Tokyo, Japan, 1985.
- Harris, L. "Artificial Reef Structures for Shoreline Stabilization and Habitat
Enhancement." *Proceedings of the 3rd International Surfing Reef
Symposium*, 176-178, Raglan, New Zealand, 2003.
- Holman, J. *Experimental Methods for Engineers*. McGraw-Hill Book Company.
New York, New York. 1989
- Hughes, S. *Physical Models and Laboratory Techniques in Coastal Engineering*,
World Scientific: Hackensack, New Jersey, 1993.
- Mansard, E., and Funke, E. "The measurement of incident and reflected Spectra
using a least squares method," ICCE, *Coastal Engineering*, Editor: Edge, B.
Chapter 8 154-172, Sydney, Australia, 1980.
- Young, M., and Testik, F. "Wave Reflection By Submerged Vertical and
Semicircular Breakwaters." *Ocean Engineering* Editor: Incecik, A., Volume
38, Issue 10, 1269-1276, New York, New York, 2011

- Mouraenko, O. Moffatt & Nichols, Personal Communication, 2013.
- Moses, G., and Rao, S. "Behavior of Marine Clay Subjected to Cyclic Loading with Sustained Shear Stress." *Marine Georesources & Geotechnology*, Editors: Chaney, R. and Wiltshire, J., Volume 25, Issue 2, 81-96, Philadelphia, Pennsylvania, 2007
- Rambabu, C., and Mani J. "Numerical Prediction of Performance of Submerged Breakwaters." *Ocean Engineering* Editors: McCormick, M. and Bhattacharyya, R., Volume 32, Issue 10, 1235-1246, New York, New York, 2005
- Randall, R. *Elements of Ocean Engineering*. Society of Naval Architects and Marine Engineers. Jersey City, New Jersey, 2010
- Randall, R., Knoll, A., Zhi, Y., and Girani, J. "Model Testing of an Artificial Submerged Reef, Haynes Coastal Engineering Laboratory Technical Report" submitted to Texas General Land Office, July 31, 2013.
- Sorensen, R. *Basic Coastal Engineering*. Springer. New York, New York, 2006
- Tomasicchio, U. "Submerged breakwaters for the defense of the shoreline at Ostia Field experiences, comparison." ICCE, *Coastal Engineering Proceedings*, Editor: Edge, B. 2404-2417, Orlando, Florida, 1996.
- US Army Corps of Engineers. *Coastal Engineering Manual EM 1110-2-1100*. USACE. Washington DC, 2008
- US Army Corps of Engineers. *Coastal Engineering Manual EM 1110-2-1617*. USACE. Washington DC, 1992

US Army Corps of Engineers. *Shore Protection Manual Volume 1*. USACE.

Washington DC, 1984

Vennard, J. and Street, R. *Elementary Fluid Mechanics*. New York, New York, 1982

APPENDIX A. FORCE GAUGE CALIBRATION AND FORCE PLOT DATA

The calibration data and curves for the 4 vertical and 2 horizontal force gauges are shown in Figure 44, Figure 45, Figure 46, Figure 47, and Figure 48 and Table 13 on the following pages. Table 14 contains force data for the irregular wave plots in the main text. Table 15 contains force data for the regular wave plots in the main text. Table 16 contains the prototype and model average and maximum values for all of the individual and combinations of force gauges.

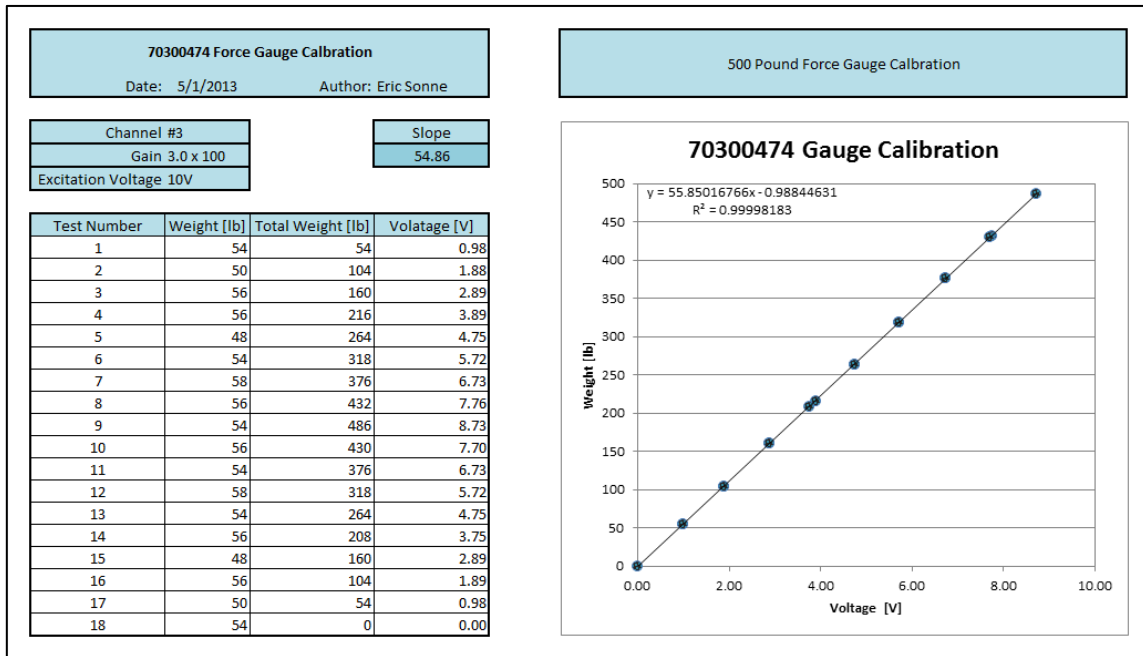


Figure 44. Vertical force gauge calibration (SN: 70300474).

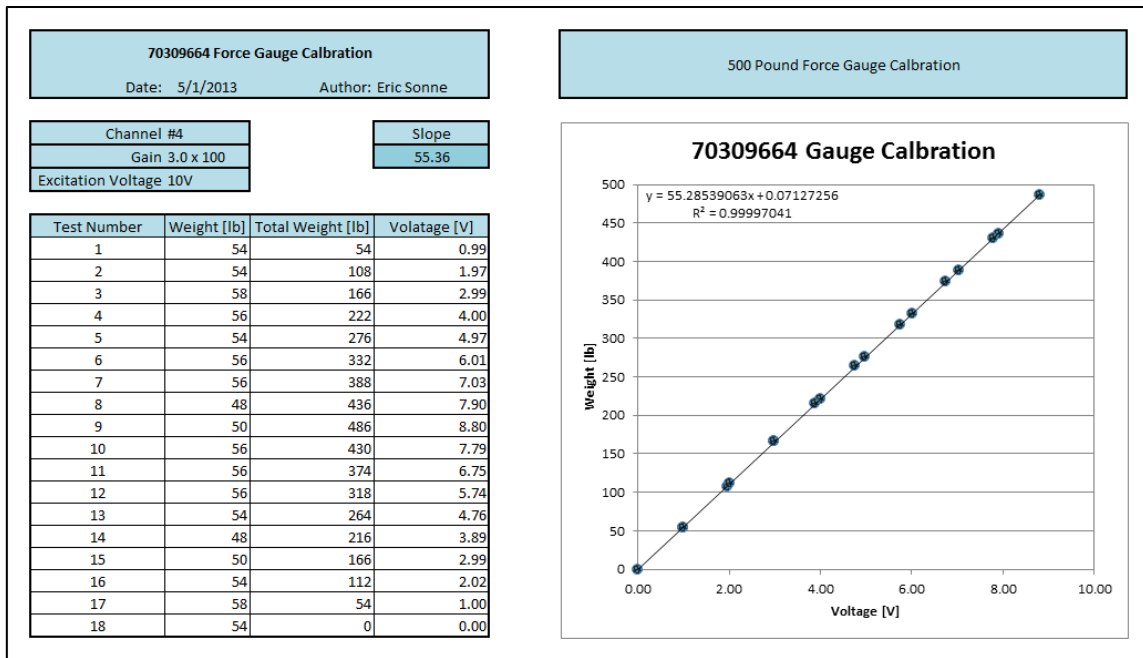


Figure 45. Vertical force gauge calibration (SN: 70309664).

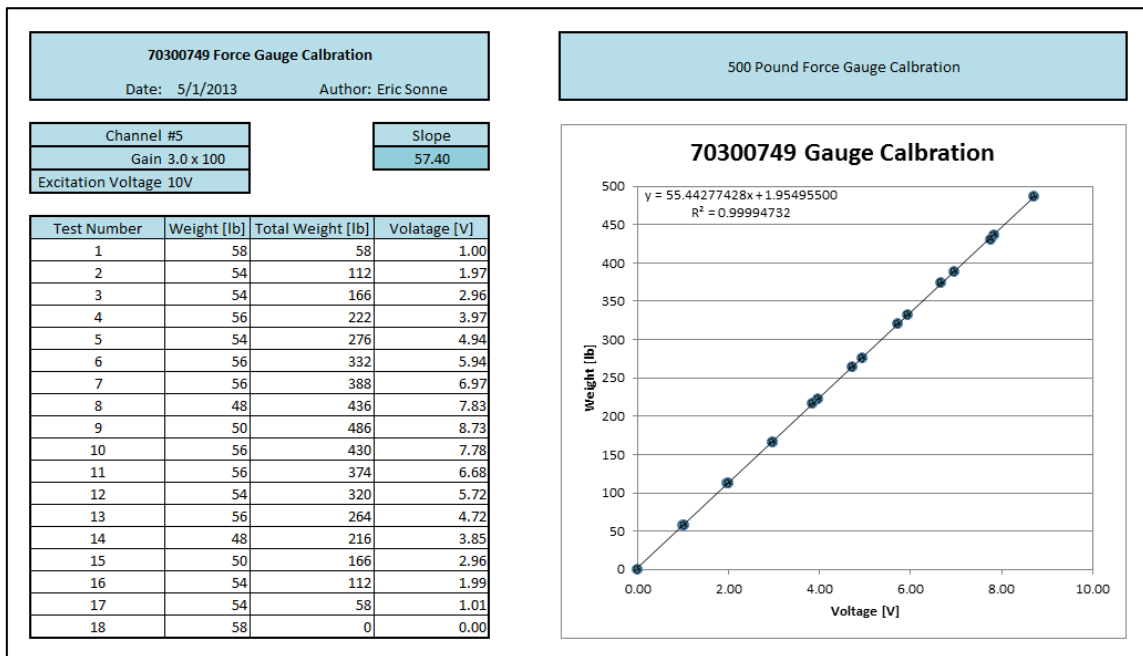


Figure 46. Vertical force gauge calibration (SN: 70300749).

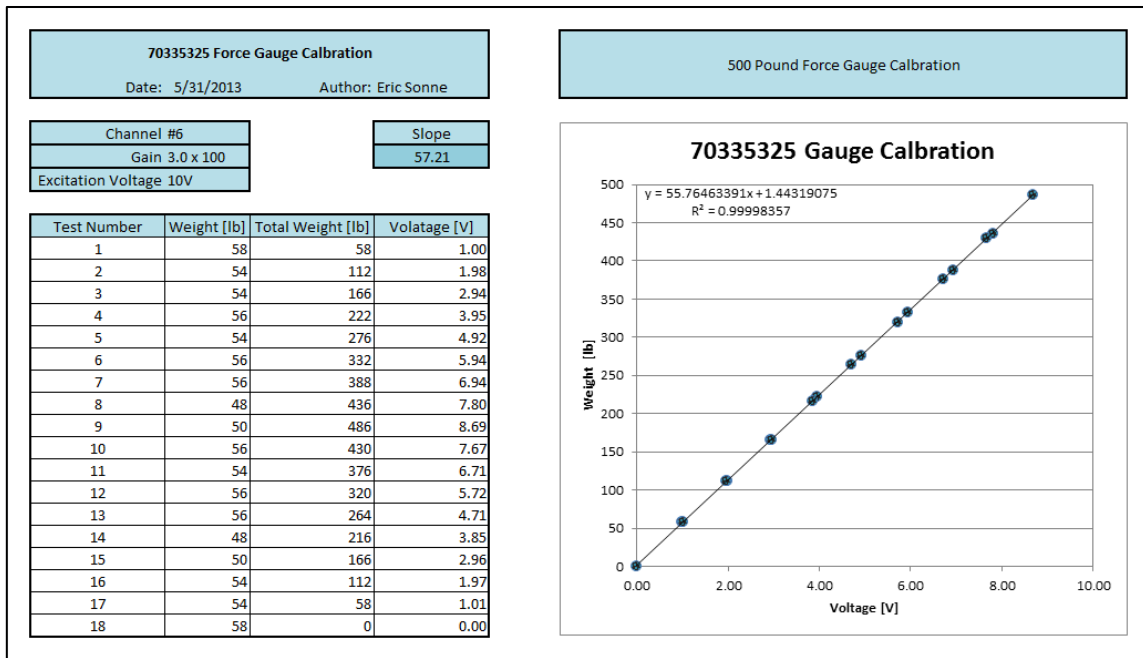


Figure 47. Vertical force gauge calibration (SN: 70335325).

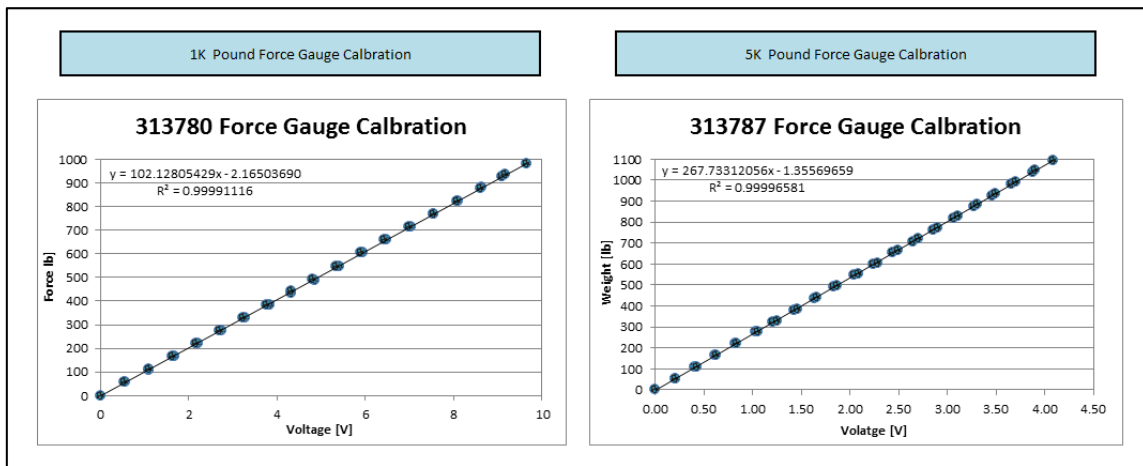


Figure 48. Horizontal force gauge calibration (left) 1,000-lb submersible and (right) 5,000-lb submersible.

Table 13. Horizontal force gauge calibration (left) 1,000-lb submersible (right) 5,000-lb submersible.

313780 Force Gauge Calibration				313787 Force Gauge Calibration			
Date: 4/6/2013		Author: Eric Sonne		Date: 4/30/2013		Author: Eric Sonne	
Channel #1		Slope		Channel #2		Slope	
Gain 3.2 x 100		99.96		Gain 6.1 x 100		266.38	
Excitation Voltage 10V				Excitation Voltage 10V			
Test Number	Weight [lb]	Total Weight [lb]	Volatage [V]	Test Number	Weight [lb]	Total Weight [lb]	Volatage [V]
1	56	56	0.56	1	54	54	0.20
2	54	110	1.11	2	54	108	0.40
3	56	166	1.67	3	56	164	0.61
4	54	220	2.21	4	56	220	0.82
5	54	274	2.74	5	56	276	1.03
6	54	328	3.28	6	48	324	1.21
7	56	384	3.84	7	56	380	1.42
8	50	434	4.32	8	56	436	1.63
9	56	490	4.86	9	54	490	1.83
10	58	548	5.41	10	56	546	2.04
11	56	604	5.95	11	54	600	2.24
12	54	658	6.48	12	54	654	2.44
13	56	714	7.03	13	54	708	2.65
14	54	768	7.55	14	54	762	2.85
15	56	824	8.09	15	56	818	3.06
16	56	880	8.64	16	56	874	3.27
17	48	928	9.10	17	50	924	3.46
18	54	982	9.64	18	56	980	3.66
19	48	934	9.17	19	58	1038	3.88
20	56	878	8.62	20	56	1094	4.09
21	54	824	8.08	21	48	1046	3.90
22	54	770	7.55	22	56	990	3.70
23	56	714	6.98	23	56	934	3.49
24	56	658	6.43	24	50	884	3.31
25	54	604	5.90	25	54	830	3.11
26	56	548	5.35	26	56	774	2.90
27	56	492	4.80	27	54	720	2.70
28	50	442	4.32	28	56	664	2.49
29	58	384	3.77	29	58	606	2.28
30	56	328	3.22	30	54	552	2.08
31	54	274	2.69	31	56	496	1.87
32	54	220	2.16	32	54	442	1.66
33	54	166	1.63	33	56	386	1.46
34	54	112	1.09	34	56	330	1.25
35	56	56	0.54	35	54	276	1.05
36	56	0	0.00	36	56	220	0.83
				37	56	164	0.62
				38	54	110	0.42
				39	56	54	0.20
				40	54	0	0.00

Table 14. Force data used for irregular wave plots in main text (first row is period (s), second row is force (lb), second column is significant wave height and wave direction).

Max Total Horizontal	0.75-ft --- 0°	2	2.5	3	3	3		
		27.75	45.96	53.39	53.38	56.67		
	1.00-ft --- 0°	2	2	2.5	2.5	2.5	3	3
		37.69	38.97	52.72	53.63	73.95	72.94	72.35
	0.75-ft --- 10°	2	2	2.5	3	3		
	24.97	26.32	48.00	52.63	53.14			
1.00-ft --- 10°	2	2.5	2.5	3	3	3		
	32.91	58.01	55.28	67.88	66.82	71.37		
Min Total Horizontal	0.75-ft --- 0°	2	2.5	3	3	3		
		-36.63	-35.76	-34.12	-35.94	-37.37		
	1.00-ft --- 0°	2	2	2.5	2.5	2.5	3	3
		-39.45	-30.86	-33.88	-34.78	-34.44	-38.18	-34.77
	0.75-ft --- 10°	2	2	2.5	3	3		
	-31.90	-32.01	-36.67	-41.74	-42.70			
1.00-ft --- 10°	2	2.5	2.5	3	3	3		
	-27.55	-41.28	-36.62	-32.10	-33.07	-33.68		
Max Total Vertical	0.75-ft --- 0°	2	2.5	3	3	3		
		14.15	12.94	15.34	14.28	15.39		
	1.00-ft --- 0°	2	2	2.5	2.5	2.5	3	3
		15.69	16.67	17.79	18.85	14.77	13.89	13.45
	0.75-ft --- 10°	2	2	2.5	3	3		
	16.08	16.90	16.27	15.03	12.80			
1.00-ft --- 10°	2	2.5	2.5	3	3	3		
	16.17	19.79	18.67	15.55	15.95	15.45		
Min Total Vertical	0.75-ft --- 0°	2	2.5	3	3	3		
		-14.89	-13.20	-10.67	-17.23	-17.03		
	1.00-ft --- 0°	2	2	2.5	2.5	2.5	3	3
		-19.37	-22.76	-16.66	-22.18	-23.98	-21.68	-24.00
	0.75-ft --- 10°	2	2	2.5	3	3		
	-15.68	-17.05	-17.71	-16.40	-18.54			
1.00-ft --- 10°	2	2.5	2.5	3	3	3		
	-21.26	-24.40	-24.74	-22.54	-23.45	-22.25		
Max Total Front Vertical	0.75-ft --- 0°	2	2.5	3	3	3		
	Front	6.18	5.34	5.10	7.58	7.53		
	1.00-ft --- 0°	2	2	2.5	2.5	2.5	3	3
	Front	8.07	9.97	5.37	8.64	6.19	5.58	6.84
	0.75-ft --- 10°	2	2	2.5	3	3		
Front	8.85	9.36	7.98	7.66	7.38			
1.00-ft --- 10°	2	2.5	2.5	3	3	3		
Front	9.30	9.42	8.25	7.62	6.82	6.93		
Min Total Front Vertical	0.75-ft --- 0°	2	2.5	3	3	3		
	Front	-7.54	-10.64	-8.23	-16.53	-17.01		
	1.00-ft --- 0°	2	2	2.5	2.5	2.5	3	3
	Front	-12.13	-14.76	-11.43	-17.70	-23.55	-17.54	-23.58
	0.75-ft --- 10°	2	2	2.5	3	3		
Front	-11.08	-11.16	-16.11	-15.70	-16.37			
1.00-ft --- 10°	2	2.5	2.5	3	3	3		
Front	-13.67	-19.39	-19.24	-22.28	-23.77	-22.27		
Max Total Rear Vertical	0.75-ft --- 0°	2	2.5	3	3	3		
	Rear	8.67	11.14	11.49	11.70	11.78		
	1.00-ft --- 0°	2	2	2.5	2.5	2.5	3	3
	Rear	11.22	9.97	14.50	14.85	16.30	16.88	15.90
	0.75-ft --- 10°	2	2	2.5	3	3		
Rear	9.14	9.02	13.06	13.17	12.05			
1.00-ft --- 10°	2	2.5	2.5	3	3	3		
Rear	10.84	16.54	15.50	15.44	15.96	15.57		
Min Total Rear Vertical	0.75-ft --- 0°	2	2.5	3	3	3		
	Rear	-8.43	-10.76	-8.59	-8.50	-9.00		
	1.00-ft --- 0°	2	2	2.5	2.5	2.5	3	3
	Rear	-11.01	-11.18	-10.87	-10.75	-11.26	-12.23	-9.45
	0.75-ft --- 10°	2	2	2.5	3	3		
Rear	-7.36	-8.09	-10.97	-9.02	-9.81			
1.00-ft --- 10°	2	2.5	2.5	3	3	3		
Rear	-9.84	-10.53	-11.14	-8.84	-8.72	-8.83		

Table 15. Force data used for regular wave plots in main text (first row is period (s), second row is force (lb), second column is significant wave height and wave direction).

Max Total Horizontal	0.75-ft --- 0°	2	2	3	3	2.25	2.5	2.75
		24.81	22.71	32.84	33.41	27.84	24.19	29.66
	1.00-ft --- 0°	2	2	3	3	2.25	2.5	2.75
		37.01	40.77	62.64	61.75	49.32	43.36	58.14
Min Total Horizontal	0.75-ft --- 0°	2	2	3	3	2.25	2.5	2.75
		-20.46	-20.06	-24.93	-23.46	-19.85	-19.52	-19.30
	1.00-ft --- 0°	2	2	3	3	2.25	2.5	2.75
		-32.83	-39.58	-31.90	-43.81	-32.86	-27.86	-26.94
Max Total Vertical	0.75-ft --- 0°	2	2	3	3	2.25	2.5	2.75
		8.81	8.84	5.78	5.79	7.66	8.66	6.53
	1.00-ft --- 0°	2	2	3	3	2.25	2.5	2.75
		16.75	17.18	11.81	10.55	12.19	16.70	11.22
Min Total Vertical	0.75-ft --- 0°	2	2	3	3	2.25	2.5	2.75
		-12.98	-11.50	-8.02	-8.27	-10.55	-9.19	-9.69
	1.00-ft --- 0°	2	2	3	3	2.25	2.5	2.75
		-17.20	-18.15	-13.22	-13.50	-18.62	-15.30	-17.24
Max Total Front Vertical	0.75-ft 0° Front	2	2	3	3	2.25	2.5	2.75
		4.95	5.25	3.81	3.56	4.05	4.64	3.59
	1.00-ft 0° Front	2	2	3	3	2.25	2.5	2.75
		8.01	8.69	4.93	4.86	5.82	6.68	6.02
Min Total Front Vertical	0.75-ft 0° Front	2	2	3	3	2.25	2.5	2.75
		-9.25	-9.16	-9.98	-9.84	-8.84	-8.22	-8.97
	1.00-ft 0° Front	2	2	3	3	2.25	2.5	2.75
		-13.05	-13.93	-18.50	-18.37	-15.62	-15.38	-17.41
Max Total Rear Vertical	0.75-ft 0° Rear	2	2	3	3	2.25	2.5	2.75
		6.77	6.70	7.21	7.28	7.95	7.08	8.86
	1.00-ft 0° Rear	2	2	3	3	2.25	2.5	2.75
		11.86	12.21	12.18	12.48	12.79	13.31	15.65
Min Total Rear Vertical	0.75-ft 0° Rear	2	2	3	3	2.25	2.5	2.75
		-5.67	-4.67	-5.24	-8.78	-4.61	-3.95	-4.86
	1.00-ft 0° Rear	2	2	3	3	2.25	2.5	2.75
		-8.22	-8.31	-10.62	-9.72	-8.67	-5.14	-7.78

Table 16. Force data summary of all measurements (regular and irregular wave tests) for model and prototype scales

Wave Period	Max Individual Horizontal – Model								Max Individual Horizontal - prototype							
	Hs = 0.75-ft Dir = 0°		Hs = 1.0-ft Dir = 0°		Hs = 0.75-ft Dir = 10°		Hs = 1.0-ft Dir = 10°		Hs = 0.75-ft Dir = 0°		Hs = 1.0-ft Dir = 0°		Hs = 0.75-ft Dir = 10°		Hs = 1.0-ft Dir = 10°	
	Avg	Max	Avg	Max	Avg	Max	Avg	Max	Avg	Max	Avg	Max	Avg	Max	Avg	Max
2.0	12.88	15.00	19.36	21.53	14.23	15.41	17.66	18.87	824	960	1239	1378	911	986	1131	1207
2.5	17.63	23.98	28.07	37.62	24.93	25.95	28.59	29.68	1128	1534	1797	2408	1596	1661	1830	1900
3.0	23.24	29.88	33.84	36.97	27.06	27.56	35.62	38.01	1487	1912	2166	2366	1732	1764	2280	2433
Wave Period	Min Individual Horizontal - Model								Min Individual Horizontal - prototype							
	Hs = 0.75-ft Dir = 0°		Hs = 1.0-ft Dir = 0°		Hs = 0.75-ft Dir = 10°		Hs = 1.0-ft Dir = 10°		Hs = 0.75-ft Dir = 0°		Hs = 1.0-ft Dir = 0°		Hs = 0.75-ft Dir = 10°		Hs = 1.0-ft Dir = 10°	
	Avg	Min	Avg	Min	Avg	Min	Avg	Min	Avg	Min	Avg	Min	Avg	Min	Avg	Min
2.0	-15.43	-25.71	-20.08	-36.56	-16.41	-17.34	-16.40	-18.17	-988	-1645	-1285	-2340	-1050	-1110	-1050	-1163
2.5	-15.92	-21.83	-18.32	-25.20	-18.51	-20.95	-21.27	-25.87	-1019	-1397	-1172	-1613	-1185	-1341	-1361	-1656
3.0	-17.40	-29.02	-19.77	-32.38	-23.32	-32.29	-18.05	-25.90	-1113	-1858	-1265	-2072	-1492	-2067	-1155	-1658
Wave Period	Max Individual Vertical - Model								Max Individual Vertical - prototype							
	Hs = 0.75-ft Dir = 0°		Hs = 1.0-ft Dir = 0°		Hs = 0.75-ft Dir = 10°		Hs = 1.0-ft Dir = 10°		Hs = 0.75-ft Dir = 0°		Hs = 1.0-ft Dir = 0°		Hs = 0.75-ft Dir = 10°		Hs = 1.0-ft Dir = 10°	
	Avg	Max	Avg	Max	Avg	Max	Avg	Max	Avg	Max	Avg	Max	Avg	Max	Avg	Max
2.0	3.37	4.74	5.11	6.37	4.85	5.84	5.53	6.82	216	304	327	408	310	374	354	436
2.5	3.58	5.79	5.62	8.44	5.43	7.19	6.67	8.95	229	371	360	540	347	460	427	573
3.0	4.04	6.58	5.18	8.54	5.20	7.63	6.22	9.89	258	421	332	546	333	488	398	633
Wave Period	Min Individual Vertical - Model								Min Individual Vertical - prototype							
	Hs = 0.75-ft Dir = 0°		Hs = 1.0-ft Dir = 0°		Hs = 0.75-ft Dir = 10°		Hs = 1.0-ft Dir = 10°		Hs = 0.75-ft Dir = 0°		Hs = 1.0-ft Dir = 0°		Hs = 0.75-ft Dir = 10°		Hs = 1.0-ft Dir = 10°	
	Avg	Min	Avg	Min	Avg	Min	Avg	Min	Avg	Min	Avg	Min	Avg	Min	Avg	Min
2.0	-4.02	-6.29	-5.90	-7.56	-5.23	-7.20	-6.27	-7.90	-257	-402	-377	-484	-335	-461	-401	-506
2.5	-4.48	-8.28	-6.83	-12.72	-6.88	-9.11	-7.76	-10.42	-287	-530	-437	-814	-440	-583	-497	-667
3.0	-5.36	-9.16	-7.93	-12.32	-6.62	-8.84	-8.18	-11.96	-343	-586	-507	-788	-424	-566	-524	-765

Table 16 Continued

Wave Period	Max Total Horizontal - Model								Max Total Horizontal - prototype							
	Hs = 0.75-ft Dir = 0°		Hs = 1.0-ft Dir = 0°		Hs = 0.75-ft Dir = 10°		Hs = 1.0-ft Dir = 10°		Hs = 0.75-ft Dir = 0°		Hs = 1.0-ft Dir = 0°		Hs = 0.75-ft Dir = 10°		Hs = 1.0-ft Dir = 10°	
	Avg	Max	Avg	Max	Avg	Max	Avg	Max	Avg	Max	Avg	Max	Avg	Max	Avg	Max
2.0	25.09	27.75	38.61	40.77	25.64	26.32	32.91	32.91	1606	1776	2471	2610	1641	1685	2106	2106
2.5	35.07	45.96	55.91	73.95	48.00	48.00	56.64	58.01	2245	2941	3579	4733	3072	3072	3625	3712
3.0	45.94	56.67	67.42	72.94	52.89	53.14	68.69	71.37	2940	3627	4315	4668	3385	3401	4396	4568
Wave Period	Min Total Horizontal - Model								Min Total Horizontal - prototype							
	Hs = 0.75-ft Dir = 0°		Hs = 1.0-ft Dir = 0°		Hs = 0.75-ft Dir = 10°		Hs = 1.0-ft Dir = 10°		Hs = 0.75-ft Dir = 0°		Hs = 1.0-ft Dir = 0°		Hs = 0.75-ft Dir = 10°		Hs = 1.0-ft Dir = 10°	
	Avg	Min	Avg	Min	Avg	Min	Avg	Min	Avg	Min	Avg	Min	Avg	Min	Avg	Min
2.0	-25.71	-36.63	-35.68	-39.58	-31.96	-32.01	-27.55	-27.55	-1646	-2344	-2284	-2533	-2045	-2049	-1763	-1763
2.5	-27.64	-35.76	-32.74	-34.78	-36.67	-36.67	-38.95	-41.28	-1769	-2288	-2095	-2226	-2347	-2347	-2493	-2642
3.0	-31.16	-37.37	-37.17	-43.81	-42.22	-42.70	-32.95	-33.68	-1994	-2392	-2379	-2804	-2702	-2733	-2109	-2156
Wave Period	Max Total Vertical - Model								Max Total Vertical - prototype							
	Hs = 0.75-ft Dir = 0°		Hs = 1.0-ft Dir = 0°		Hs = 0.75-ft Dir = 10°		Hs = 1.0-ft Dir = 10°		Hs = 0.75-ft Dir = 0°		Hs = 1.0-ft Dir = 0°		Hs = 0.75-ft Dir = 10°		Hs = 1.0-ft Dir = 10°	
	Avg	Max	Avg	Max	Avg	Max	Avg	Max	Avg	Max	Avg	Max	Avg	Max	Avg	Max
2.0	10.60	14.15	16.57	17.18	16.49	16.90	16.17	16.17	679	906	1061	1099	1055	1082	1035	1035
2.5	10.80	12.94	17.03	18.85	16.27	16.27	19.23	19.79	691	828	1090	1206	1042	1042	1231	1267
3.0	11.32	15.39	12.43	13.89	13.92	15.03	15.65	15.95	724	985	795	889	891	962	1002	1021
Wave Period	Min Total Vertical - Model								Min Total Vertical - prototype							
	Hs = 0.75-ft Dir = 0°		Hs = 1.0-ft Dir = 0°		Hs = 0.75-ft Dir = 10°		Hs = 1.0-ft Dir = 10°		Hs = 0.75-ft Dir = 0°		Hs = 1.0-ft Dir = 0°		Hs = 0.75-ft Dir = 10°		Hs = 1.0-ft Dir = 10°	
	Avg	Min	Avg	Min	Avg	Min	Avg	Min	Avg	Min	Avg	Min	Avg	Min	Avg	Min
2.0	-13.12	-14.89	-19.37	-22.76	-16.37	-17.05	-21.26	-21.26	-840	-953	-1240	-1457	-1047	-1091	-1361	-1361
2.5	-11.20	-13.20	-19.53	-23.98	-17.71	-17.71	-24.57	-24.74	-717	-845	-1250	-1534	-1133	-1133	-1573	-1584
3.0	-12.24	-17.23	-18.10	-24.00	-17.47	-18.54	-22.75	-23.45	-784	-1103	-1158	-1536	-1118	-1186	-1456	-1501

Table 16 Continued

Wave Period	Max Total Front Vertical - Model								Max Total Front Vertical - prototype							
	Hs = 0.75-ft Dir = 0°		Hs = 1.0-ft Dir = 0°		Hs = 0.75-ft Dir = 10°		Hs = 1.0-ft Dir = 10°		Hs = 0.75-ft Dir = 0°		Hs = 1.0-ft Dir = 0°		Hs = 0.75-ft Dir = 10°		Hs = 1.0-ft Dir = 10°	
	Avg	Max	Avg	Max	Avg	Max	Avg	Max	Avg	Max	Avg	Max	Avg	Max	Avg	Max
2.0	5.46	6.18	8.69	9.97	9.10	9.36	9.30	9.30	350	396	556	638	583	599	595	595
2.5	4.99	5.34	6.72	8.64	7.98	7.98	8.83	9.42	319	342	430	553	510	510	565	603
3.0	5.52	7.58	5.55	6.84	7.52	7.66	7.12	7.62	353	485	355	438	481	490	456	488
Wave Period	Min Total Front Vertical - Model								Min Total Front Vertical - prototype							
	Hs = 0.75-ft Dir = 0°		Hs = 1.0-ft Dir = 0°		Hs = 0.75-ft Dir = 10°		Hs = 1.0-ft Dir = 10°		Hs = 0.75-ft Dir = 0°		Hs = 1.0-ft Dir = 0°		Hs = 0.75-ft Dir = 10°		Hs = 1.0-ft Dir = 10°	
	Avg	Min	Avg	Min	Avg	Min	Avg	Min	Avg	Min	Avg	Min	Avg	Min	Avg	Min
2.0	-8.65	-9.25	-13.47	-14.76	-11.12	-11.16	-13.67	-13.67	-553	-592	-862	-945	-712	-714	-875	-875
2.5	-9.43	-10.64	-17.02	-23.55	-16.11	-16.11	-19.31	-19.39	-604	-681	-1089	-1507	-1031	-1031	-1236	-1241
3.0	-12.31	-17.01	-19.50	-23.58	-16.04	-16.37	-22.77	-23.77	-788	-1089	-1248	-1509	-1026	-1048	-1458	-1522
Wave Period	Max Total Rear Vertical - Model								Max Total Rear Vertical - prototype							
	Hs = 0.75-ft Dir = 0°		Hs = 1.0-ft Dir = 0°		Hs = 0.75-ft Dir = 10°		Hs = 1.0-ft Dir = 10°		Hs = 0.75-ft Dir = 0°		Hs = 1.0-ft Dir = 0°		Hs = 0.75-ft Dir = 10°		Hs = 1.0-ft Dir = 10°	
	Avg	Max	Avg	Max	Avg	Max	Avg	Max	Avg	Max	Avg	Max	Avg	Max	Avg	Max
2.0	7.38	8.67	11.32	12.21	9.08	9.14	10.84	10.84	472	555	724	782	581	585	694	694
2.5	9.11	11.14	14.74	16.30	13.06	13.06	16.02	16.54	583	713	943	1043	836	836	1025	1058
3.0	9.89	11.78	14.36	16.88	12.61	13.17	15.66	15.96	633	754	919	1081	807	843	1002	1022
Wave Period	Min Total Rear Vertical - Model								Min Total Rear Vertical - prototype							
	Hs = 0.75-ft Dir = 0°		Hs = 1.0-ft Dir = 0°		Hs = 0.75-ft Dir = 10°		Hs = 1.0-ft Dir = 10°		Hs = 0.75-ft Dir = 0°		Hs = 1.0-ft Dir = 0°		Hs = 0.75-ft Dir = 10°		Hs = 1.0-ft Dir = 10°	
	Avg	min	Avg	min	Avg	min	Avg	min	Avg	min	Avg	min	Avg	min	Avg	min
2.0	-6.26	-8.43	-9.68	-11.18	-7.72	-8.09	-9.84	-9.84	-400	-539	-620	-716	-494	-518	-630	-630
2.5	-7.36	-10.76	-9.50	-11.26	-10.97	-10.97	-10.83	-11.14	-471	-689	-608	-721	-702	-702	-693	-713
3.0	-8.02	-9.00	-10.51	-12.23	-9.41	-9.81	-8.80	-8.84	-513	-576	-672	-783	-602	-628	-563	-566

APPENDIX B. CONSTRUCTION AND MODEL TEST PHOTOS



Figure 49. Breakwater model being checked at Brazos Industries



Figure 50. Support frame construction



Figure 51. Support frame attachment plate (left) floor tie down (right)



Figure 52. Support frame with guide wires, without breakwater



Figure 53. Wave absorber on south wall



Figure 54. Installation of the breakwater (setting floor clearance)

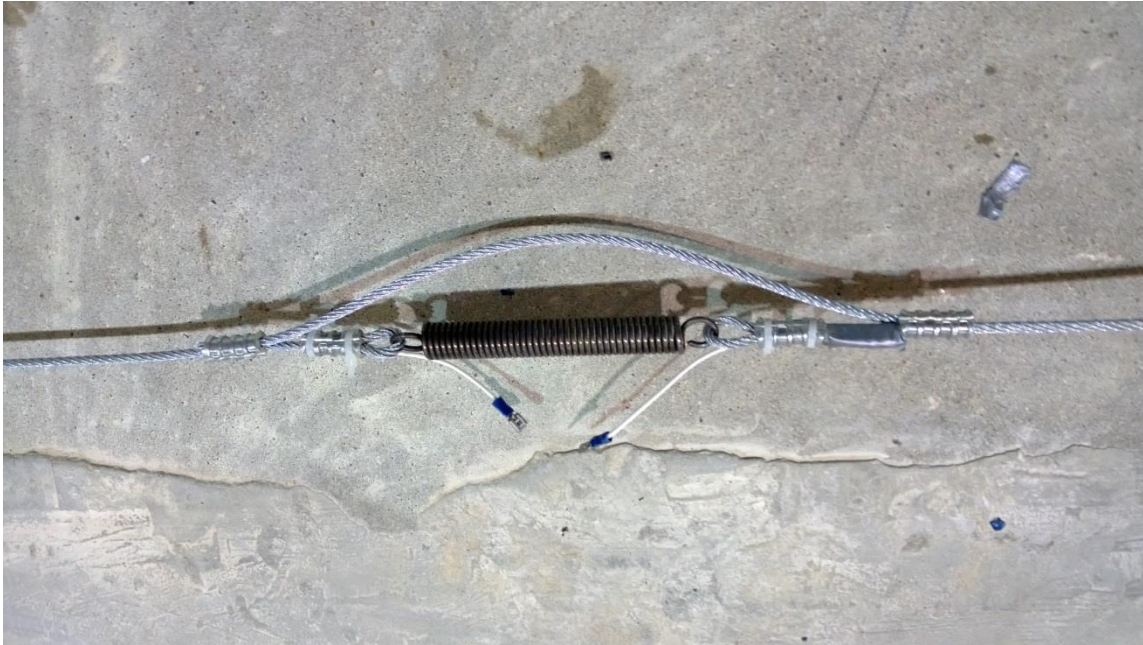


Figure 55. Longitudinal spring plus overload wire in tripped position



Figure 56. Rear horizontal force reaction cables with supports



Figure 57. Front horizontal force reaction cable with force gauge and support



Figure 58. Longitudinal view of breakwater force test setup

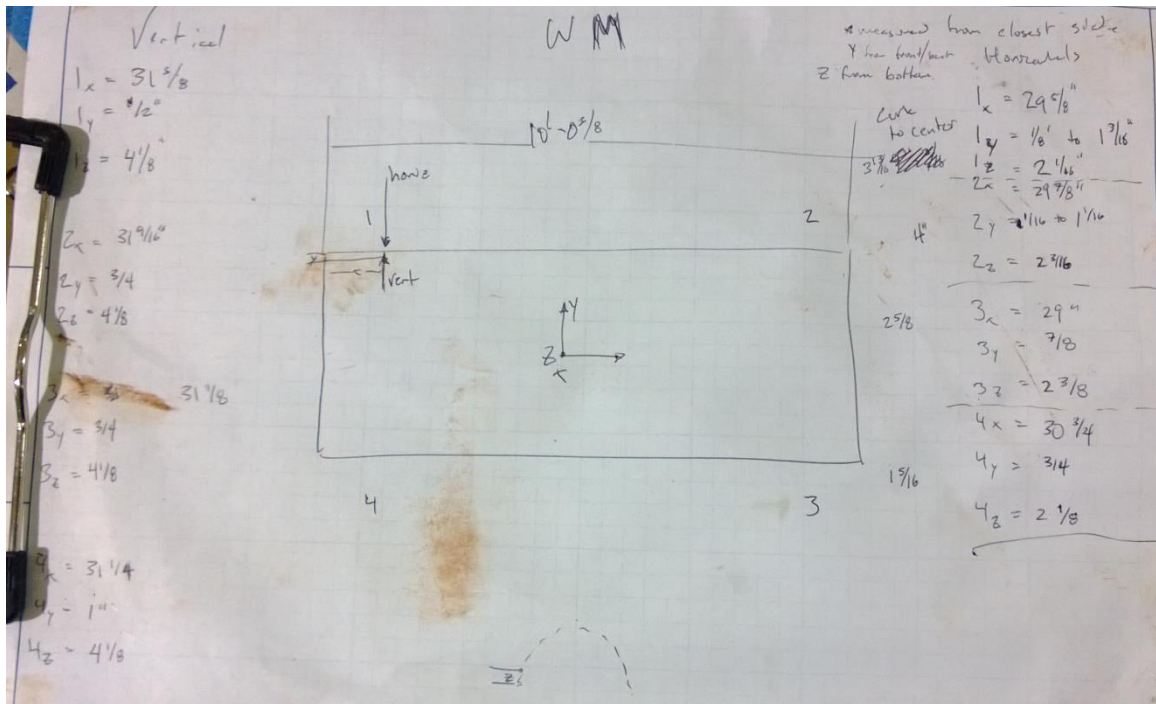


Figure 59. Final force cable attachment point locations

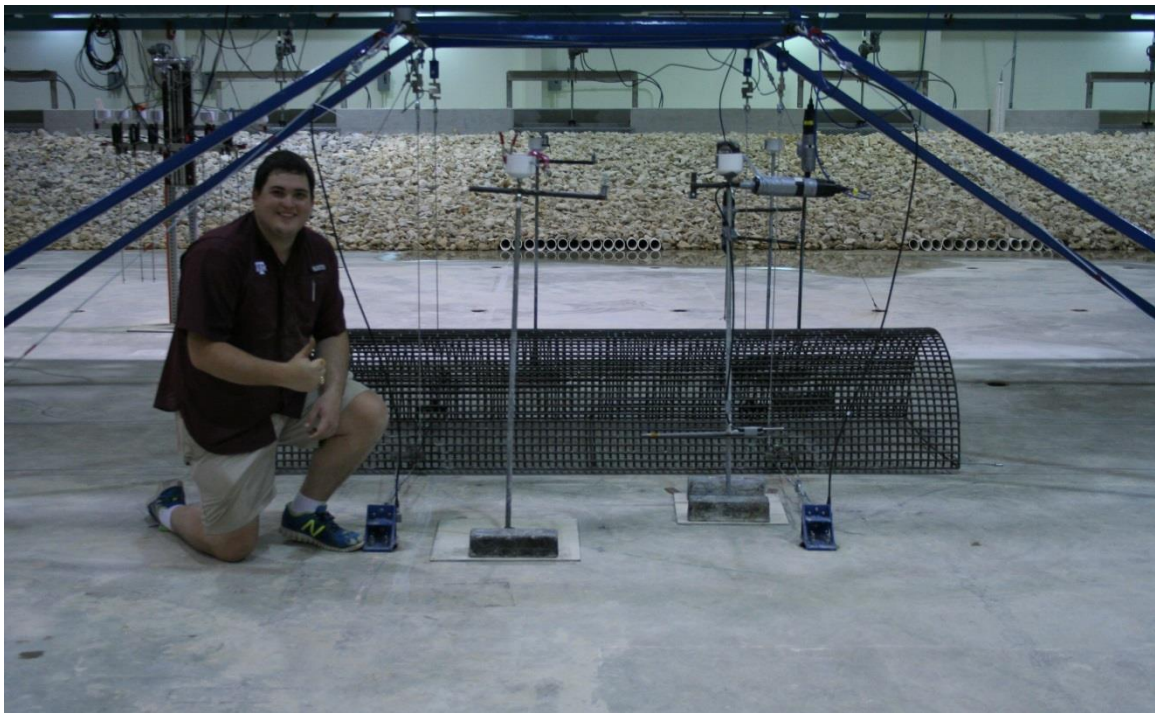


Figure 60. Author Alex Knoll with final force test setup



Figure 61. During force testing of breakwater



Figure 62. 40 ft breakwater wave transmission reflection setup